19th Swiss Conference on Biomaterials

Program & Abstract

Tuesday & Wednesday
June 25 & 26, 2013

Congress Center, Davos
Room Aspen

SSB Swiss Society for Biomaterials
Société Suisse des Biomatériaux
Schweizerische Gesellschaft für Biomaterialien
Società Svizzera Biomateriali

AO Foundation

Contents

Welcome by the President of the SSB

Dear SSB 2013 participants,

In the name of the Executive Committee of the Swiss Society for Biomaterials, I would like to welcome you to the 19th Swiss Conference on Biomaterials.

This year we have decided to propose an original conference format with a first afternoon session dedicated to young scientists, followed by a second day focused on the theme of this year: Polymers and Biomaterials. We are happy to present this year again a scientific program with an outstanding pool of speakers and poster presenters. What is more, the SSB is taking the opportunity of the extended meeting duration to invite you to a get-together dinner during which you will be able to establish many new contacts, and hopefully lay the foundations of new promising projects. On another note, the Executive Committee of the SSB has put in hand during the last year a wide-ranging reflection on the objectives and future orientations of the Society, which will be presented during the General Assembly on June 26. We invite you to attend this important meeting as well.

The SSB is proud and happy to welcome you in Davos. Not only because of its magnificent location, but also because the name of Davos is linked very closely to the history of biomaterials research in Switzerland. I would like to express my deepest gratitude to the AO Research Institute and the Organization Committee for having accepted to host our Conference this year. I would like to thank also the Scientific Committee, our sponsors, and of course you all, dear SSB 2013 participants, for your trust and continuous support.

Have a great meeting!

Dr. Paul-Henri Vallotton

SSB President

ssb.biomaterials.ch

Organization Committee

- **David Eglin,** AO Research Institute Davos, Musculoskeletal Regeneration Program, Davos
- **Matteo D'Este**, AO Research Institute Davos, Musculoskeletal Regeneration Program, Davos
- **Daniela Schraner** (Meeting Secretary), AO Research Institute Davos, Musculoskeletal Regeneration Program, Davos

Scientific Committee

- **Pierre-Etienne Bourban**, Ecole Polytechnique Fédérale de Lausanne, Laboratoire de Technologie des Composites et Polymères, Lausanne
- **David Eglin**, AO Research Institute Davos, Musculoskeletal Regeneration Program, Davos
- **Bert Müller**, University of Basel, Biomaterials Science Center, Basel
- **Christine Wandrey,** Ecole Polytechnique Fédérale de Lausanne, Laboratory for Regenerative Medicine and Pharmacobiology, Lausanne

Invited Speakers

- **Michel Dalstra**, Aarhus University, Departement of Dentistry, Aarhus, Denmark
- **Matthias P. Lutolf,** Ecole Polytechnique Fédérale de Lausanne, Laboratory of Stem Cell Bioengineering, Lausanne

Sponsors of the 19th Swiss Conference on Biomaterials

nolax

SUNSTAR
Degradable Solutions AG

RMS Testing · Research · Consulting
www.rms-foundation.ch

Endorsed by

eCELLS&MATERIALS

endorsed by biomat.net

To all members of the SSB and interested people

You are cordially invited to the

19th General Assembly of the SSB

Davos, Congress Center,
Wednesday, June 26, 2013

11:00 – 11:45

AGENDA

1. Approval of the agenda
2. Protocol of the 18th General Assembly
3. Report of the president
4. Report of the treasurer
5. Budget 2013
6. Election of the new Executive Committee Members
7. Election of the President (1 year term)
8. Sponsoring
9. SSB 2014
10. Modifications of the Bylaws
11. Official integration of tissue engineering in SSB purpose and activities
12. Varia

The Executive Committee is looking forward to meeting you in Davos.

Kind regards,

For the Swiss Society for Biomaterials,

Paul-Henri Vallotton
President

Christine Wandrey
Secretary

Official Journal of
Swiss Society for Biomaterials (SSB), AOTrauma, AOCMF, Tissue and Cell Engineering Society (TCES)
http://www.ecmjournal.org ISSN 1473-2262 NLM: 100973416 2011 Impact Factor 9.65

eCM True Open Access Journal, published by AO Research Institute Davos. **eCM** provides a forum for publication of preclinical research in the musculoskeletal field (Trauma, Maxillofacial (including dental), Spine and Orthopaedics) and the cells and materials used in the replacement, repair or regeneration of these tissues.

eCM Scope

Assessment of materials for biomedical use in the musculoskeletal field & interaction with tissues/ prokaryotic / eukaryotic cells.

- Manuscripts must have an important biological dimension reporting effects at the cellular, tissue or organismic levels.

Tissue Engineering and Regenerative Medicine.

- Manuscripts concerning aspects of the repair or regeneration of connective and mineralized tissues within the musculoskeletal field will be considered.

Structure, function, biology of connective and mineralized tissues.

- Manuscripts concerning the structure of bone, teeth, cartilage, intervertebral discs, skeletal muscle, tendons and ligaments within the musculoskeletal field will be considered.

Stem and Progenitor Cells.

- All manuscripts concerning stem cell characterization and mechanisms of differentiation as they relate to the connective and mineralized tissues of the musculoskeletal field will be considered.

eCM carries original research papers, reviews and tutorials on the advances made within the journal scope. All articles are peer-reviewed and reviewer comments, together with responses by authors, are published as an integral part of the paper. Technical notes are not entertained. Note: musculoskeletal field includes bone, teeth, cartilage, intervertebral discs, skeletal muscle (not smooth or cardiac muscle), tendons and ligaments.

Ten good reasons for publishing a paper in eCM

1. World-wide open access.
2. Authors retain copyright to their articles.
3. Rigorous (high standard) open peer reviewing ((reviewers have to specifically request their name to be withheld).
4. Indexed by ISI within: Science Citation Index Expanded, Materials Science Citation Index (from 2012 additionally to "Engineering Biomedical" and "Cell & Tissue Engineering" categories), Journal Citation Reports /Science Edition, Biosis Previews and Biological abstracts. Indexed in CAS, *Index Medicus,* Medline and Scopus databases and can be searched directly from Pubmed, Biomedsearch, DOAJ and Open J Gate. NLM: 100973416.
5. Five-year Impact Factor# 4.953. (3rd in Biomaterials) Yearly Impact Factors: 2012 3.028, 2011 9.65, 2010 5.378, 2009 4.289. Article Influence Score* 1.46 (2nd in Biomaterials)
6. 17187 registered readers world-wide, over 3000 PubMed monthly linkouts & 7000 monthly visits (Google analytics).
7. Discussion with reviewers feature, which is an integral section of the paper allows sensible arguments to be included (as would occur in a conference).
8. Speed of publication, 40 days average from submission to first decision, ~3 weeks after acceptance, paper is online.
9. Transparent route to becoming a member of the International Editorial Review Board.
10. Founded by scientists for the benefit of Science rather than profit.

eCM Journal
AO Research Institute Davos Clavadelerstrasse 8, 7270
Davos, Switzerland Phone: +41 81 414 24 41, Fax: +41
81 414 22 99
Daniela Schraner: admin@ecmjournal.org, www.ecmjournal.org

19th Swiss Conference on Biomaterials

Final Program

SSB Swiss Society for Biomaterials
Société Suisse des Biomatériaux
Schweizerische Gesellschaft für Biomaterialien
Società Svizzera Biomateriali

AO Foundation

Program

Tuesday, June 25, 2013

15:15 Registration of the Participants / Welcome Coffee

16:15 D. Eglin / RG. Richards - Welcome to Davos

16:20 Opening Address from SSB President

Session 1

16:30 **L. Galea, RMS Foundation, CH**

«Recrystallization and polymer impregnation improve strength and toughness of calcium phosphate ceramics»

16:45 **P. Chavanne, FHNW, CH**

«Gelatin infiltration of 3D printed hydroxyapatite scaffolds for potential use in regenerative medicine»

17:00 **N. Walters, UCL Eastman Dental Institute, UK**

«Novel fibre-reinforced dental and orthopaedic composites with improved toughness and fatigue properites»

17:15 **W. Querido, CNRS LRC7228, Universite de Haute-Alsace, FR**

«Potential role of strontium renelate for bone tissue engineering approaches»

17:30 **J. Idaszek, Warsaw University of Technology, PL**

«PCL-based scaffolds with degradation profiles tuned to various treatment strategies of bone»

17:45 **X-H. Qin, TU Vienna, Austrian Cluster for Tissue Regeneration, AT**

«Two-photon microfabrication of artificial ECM hydrogel via thiol-ene chemistry»

18:00 **T. Esteva, ETHZ, CH**

«Coated y-PGA-Phe nanoparticles for siRNA delivery»

18:15 **D. Morrison, Universtiy of Glasgow, UK**

«Can we alter the cell's response to PEEK with nanopatterning and

plasma treatment?»

19:15 Dinner at Schatzalp

Wednesday, June 26, 2013

08:00 Registration of the Participants

Session 2

08:30 **Keynote Speaker: Dr. M. P. Lutolf, EPFL, CH**

« Rapid discovery of 3D artificial stem cell niches»

09:15 **Prof. M. Zinn, EMPA, CH**

«Soft polymeric surface coatings made from olefinic mediumchain-length poly(3-hydroxyalkanoate)»

09:30 **Dr. R. Mahou, EPFL, CH**

«Engineering polymer hydrogels for MSC immobilization and transplantation»

09:45 **Dr. M. Cuénoud, EPFL, CH**

«Hybrid polylactide foams for osteochondral tissue engineering»

10:00 Coffee Break

10:30 **Prof. M. Zenobi-Wong, ETHZ, CH**

«Cartilage mimetic hydrogels promote a proliferative, chondrogenic phenotype»

10:45 **Dr. P. Urwyler, University of Basel, CH**

«Comparing physical properties of PEKK and PEEK»

11:00 General Assembly of the SSB

11:45 Poster Session and Buffet Lunch

Wednesday, June 26, 2013

Session 3

13:30 **Keynote Speaker: Prof. M. Dalstra, Aarhus University, DK**

«X-ray microtomography of bone and other mineralized tissues»

14:15 **Prof. E. Carreño-Morelli, University of Applied Sciences Western Switzerland, CH**

«Porous titanium by powder injection moulding of titanium hydride and PMMA space holders»

14:30 **Dr. F. Borcard, EPFL, CH**

«Chemical functionalization of bioceramics for the development of bone implants»

14:45 **Dr. M. Obarzanek-Fojt, EMPA, CH**

«From implantation to degradation – Are PLLA/MWCNT composite materials really cytocompatible?»

15:00 Concluding Remarks and Awards

15:45 End of Meeting

19th Swiss Conference on Biomaterials

Overview Oral Presentations

SSB Swiss Society for Biomaterials
Société Suisse des Biomatériaux
Schweizerische Gesellschaft für Biomaterialien
Società Svizzera Biomateriali

AO Foundation

Oral Presentations

Session 1

Session 2

Session 3

19th Swiss Conference on Biomaterials

Abstracts Oral Presentations

SSB Swiss Society for Biomaterials
Société Suisse des Biomatériaux
Schweizerische Gesellschaft für Biomaterialien
Società Svizzera Biomateriali

AO Foundation

Recrystallization and polymer impregnation improve strength and toughness of calcium phosphate ceramics

L. Galea[1,4], M. Peroglio[2], D. Eglin[2], T. Graule[3,4], M. Bohner[1]

[1] RMS Foundation, Bettlach, CH. [2] AO Research Institute, Davos, CH. [3] EMPA, Dübendorf, CH. [4] TU Bergakademie, Freiberg, DE

INTRODUCTION: Porous calcium phosphate (CaP) ceramics are widely used as bone graft substitute materials, but these ceramics are brittle and have low tensile strength. Mechanical properties of structural ceramics are usually improved by microstructural changes like decrease of grain size or impregnation with a tough polymer [1]. Our approach was thus to combine a recently developed recrystallization process of the ceramic by hydrothermal treatment with a subsequent impregnation with poly(ε-caprolactone) (PCL).

METHODS: Microporous (30%) cylindrical blocks of α-tricalcium phosphate (α-TCP) were produced with an oil-in-water emulsion process [2] followed by sintering (1500°C, 12h). Hydrothermal incubation was performed for 24h at 200°C, followed by drying (60°C, 48h). Half of the samples were impregnated under vacuum with a PCL (Mn = 80 000 g/mol) solution in ethyl acetate (35 g/L). The samples size and weight were measured, and the samples were mechanically tested, analyzed by XRD, and observed by SEM at all processing steps. Brazilian tests were used to determine the diametral tensile strength, σ_{dts}. The strain energy density, G, was calculated as integral of the force-displacement curve, at maximum force, divided by the sample section. Student's t-test were performed (significance at $p < 0.05$).

RESULTS: PCL amount was 5.1±0.5 vol%. After hydrothermal treatment, SEM and XRD analysis revealed recrystallization of the ceramic with the appearance of fine (0.1-0.5µm) calcium deficient hydroxylapatite (CDHA) needles (Fig 1). PCL was found in the first hundreds of micrometer of the blocks (Fig 1). Incubation increased σ_{dts} and G of the ceramic blocks (Fig 2). PCL impregnation significantly increased σ_{dts} for incubated samples and improved G for non-incubated blocks (Fig 2).

DISCUSSION & CONCLUSIONS: The fine and entangled crystal structure obtained after incubation might explain the gain in strength and toughness, more than a change in chemistry. Indeed, mechanical properties of α-TCP and CDHA are very similar [3]. PCL strength being much lower than CaP strength, it is surprising that it increased σ_{dts} of the incubated samples. This may be explained by the higher surface area of the ceramic, leading to a better bonding between the PCL coating and the fine nanoscale, high aspect ratio CaP structures [4]. This phenomenon was not observed in the non-incubated samples, which contained microscale porosity. PCL fibrils led to an increase in the toughness of non-incubated samples (Fig 1B), as attested by the increased rupture energy [1]. For incubated samples, this effect might be hidden by the strong increase due to structural changes from incubation. Hence, combination of hydrothermal incubation and polymer impregnation is necessary to synergistically improve σ_{dts} and G of porous CaP.

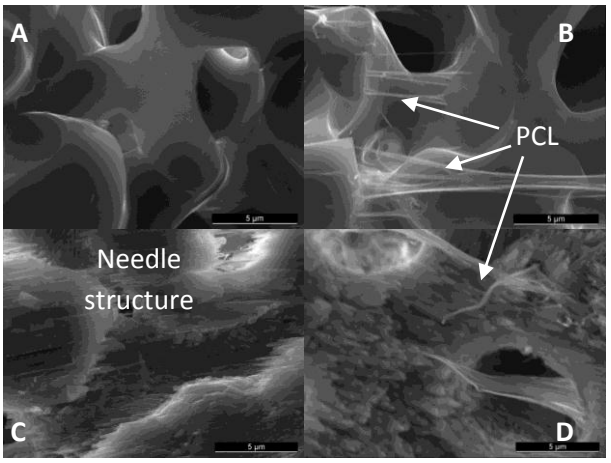

Fig. 1: SEM images of non-incubated (A-B) and incubated (C-D) blocks, without (A+C) and with (B+D) PCL impregnation. Scale bars are 5µm.

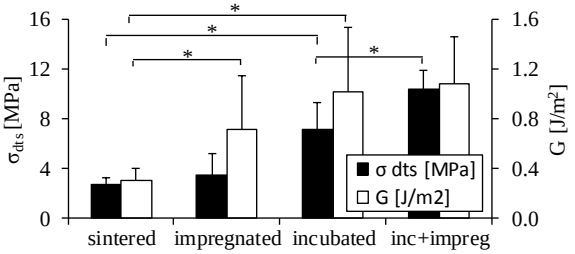

*Fig. 2: Strength σ_{dts} and energy density G as a function of incubation and impregnation (*p<0.05)*

REFERENCES: [1] M. Peroglio et al (2011) *Acta Biomaterialia* **6**(11):4369-4379. [2] M. Bohner et al (2005) *Biomaterials* **26**(31):6099-6105. [3] L Liang et al (2010) *Acta Biomaterialia* **6**(9):3763-3771. [4] Roohani-Esfahani et al. (2010) *Biomaterials* **31**(21): 5498-5509.

Gelatin infiltration of 3D printed hydroxyapatite scaffolds for potential use in regenerative medicine

P. Chavanne[1], S.Stevanovic[1], O.Braissant[2], U.Pieles[1] P.Gruner[3], R.Schumacher[1]

[1]FHNW - School of Life Sciences, Muttenz, CH, [2] LOB2 - Laboratory of Biomechanics & Biocalorimetry, University of Basel, CH, [3]Medicoat AG, Mägenwil, CH

INTRODUCTION: The present study investigates the fabrication of hydroxyapatite (HA) scaffolds with CAD designed macro porosity by means of powder based 3D-printing. Hydroxyapatite (HA) as the major inorganic component of bone, is well accepted to be osteoconductive and, therefore, qualified for scaffolds in regenerative medicine [1]. To reach mechanically stable structures a post processing infiltration method with gelatin was applied. The collagen-based gelatin has a high degree of biological functional groups and is often used in pharmaceuticals due to its good cell viability and lack of antigenicity [2]. 3D-printed HA scaffolds in combination with the developed gelatin infiltration result in bio-active scaffolds with promising mechanical properties.

METHODS: An adapted 3D-printing system (Z-Corp, Z-510) with an acidic binder solution was used to produce HA specimens with open porous macro-scale structures. The sintered specimens were infiltrated with a gelatin solution and dried for 1h @ 30°C. The infiltration process was repeated 4x and 10x. To analyse the mechanical properties and surface structure, measurements of porosimetry (Archimedes), compressive strength (CS) and scanning electron microscopy (SEM) were performed.

RESULTS: The SEM pictures showed HA crystals enclosed by gelatin after infiltration [Fig. 1]. The compressive strength of the 3D printed specimens averaged before infiltration 0.8 MPa (s=0.03).

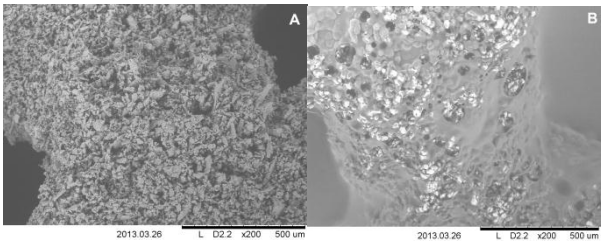

Fig. 1: SEM image of 3D-printed HA before the infiltration (A) and after 10x infiltration process (B), the enclosing gelatin is clearly visible (smooth / dark regions).

After 4x infiltration process the CS increased to 3.7 MPa (s=0.01) and after 10x it ended up at 12.6 MPa (s=0.52) [Fig. 2]. However, the porosity decreased after 4x infiltration from 90 % to 35 % and only marginal to 34 % porosity after 10x.

DISCUSSION & CONCLUSIONS: The combination of gelatin and HA, processed with optimized 3D-printing and infiltration methods, results in customizable scaffolds with promising mechanical properties. Literature claims that higher stability can be attributed to crack bridging provided by the applied gelatin coating, which results in an increased compressive strength [3]. However, the insolubility of the specimens needs to be further improved to ensure mechanical stability in body like environments. Furthermore the primary infiltration approach is only applicable to the outermost layer. Further on, a reduction of this effect would additionally increase the compressive strength.

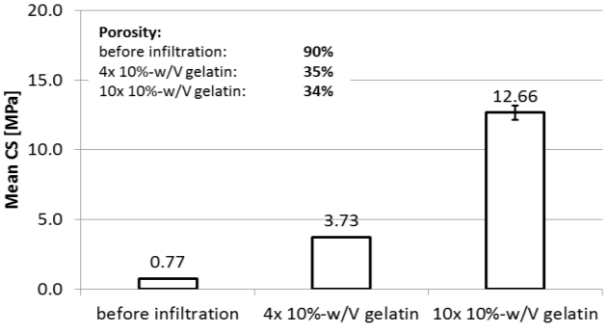

Fig. 2: Compressive strength and porosity values of specimens before and after the infiltration processes.

REFERENCES: 1 F. Fierz, F. Beckmann, et al (2008) *Biomater*, **29**:3799-3806. 2 H. Kim, H. Kim and V. Salih (2005) *Biomater*, **26**:5221-5230.3. M. Dressler, F. Dombrowski, et al. (2011) *J Eur Ceram Soc*, **31**:523-529

ACKNOWLEDGEMENTS: Support by the Swiss-Nanoscience Institute (SNI) and Swiss National Science Foundation (SNSF) is gratefully acknowledged.

Novel fibre-reinforced remineralising dental and orthopaedic composites with improved toughness and fatigue properties

NJ. Walters[1], MA. Khan & AM. Young[1]

[1] *Department of Biomaterials & Tissue Engineering, UCL Eastman Dental Institute, London, UK*

INTRODUCTION: Novel remineralising dental resin-based composites are under development for more conservative tooth restoration. The materials consist of a liquid phase containing monomers and photoinitiators, mixed with a powder phase containing glass particles and fibres and calcium phosphates (CaP) monocalcium phosphate monohydrate (MCPM) and beta-tricalcium phosphate (β-TCP) at 1:1 mass ratio. Interaction effects between CaP and fibres have previously been shown to double toughness, whilst maintaining strength comparable to current market-leading composites (90-180 MPa) [1]. Similar chemically-initiated materials are also being developed for bone repair. The composites have been shown to form brushite in the core of the material upon curing and to precipitate hydroxyapatite on the surface in simulated body fluid, but not artificial saliva. This remineralisation may result in decreased de-bonding at the junction between the material and the tissue, where polymerisation shrinkage usually occurs, without roughening the aesthetic surface of dental restorations. Additionally, use of novel diluent monomer polypropylene glycol (PPGDMA) has recently been shown to improve curing without increasing shrinkage, and use of polymerisable co-initiator *N*(*p*-tolyl)glycine-glycidyl methacrylate (NTG-GMA) has been shown to increase adhesion to dentine [2]. Furthermore, both PPGDMA and NTG-GMA may improve biocompatibility compared to conventional monomers, due to their higher relative molecular masses and their more complete incorporation upon polymerisation.

METHODS: Discs of composite (diameter 10.2mm, height 1mm) were prepared by mixing the liquid phase, containing monomers urethane dimethacrylate (UDMA), PPGDMA and 2-hydroxyethyl methacrylate (HEMA), photoinitiator camphorquinone and co-initiator NTG-GMA with various powder phases containing glass particles, fibres and calcium phosphates. Yield stress and toughness were determined using a biaxial flexural test with a ball-on-ring jig, as previously described [1]. The mean yield stress of each formulation was used to estimate the yield load for each individual specimen, taking into account the exact height of each specimen. Fatigue testing using the same jig was performed by cyclic loading at 1Hz for 1,000 cycles, with a preload of 5N and a peak load of 80% of the estimated yield. The staircase approach was then applied: for each sample, the peak load was either lowered or raised by 5%, depending on whether the previous specimen failed or not.

RESULTS: Basic composites containing glass particles only in the powder phase had a yield stress of $164^{\pm16}$ MPa and toughness of $17^{\pm5}$ MPa. Remineralising composites containing 15 wt% fibres and 30 wt% CaP had a yield stress of $101^{\pm6}$ MPa and toughness of $39^{\pm3}$ MPa. Under fatigue testing, 60% of basic composite specimens failed under cyclic loading at 70, 75 or 80% of the estimated failure load. One hundred per cent of remineralising composite specimens survived loading at 75% of the estimated failure load, with some specimens surviving 80 and 85% of the estimated failure load.

DISCUSSION & CONCLUSIONS: A novel class of remineralising dental and orthopaedic composites that are currently being developed have improved toughness and fatigue properties compared to basic composites, with yield stress comparable to some market-leading materials. This is due to the reinforcement provided by the fibres, which is augmented by the interaction between the CaP and the calcium in the glass fibres. Improved toughness and fatigue capabilities are important for improving longevity of posterior tooth restorations, which must be able to withstand high load, and repair treatments of load-bearing bone tissue.

REFERENCES: [1] N. Walters & A. M. Young (2012) *Low Shrinkage Dental Composites with High Strength and Toughness*, J. Dent. Res. 91(Spec. Iss. C):288. [2] N. J. Walters, M. A. Khan, S. Liaqat & A. M. Young (2013) *Novel Remineralising, Antimicrobial Dental & Orthopaedic Composites*, Proceedings of Tissue Engineering and Regenerative Medicine International Society European Chapter, June 17-20 2013, Istanbul, Turkey.

ACKNOWLEDGEMENTS: The authors are very grateful to Dr. George Georgiou for support with fatigue testing.

Potential role of strontium ranelate for bone tissue engineering approaches

W. Querido[1,2], K. Anselme[2], M. Farina[1]

[1] *Instituto de Ciências Biomédicas, Universidade Federal do Rio de Janeiro, Rio de Janeiro, Brasil.* [2] *Institut de Sciences des Matériaux de Mulhouse (IS2M), CNRS LRC7228, Université de Haute-Alsace, Mulhouse, France.*

INTRODUCTION: Some recent studies[1,2,3] have shown that the anti-osteoporotic drug strontium ranelate could play a promising role on improving the osseointegration of bone implants. In these studies, systemic treatment was shown to enhance the microarchitecture/volume of the surrounding bone tissue and the mechanical fixation of the implants. The better understanding of the effects leading to this improvement may play a key role on establishing future applications of the drug on bone tissue engineering approaches. In this study, we evaluate direct effects of strontium ranelate treatment on the formation of mineralized matrix by osteoblast cells cultured on a biomaterial.

METHODS: Mouse osteoblast cells were cultured for 28 days either directly on 24-well plates or on polished pure titanium substrates. The cultures were done under mineralizing conditions (medium with 10 mM β-glycerophosphate and 50 µg/mL ascorbic acid). Strontium ranelate was added to the medium at 0.5 mM Sr^{2+}. The chemical nature and composition of the intact matrix was evaluated by attenuated total reflection Fourier transform infrared spectroscopy (ATR-FTIR) and energy-dispersive X-ray spectroscopy (EDS).

RESULTS: In all cell cultures, there was the production of a typical mineralized matrix, easily noticed by the naked eye. In the 24-well plates, this matrix was observed as dark nodular deposits by transmission optical microscopy, while on the titanium substrates, the matrix was seen as white deposits under a stereomicroscope. It was clear in both cases that treatment with strontium ranelate promoted a marked increase in the formation of mineralized matrix (*Figure 1*). Further analysis by ATR-FTIR showed that all matrices were similar to that described in bone, with spectra comprising typical bands of PO_4^{3-} and CO_3^{2-} from bone apatite and of Amide I and II from peptide bonds found in collagen. This may indicate that strontium ranelate treatment did not have deleterious effects on the overall bone-like nature of the matrix. However, EDS analysis showed a clear incorporation of Sr into the matrices produced under treatment, which could affect the matrix/biomaterial interface and may call for further studies.

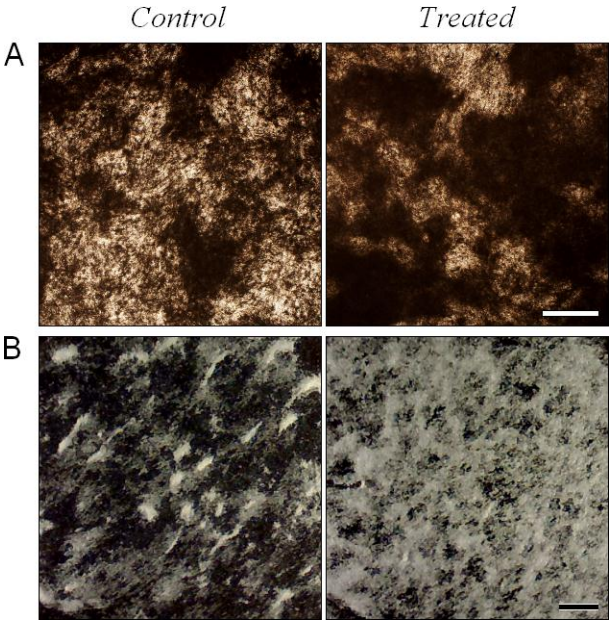

Figure 1: Formation of mineralized matrix by osteoblast cells cultured on (A) 24-well plates and (B) polished pure titanium substrates. The matrix is seen as (A) dark deposits by optical microscopy and (B) white deposits under a stereomicroscope. Scale bars: (A) 0.5 mm and (B) 1 mm.

DISCUSSION & CONCLUSIONS: We show a direct effect of strontium ranelate on promoting the formation of bone-like mineralized matrix by osteoblast cells in culture, both in standard cell culture plates and on titanium substrates. We highlight with these preliminary results a potential role of strontium ranelate for future bone tissue engineering approaches.

REFERENCES: [1] L Maimoun, TC Brennan, I Badoud, *et al* (2010) Bone **46**(5):1436-41. [2] Y Li, G Feng, Y Gao, *et al* (2010) J Orthop Res **28**(5):578-82. [3] Y Li, X Li, G Song, *et al* (2012) Clin Oral Implants Res **23**(9):1038-44.

ACKNOWLEDGEMENTS: This study was supported by FAPERJ and CNPq (Brazil) and by the CAPES/COFECUB program n° 628/09 (Brazil/France cooperation).

PCL-based scaffolds with degradation profiles tuned to various treatment strategies of bone

J. Idaszek[1,2], V. Zell[2], A. Bruinink[2], W. Swieszkowski[1]

[1] *Faculty of Materials Science and Engineering, Warsaw University of Technology, Warsaw, PL.*

[2] *Materials-Biology Interactions Laboratory, EMPA, Swiss Federal Laboratories for Materials Science and Technology, St. Gallen, CH*

INTRODUCTION: Fused deposition modelling (FDM) is one of the rapid prototyping techniques and is based on deposition of molten polymer in the shape of fibres in a layered fashion. FDM allows to fabricate scaffolds with fully interconnected pores and controlled architecture, morphology and porosity, thus enables true engineering of the scaffolds [1]. Poly(ε-caprolactone), PCL, is the most FDM-compatible thermoplastic polyester among the FDA-approved biodegradable polymers. However, this polymer exhibits very long degradation rate and relatively poor bioacceptance.

The aim of this study was to develop a new type of PCL-based scaffolds which degradation can be tuned for different treatment strategies of bone tissue regeneration.

METHODS: Composite scaffolds containing PCL (70 wt%), tricalcium phosphate (TCP; 5 wt%) and poly(lactide-*co*-glycolide) (PLGA; 25 wt%) with various molecular weight and composition (LA50_1, LA50_2, LA75 and LA82) were submitted to degradation in Simulated Body Fluid (SBF) at 37 °C for a period up to 24 weeks. After fixed periods of time changes of mass, water absorption, mechanical properties and surface morphology were determined. Human Bone Marrow Mesenchymal Stromal Cells (HBMCs) were cultured in form of multicellular spheroids on the 3D scaffolds for a period of 7 days [2]. Neat PCL and composite scaffolds (95wt% PCL and 5 wt% of TCP; PCL-TCP) were used as controls in the cell outgrowth experiment.

RESULTS: Addition of various PLGAs resulted in different degradation profiles (Fig. 1). The 5% mass loss (onset of deterioration of mechanical properties [3]) could be tailored to 3-24 weeks. Cell outgrowth area was significantly higher on ternary composite 504H that neat PCL scaffolds.

DISCUSSION & CONCLUSIONS: Our approach allowed to accelerate degradation of PCL-based scaffolds (both at the macroscopic and molecular level) and tune it to fit to particular application (i.e. biodegradable implant or tissue engineering product). Additionally, it improved HBMC outgrowth out of multicellular spheroids. It is assumed that 3D relative to 2D cultures have an improved prognostic value for the *in vivo* response. However, the underlying mechanism of improved cells outgrowth still has to be determined.

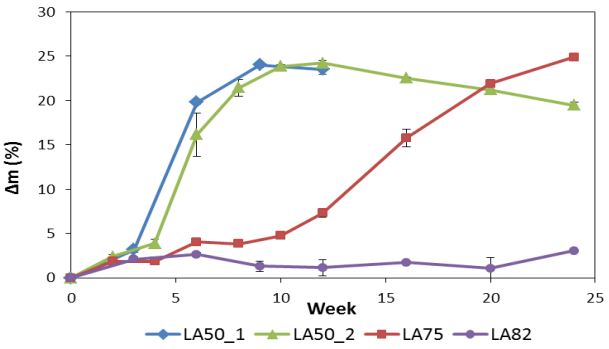

Fig. 1: Mass change of scaffolds made of different ternary composites during degradation in SBF over a period up to 24 weeks.

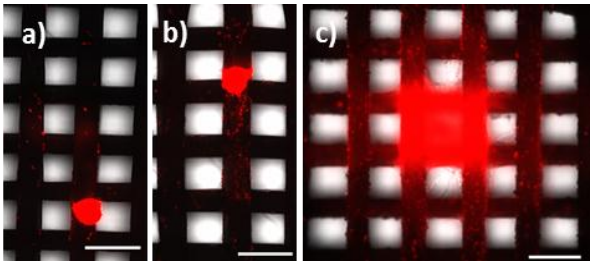

Fig. 2: HMBC outgrowth out of multicellular spheroids kept on: a) PCL; b) PCL-TCP; c)LA50_1. Scale bar 500 µm.

REFERENCES: [1] D. Hutmacher (2000) *Biomaterials* **21**: 2529-43. [2] M. Moczulska et al (2012) *J Biomed Mater Res A* **100**: 882-93. [3] J. Idaszek et al (2012) *Composites Theory and Practice* **12**: 228-31.

ACKNOWLEDGEMENTS: This study was supported by the BIO-IMPLANT project (Grant No. POIG.01.01.02-00-022/09). The stay of Joanna Idaszek at Empa was supported by the European Union in the framework of European Social Fund through the Warsaw University of Technology Development Programme, realized by Center for Advanced Studies.

Two-photon microfabrication of artificial ECM hydrogel via thiol-ene chemistry

X-H. Qin, J. Torgersen, S. Mühleder, W. Holnthoner, A. Ovsianikov, J. Stampfl, H. Redl, R. Liska
TU Vienna, Austrian Cluster for Tissue Regeneration, Austria

INTRODUCTION: Development of 3D hydrogels capable of promoting cell viability and certain cell-ECM interactions is critical for tissue engineering. However, the lack of a general approach to rapidly construct 3D engineered hydrogels remains a major challenge.[1] Two-photon polymerization (TPP) strategy presents the most promise to create ECM-mimetic hydrogels because it enables the true 3D-printing of user-dictated shapes with μm-scale resolution. Our previous work has proved: 1) vinyl esters are much less cytotoxic than acrylates;[2] 2) reactivity-limitation of vinyl esters could be resolved by using thiol-ene chemistry.[3] Herein, we explore the use of thiol-ene chemistry for TPP of hydrogels. Presented is the synthesis of naturally-derived macromers that are thiol-ene photo-clickable and TPP microfabrication of hydrogels with user-defined geometries. [3]

METHODS: Gelatin hydrolysate vinyl ester (GH-VE) was prepared through aminolysis reaction between lysine units of GH and excessive divinyl adipate (DVA). Products were purified by dialysis and lyophilization and further analyzed via ^{1}H-NMR and MALDI-TOF-MS. Cytotoxicities of GH-VE on MG63 cells were measured via MTT assay. Reduced BSA (BSA-SH) were used as model macrothiols to donate varying amount of cysteines for thiol-ene polymerization where cysteine concentration was quantified via Ellman's test. One-photon photoreactivity of GH-VE/BSA-SH formulations were evaluated via in-situ photo-rheometry. A water-soluble two-photon active chromophore (WSPI) was used as photoinitiator.[1] A Ti:sapphire laser system (800 nm) was used for TPP microfabication.

RESULTS: Synthesis and characterization Schematic design and synthesis of thiol-ene photopolymerized hydrogels are shown in Fig. 1. Specifically, ^{1}H-NMR analysis quantitatively showed that 0.57 mmol vinyl groups were present in one gram of GH-VE. Further calculation suggested that 2.7 DVA moieties on average were immobilized in one GH-VE peptide. In addition, MTT assay showed that GH-VE macromer presented negligible cytotoxicity on MG63 cells which suggests that the modification did not increase toxicity. Quantification of concentration of free cysteines showed that around 2-12 cysteines were accessible upon reduction. Photo-rheometry measurements showed that one-photon curing kinetics of such thiol-ene hydrogels were tunable by changing the cysteine concentration.

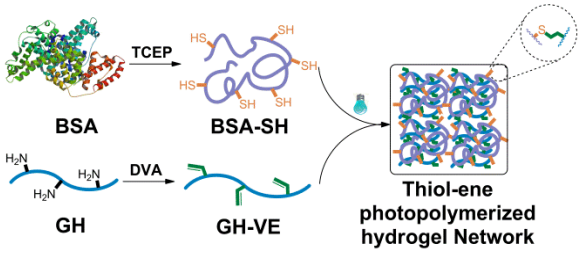

Fig. 1: Hydrogel formation by thiol-ene photopolymerization.

TPP fabrication We firstly designed a 3D CAD model consisting of three layers of packed cylinders with a hexagonal arrangement. By using the TPP technique, well-defined hydrogel network structures were written within the GH-VE/BSA-SH matrix in a high writing speed (50 mm/s). Laser scanning microscope (LSM) images thereof are shown in Fig. 2. The structures' feature sizes were around tens of microns, which is biologically-relevant.

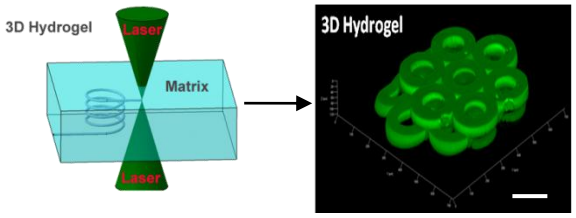

Fig. 2: TPP setup and LSM images of microfabricated 3D hydrogels (scale bar:100 μm)

DISCUSSION & CONCLUSIONS: In all, a new approach to directly assemble 3D biomimetic hydrogels is presented. The fusion of rationally-designed hydrogel precursors, the robust thiol-ene chemistry and TPP technique would enable the creation of customized ECM microenvironment and promote further biologically-relevant studies.

REFERENCES: [1] J. Torgersen, X. Qin, et al (2013) *ADV FUNCT MATER*, in press. [2] C. Heller, R. Liska, et al (2009) *J POLYM SCI POL CHEM* **47**: 6941-54. [3] A. Mautner, X. Qin, et al (2013) *J POLYM SCI POL CHEM* **51**: 203-12.

ACKNOWLEDGEMENTS: XH Qin acknowledges the PhD fellowship sponsored by the China Scholarship Council (CSC) and the Austrian Research Promotion Agency (FFG).

Coated γ-PGA-Phe nanoparticles for siRNA delivery

T. Esteva[1], D. Studer[1,2], M. Shudo[3], T. Akagi[3], M. Akashi[3], K. Maniura-Weber[2], M. Matsusaki[3], M. Zenobi-Wong[1]

[1]Cartilage Engineering and Regeneration, ETH Zürich, CH. [2]Materials-Biology Interactions Laboratory, Swiss Federal Laboratories for Materials Science and Technology, St.Gallen, CH. [3]Department of Applied Chemistry, Graduate School of Engineering, Osaka University, JP

INTRODUCTION: RNA interference (RNAi)-based technologies offer an attractive strategy for the specific silencing of disease-causing genes by inhibiting the synthesis of a target protein. An effective siRNA delivery requires the use of appropriate materials so that the siRNA can be translocated into the cell and escape immediate degradation pathways to exert its silencing function in the cytoplasm. Our work focuses on poly (γ-glutamic acid)-L-phenylalanine ethyl ester (γ-PGA-Phe) nanoparticles (NPs), a core-corona NP formed by self-assembly of the amphiphilic co-polymer. The outer negative charge of the NPs allows for a subsequent coating with positively charged polymers such as polyethyleneimine (PEI) or diethylaminoethyl (DEAE)-dextran. Both polymers exhibit a proton sponge effect at the pH encountered in endosomes, which makes them suitable candidates as siRNA carriers.

METHODS: NPs were produced by mixing 10mg/ml γ-PGA-Phe in DMSO with 100mM NaCl solution. The NPs were coated with either 20kDa DEAE-dextran (TbD Consultancy), 10kDa PEI (Alpha Aesar) or 25kDa PEI (Sigma) and subsequently mixed with 1.2µM siRNA. After each step, the NPs were analyzed for size distribution and zeta potential (ZP) (Malvern Zetasizer nano). In order to assess the siRNA complexation capability, non-bound GAPDH-Cy3 siRNA (Ambion) was quantified in the supernatant. The same NPs were used to assess the uptake into human bone marrow-derived stromal cells (hBMCs) using fluorescent microscopy as well as the gene knockdown efficiency by RT-PCR. Further, acGFP transduced cells were incubated with NPs targeting acGFP and fluorescence monitored upon siRNA delivery.

RESULTS: γ-PGA-Phe NPs were reproducibly produced with a size of 130nm and a ZP value of -40mV. Coating of the NPs with DEAE-dextran or PEI was successful and led to a complete charge reversal.

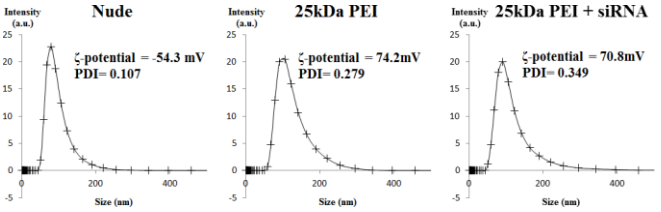

Fig. 1: Size distribution and ZP of nude γ-PGA-Phe NPs, after coating with 25kDa PEI and subsequent adsorption of siRNA

Table 1. Diameter and ZP of γ-PGA-Phe NPs after coating with 10kDa PEI, 25kDa PEI or 20kDa DEAE dextran, and subsequently siRNA

Coating	Diameter (nm)	PDI	ZP (mV)
20kDa DEAE dextran	168.3	0.184	-5.54
10kDa PEI	169.6	0.258	59.6
25kDa PEI	174.9	0.279	74.2

The further adsorption of siRNA showed above 80% efficiency on DEAE-dextran and 25kDa PEI coated NPs, respectively. GAPDH siRNA NPs were added to hBMC cultures and the intracellular localization of the NPs confirmed by confocal fluorescence microscopy. The application of acGFP siRNA NPs showed a decrease of 34% of the acGFP fluorescence, a comparable result to the one obtained with commercial polymers for siRNA delivery.

DISCUSSION & CONCLUSIONS: The reported NPs allowed for effective intracellular delivery of siRNA and silencing of target genes. Experiments are currently performed to investigate the anti-inflammatory potential of these NPs at a cartilage implant interface.

REFERENCES: [1]H Kim (2009) Macromol. Biosci. 9, 842-848. [2]T Xia (2009) ACSNano **3** 10 3273-3286. [3]W Liang, J K W Lam (2012) ISBN: 978-953-51-0662-3, InTech, DOI: 10.5772/46006

ACKNOWLEDGEMENTS: This work was supported by the Swiss National Science Foundation (Grant CR23I2_130678) and the AO Research Foundation.

Can we alter the cell's response to PEEK with nanopatterning and plasma treatment?

D. Morrison[1], N. Gadegaard[1], MJ. Dalby[1], AHC. Poulsson[2]

[1]University of Glasgow, Glasgow, UK, [2] AO Research Institute Davos, Davos, CH.

INTRODUCTION: Poly(aryl-ether-ether-ketone) (PEEK) is a semi crystalline polymer which exhibits properties which make it an attractive choice for use as an implant material, such as natural radiolucency (which it is possible to vary dependant on the amount of barium sulphate added during manufacturing) and MRI compatibility as well as good chemical and sterilization resistance[1]. Recently we have been able to injection mould highly defined Nanotopographies with PEEK and these are currently being assessed for their potential to alter osteogenic behavior of cells.

METHODS: Four different nanopatterned substrates were fabricated in an Engel victory 28 tonne injection moulder;, planar, ordered square (SQ), Hexagonal (Hex) and disordered square (NSQ) topographies were produced in both PEEK and polycarbonate (control material). PEEK processing parameters were set as prescribed by the polymer manufacturer and supplier (Invibio Biomaterials Solutions, UK). Oxygen plasma treatment was carried out using a Gala instruments plasmaprep 5 Asher. Changes to the topography due to the plasma treatment were assessed via AFM (Atomic Force Microscopy) and SEM (Scanning Electron Microscopy). Additionally surface elemental composition changes as a result of plasma treatment were investigated with X-ray photoelectron spectroscopy (XPS). SAOS-2 cells were plated at a seeding density 5600 cell/cm^2 on planar, NSQ, SQ and Hex PEEK and planar, NSQ, SQ and Hex polycarbonate substrates. Untreated and PEEK samples with 2min 200W oxygen plasma treatment were evaluated. Osteogenic behaviour was investigated by Alizarin Red S and Von Kossa staining at 3, 4 and 5 weeks and alkaline phosphatase (ALP) staining at 1, 2 and 3 weeks. Samples were assessed via cross polarised light microscopy and cell profiler computerised analysis software.

RESULTS: Our results indicate that oxygen plasma treatment improves the ability of cells to adhere to PEEK substrates. Oxygen plasma treatment is known to etch the surface of polymers with longer treatment times[2], however this study has identified treatment times long enough to improve cellular adhesion without damaging the nanotopographies introduced. While we have seen increased osteogenic behavior on plasma treated nanotopographies we are currently investigating if these two factors act synergistically or if one factor is responsible for the improvement.

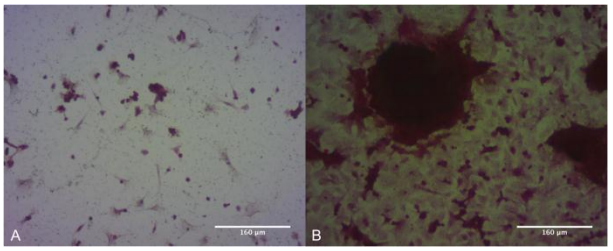

Fig. 1: Cross polarised light images of SAOS-2 cells on PEEK NSQ topographies stained with Von Kossa and nuclear fast red. On the left the NSQ nanopattern without plasma treatment (A) and on the right the NSQ nanopattern with 2min 200W oxygen plasma treatment (B).

DISCUSSION & CONCLUSIONS*:* Our work has addressed an underlying issue with PEEK's use as a biomaterial namely the poor cell adhesion[3]. Additionally our use of histological methods for assaying osteogenic behaviour has allowed us to circumvent PEEK 's auto fluorescence. Due to the improved osteogenic performance on surfaces that are both plasma treated and nanopatterned, and since these topographies have been demonstrated to have osteogenic effects when incorporated into other polymers[4] our current work is directed towards identifying the relative contributions of these two factors to the observed biological response

REFERENCES: [1] S.M. Kurtz, J.N. Devine (2007) *Biomaterials* **29**:4845-4869. [2] K. Tsougeni, N. Vourdas (2009) *Langmuir* **25**(19):11748-11759. [3]T.J. Dennes, J Schwartz (2009) *J Am Chem Soc* **131**:3456-3457 [4]M.J. Dalby, N Gadegaard, *et al* (2007) *Nature Materials* **6**:997-1003

ACKNOWLEDGEMENTS: Invibio Biomaterials Solutions for supplying PEEK.

Rapid discovery of 3D artificial stem cell niches

Matthias P. Lutolf

Laboratory of Stem Cell Bioengineering and Institute of Bioengineering, School of Life Sciences, Ecole Polytechnique Fédérale de Lausanne, CH-1015 Lausanne, Switzerland; Email: matthias.lutolf@epfl.ch

The behavior of cells in tissues is governed by the 3D microenvironment, which involves a dynamic interplay between biochemical and mechanical signals. The complexity of microenvironments and the context-dependent cell responses that arise from these interactions have posed a major challenge to understanding the underlying regulatory mechanisms. To systematically dissect the role of the various factors that determine cell fate in 3D, we have been developing experimental paradigms to simultaneously generate hundreds to thousands of unique microenvironments and probe their effects on cell fate. In this talk I will discuss our approach by way of proof-of-principle experiments in which we have measured the combined effects of microenvironment stiffness, proteolytic degradation, and three classes of signaling proteins on embryonic stem cells (ESC) fate, unveiling a comprehensive map of the interactive involvement of these parameters in regulating ESC self-renewal and neuroepithelial differentiation. Our approach is broadly applicable to gain a systems-level understanding of multifactorial 3D cell-matrix interactions and opens the door for discovering unique microenvironments that control the behavior of difficult-to-culture mammalian cells such as stem cells.

Soft polymeric surface coatings made from olefinic medium-chain-length poly(3-hydroxyalkanoate)

M. Zinn[1,3], S. Lischer[2], S. Dilettoso[3], P. Rupper[4], K. Maniura-Weber[2]

[1] Institute of Life Technologies, HES-SO, Sion, CH [2] Laboratory for Materials-Biology Interactions, Empa, St. Gallen, CH, [3] Laboratory for Biomaterials, Empa, St. Gallen, CH; [4] Laboratory for Advanced Fibers, Empa, St. Gallen, CH

INTRODUCTION: Pseudomonas putida GPo1 is able to intracellularly accumulate medium-chain-length poly (3-hydroxyal- kanoates) (mcl-PHAs) that consist of enantiomerically pure [R]-3-hydroxyfatty acids of between C6 and C14 carbon units. The polymer can be extracted, purified, and used as biodegradable and biocompatible polymer for medical applications[1]. Particular production conditions enable the tailored biosynthesis of functionalized mcl-PHA with terminal double bonds in the side-chains[2]. In this study we assessed the chemo-physical properties of mcl-PHAs produced from different mixtures of octanoic and 10-undecenoic acid and also investigated in vitro the adhesion of normal human dermal fibroblasts (NHDF) to polymer coatings.

METHODS: Poly(3-hydroxyoctanoate-*co*-3-hydroxy-10-undecenoate) was produced in a chemostat culture of *P. putida* GPo1 with tailored functionality (0, 10, 25, 50 and 100 mol% of terminal double bonds in the side-chains). The polymer was extracted, purified, characterized (GC, GPC and DSC), and solvent casted using methylene chloride on Petri dishes yielding coatings of at least 500 µm of thickness. For all cell experiments, the coatings were sterilized by heat at 80°C for 1 h, afterwards the coatings were stored at 4°C for 7 days for polymerization. Before cell seeding the coatings were incubated with 1 mL of cell culture media for 5.5 h (37°C, 95% air, 5% CO_2), the supernatant was then used for the cytotoxicity assay. NHDF (11.4 cells mm^{-2}) were applied onto the coatings) and incubated for 5 days (37°C, 95% air, 5% CO_2). On day 5 NHDF were stained for actin, vinculin and nucleus. The cytotoxicity assay was performed according to ISO-norm 10993-5: biological evaluation of medical devices, using the 3T3 mouse fibroblast cell line (ECACC No 85022108).

RESULTS: The molecular weight (Mw) of all PHAs were in the same range of 210 – 260 kDa but the melting properties differed significantly (Table 1). All polymers were hydrophobic and had a water contact angle above 85°. Interestingly, there were significant differences in the coverage of the cells on the coatings (Table 1). Best performing coatings were PHOUE (75/25; Fig. 1) and PHOUE (50/50).

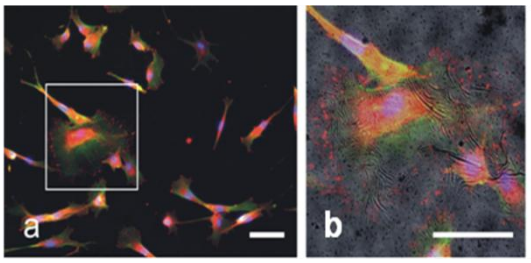

Fig. 1: NHDF stained for actin (green), vinculin (red), and nucleus (DAPI, blue) on PHOUE (75/25). a) fluorescence picture, b) overlay of fluorescene and light micrographs. Scale bar = 100 µm.

Table 1. Melting(Tm)glass transition (Tg) and adhesion of normal human dermal fibroblasts on the coatings after 5 days of incubation.

Polymer	Tm[2] [°C]	Tg[2] [°C]	NHDF P10 [cells mm^{-2}]
PHO (100)	58.1	-33.1	8.26 ± 3.19
PHOUE (90/10)	50.8	-35.9	9.24 ± 1.00
PHOUE (75/25)	44.5	-39.5	51.95 ± 5.41
PHOUE (50/50)	39.9	-44.6	42.58 ± 8.22
PHUE (100)	-	-49.3	12.29 ± 3.54

DISCUSSION & CONCLUSIONS: Despite the fact that all polymers were biocompatible, there were differences in the adherence to the coatings by NHDF. Light micrographs revealed that ruffle-like structures were formed surrounding the cells indicating that cells could exert forces to the substrates. Further studies are under evaluation in order to assess the reason for this particular effect.

REFERENCES: [1] Rai, R., *et al.* (2011) Medium chain length polyhydroxyalkanoates, promising new biomedical materials for the future. *Mat.s Sci. Eng.***72**, 29-47. [2]Hartmann, R. *et al.* (2006) Tailor-made olefinic medium-chain-length poly[(*R*)-3-hydroxyalkanoates] by *Pseudomonas putida* GPo1: Batch versus chemostat production. *Biotechnol. Bioeng.* **93**: 737-746.

ACKNOWLEDGEMENTS: The financial support by Empa and HES-SO Valais is greatly acknowledged.

Engineering Biomaterials for MSC Immobilization/Transplantation

R. Mahou[1], R. Meier[2], C. Gonelle-Gispert[2], L. Bühler[2], C. Wandrey[1]

[1]LMRP, EPFL, Lausanne, CH. [2]University of Geneva, CH.

INTRODUCTION: Cell microencapsulation for subsequent application in transplantation therapy is being widely investigated. However, the lack of optimal material is frequently identified as major drawback for promising therapy development. In this study, hybrid hydrogel microspheres (alg-PEG-M) free of polycations and producible in one step technology in biological environment have been developed and applied to immobilize human multipotent mesenchymal cells (MSC) for further application to treat liver fibrosis.

METHODS: Human MSC were immobilized in engineered microspheres by combining ionotropic gelation of sodium alginate (Na-alg) and covalent cross-linking of poly(ethylene glycol) (PEG) derivatives in one-step technology under physiological conditions. The hypothesis is that encapsulated MSC can deliver anti-inflammatory cytokines and reduce liver fibrosis. We tested then the *in vitro* viability, proliferation and differentiation capacity of human MSC after microencapsulation, as well as their anti-inflammatory effect *in vivo*.

RESULTS:

1. Encapsulation of MSC in alg-PEG-M

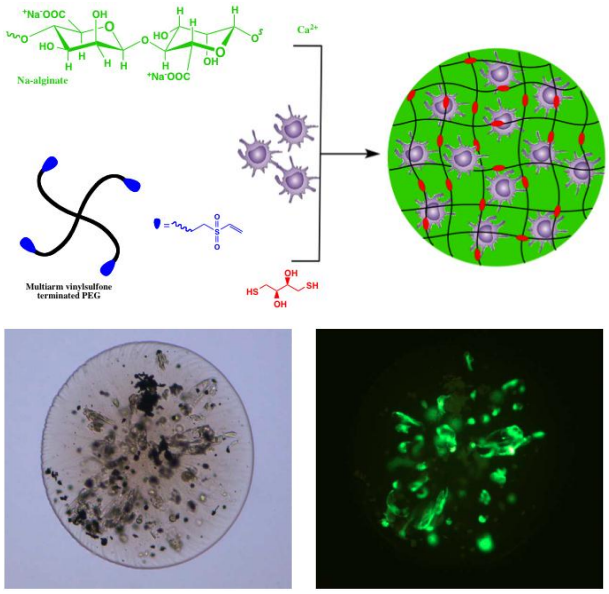

Fig.1: Formation of alg-PEG-M by combining electrostatic and covalent cross-linking (top). The viability of MSC was confirmed 7 months post-encapsulation (bottom).

2. Proliferation and differentiation

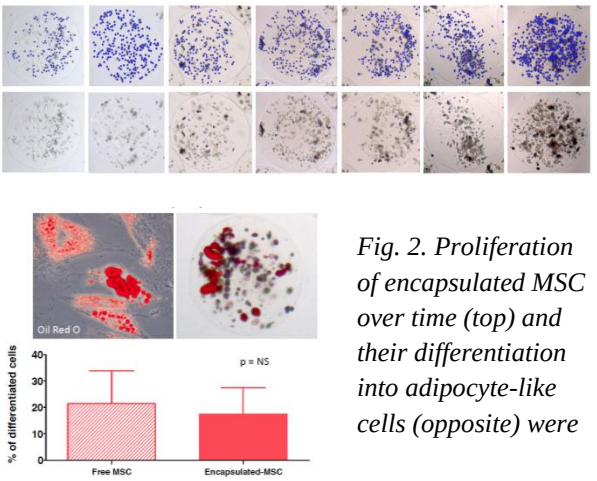

Fig. 2. Proliferation of encapsulated MSC over time (top) and their differentiation into adipocyte-like cells (opposite) were

3. Anti-fibrotic effects of encapsulated MSC

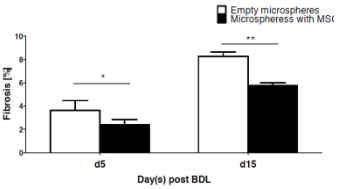

Fig. 3. Anti-fibrotic effects were proven by delayed collagen deposition (opposite)

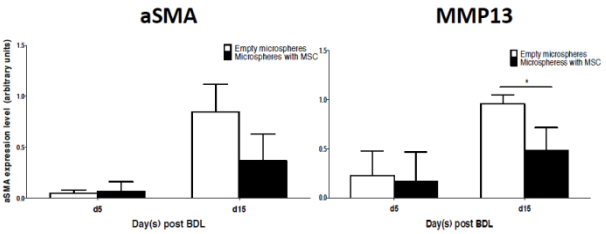

DISCUSSION & CONCLUSIONS: Human MSC maintained viability, proliferation and differentiation capacity into adipocytes after encapsulation in alg-PEG-M. Moreover, encapsulated MSC show long term viability *in vitro* and after xenotransplantation in mice. Local and distant fibrotic reactions were modulated, potentially through cytokine secretion.

REFERENCES: [1]R. Mahou (2010) Alginate-poly(ethylene glycol) hybrid microspheres with adjustable physical properties *Macromolecules*, 43, 1371–1378. [2] R. Mahou (2013) Combined electrostatic and covalent polymer networks for cell microencapsulation.

ACKNOWLEDGEMENTS: The Swiss National Science Foundation supported this research (Grants 205321-116397/1, 205320_130572/1, 205321_141286/1).

Hybrid polylactide foams for osteochondral tissue engineering

M. Cuénoud[1], P-E. Bourban[1] , CJG. Plummer[1] and J-AE. Månson[1]

[1] *Laboratoire de Technologie des Composites et Polymères (LTC), Ecole Polytechnique Fédérale de Lausanne (EPFL), Lausanne, CH.*

INTRODUCTION: Damaged articular cartilage has limited regeneration capacity, which may lead to severe pain and disability. Cartilage repair is therefore considered to be a major dilemma in the field of orthopedic medicine[1]. Our institute is currently developing new solvent-free processing routes for the next generation of bioresorbable synthetic polylactide (PLA)-based bone and cartilage replacement materials[2]. The present study focused on scaffolds with reduced elastic moduli produced by supercritical carbon dioxide ($C0_2$) foaming of polylactides (PLA) plasticized by poly(ethylene glycol) (PEG). The effects of the processing parameters and sterilization methods on the scaffold performance were investigated.

METHODS: Homogenous blends of Poly-L-lactide (PLLA) and Poly-DL-lactide (PLDLA) with 20wt% PEG were obtained by melt-extrusion. The extruded raw polymers and blends were foamed under different conditions using a high-pressure, high-temperature autoclave, and selected foams were sterilized by γ or X-ray irradiation, or treatment with ethylene oxide. The resulting morphologies were observed by scanning electron microscopy and micro-computed tomography, and the thermal response was investigated by differential scanning calorimetry. The mechanical properties were measured in compression at 37 °C.

RESULTS: Interconnected, open-pore foams with porosities of more than 75 %, cell diameters in the range 200 to 700 µm and compression moduli of a few MPa were obtained. It was also observed that addition of PEG resulted in foams with increased pore diameters and lower foam densities than the neat polylactide, but also increased pore coalescence at high saturation pressures, effects that were accounted for by the large decrease in melt viscosity on addition of PEG. Furthermore, the compression moduli of the foams were shown to be strongly reduced on addition of PEG, which was assumed to be a direct consequence of the plasticization of the polylactide by PEG and the accompanying decrease in glass transition temperature[3], implying the amorphous content to be in the rubbery state at *in vivo* temperature, as required. Thus, foams with moduli ranging from 0.3 to 15 MPa could be prepared from the different PLA/PEG blends studied. Moreover, bilayered scaffolds were produced by assembling the plasticized foams with a biocomposite foam using an adapted fusion bonding method (Fig. 1 c). This allowed control of interfacial properties such as the bonding strength, and the interface density and permeability. These hybrid scaffolds exhibited well-defined layers with suitable properties for the repair of bone and cartilage, respectively. Finally, X-ray and γ irradiation was shown to strongly degrade the polymer matrix. However, it was found that treatment with ethylene oxide gas could be used to sterilize the scaffolds without significantly modifying their properties.

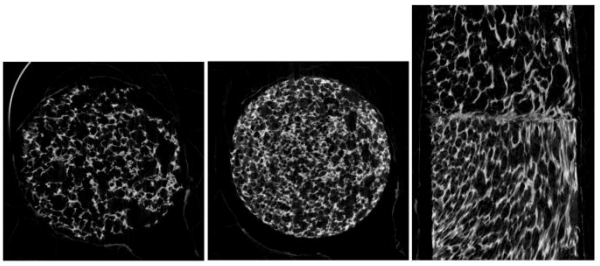

Fig. 1: Cross-sectional micro-computed tomography images of (a) PLLA-PEG, (b) PLLA-βTCP and (c) bilayered PLLA- βTCP (bottom) and PLLA-PEG (top) foams.

DISCUSSION & CONCLUSIONS: Foams produced from PLLA have already been shown to be suitable for bone repair[4], and the present work demonstrates that similar morphologies may be obtained with PLLA-PEG and PLDLA-PEG blends with significantly reduced moduli. The combination of these foams into a bilayered scaffold opens up exciting new possibilities for applications such as cartilage repair.

REFERENCES: [1] T.A.E Ahmed, M. T Hincke (2010) *Tissue Engineering – Part B: reviews*, **16**:305. [2] M Cuénoud, P.-E Bourban, *et al* (2012) *Journal of cellular plastics*, **48**:5. [3] M Cuénoud, P.-E Bourban, C.J.G Plummer, *et al* (2011) *Journal of Applied Polymer Science*, **121**:4. [4] U van der Pol, L Mathieu, *et al (2010) Acta Biomateriala*, **6**:3755.

ACKNOWLEDGEMENTS: The authors thank Prof. D. P. Pioletti for valuable discussions, the EPFL-CIME for the SEM images and the Swiss National Science Foundation (grant 205320-132809) for funding this research.

Cartilage mimetic hydrogels promote a proliferative, chondrogenic phenotype

M. Zenobi-Wong[1], R. Mhanna[1], G Palazzolo[1], J Becher[2], M Schnabelrauch[2]

[1] Cartilage Engineering + Regeneration, ETH Zürich, CH. [2] Innovent Technologieentwicklung Jena, Germany

INTRODUCTION: The cartilage extracellular matrix (ECM) is characterized by a network of collagen 2 fibrils interspaced with highly sulfated proteoglycans. These two features of cartilage inspired the development of two biomimetic hydrogels. As sulfation is thought to influence the bioactivity of polymers[1], we synthesized a sulfated version of alginate to mimic the high fixed negative charge density of the glycosaminoglycans. Secondly, the collagen mimetic peptide GFOGER was used to crosslink PEG hydrogels using Michael addition chemistry. We hypothesized these materials would promote expression of cartilage specific genes compared to unmodified polymers. To test this, chondrocytes and stem cells were encapsulated in the hydrogels and the phenotype of the cells explored.

METHODS: Alginate tetrabutyl ammonium salt was suspended in DMF to which a 5-fold excess of SO_3/pyridine per disaccharide repeating unit was added. The solution was precipitated in acetone, brought to pH=12 and then neutralized. The precipitate was filtered, dissolved in water and purified by dialysis. Bovine chondrocytes (P3-4) were encapsulated in 2% sulfated and 2% unmodified alginate by immersion in 100 mM $CaCl_2$. Human mesenchymal stem cells were encapsulated in degradable or non-degradable PEG gels modified with 100 µM RGD, 100 µM GFOGER or no adhesion peptide (QGel, Lausanne, Switzerland). Samples were evaluated for cell proliferation (BrdU assay, Millipore) and RhoA activity. The expression of chondrogenic markers was measured using RT-qPCR and immunostaining for collagen 2. Samples were stained with DAPI and phalloidin and imaged using confocal microscopy.

RESULTS: Cell proliferation was enhanced in both sulfate- (5-fold) and GFOGER- (2-fold) modified gels compared to non-modified controls. Interestingly, in both cartilage mimetic systems, collagen 2 expression was maintained in spite of the increased proliferative activity (Fig 1). The cells were more spread in the modified hydrogels and they showed a higher RhoA activity level, suggesting this pathway might play a role in inducing the higher proliferation rates[2].

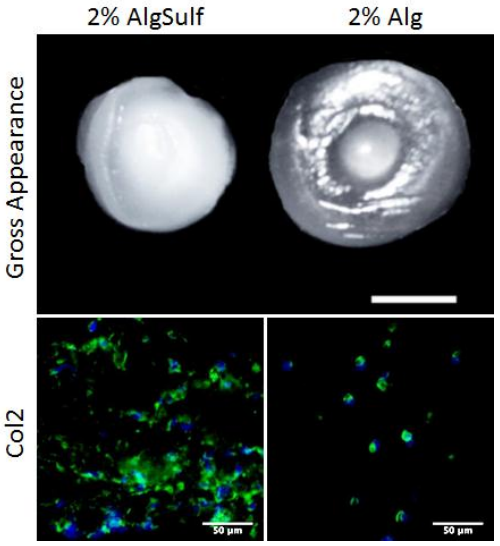

Fig. 1: Chondrocytes embedded in sulfated alginate had a white opaque appearance after 35 days culture. The sulfated alginate induced high proliferation, yet the cells continued to express collagen 2 (green = collagen 2, blue = nuclei).

DISCUSSION & CONCLUSIONS: We used the highly sulfated nature of aggrecan and the high abundance of collagen as inspiration to engineer better mimics of the cartilage ECM. Both systems resulted in a higher number of collagen 2 positive chondrocytes. These results suggest that the modified polymers could stimulate cell proliferation **without** the precipitous loss of collagen 2 expression which normally accompanies expansion in monolayer culture. The use of growth promoting cartilage mimetic hydrogels could have great relevance for improving the outcome of cell-based treatments like autologous chondrocyte implantation (ACI).

REFERENCES: [1] M.R. Mariappan, E.A. Alas, J.G. Williams, et al (1999) *Wound Repair Reg.* **7**:400-6. [2] G.Wang, A.Woods, S. Sabari, et al. (2004) *J Biol Chem.* **279**:13205-14.

ACKNOWLEDGEMENTS: The work was funded by the European Union Seventh Framework Programme (FP7/2007-2013) under grant agreement n° NMP4-SL-2009-229292 (Find&Bind).

Comparing physical properties of PEKK and PEEK

P. Urwyler[1], X. Zhao[1], A. Pascual[2], U. Pieles[3], H. Schift[4], B. Müller[1]

[1] Biomaterials Science Center, University of Basel, CH. [2] Institute of Polymer Engineering, University of Applied Sciences and Arts Northwestern Switzerland, Windisch, CH. [3] Institute for Chemistry and Bioanalytics, University of Applied Sciences and Arts Northwestern Switzerland, Muttenz, CH. [4] Laboratory for Micro- and Nanotechnology, Paul Scherrer Institut, Villigen, CH

INTRODUCTION: High-performance thermo-plastics including polyetheretherketone (PEEK) and polyetherketoneketone (PEKK) are key biomaterials for load-bearing implants. Plasma treatment is a common process to chemically activate polymer surfaces, which is a prerequisite to achieve proper cell attachment. Oxygen plasma treatment of PEEK films results in well reproducible nanostructures [1]. Our goal is the development of nanostructures on surfaces of implants that induce alterations in cell shape and cell differentiation to reach osteointegration of load-bearing polymer implants.

METHODS: Commercially available 100 µm-thick amorphous PEEK (APTIV™ 2000 series, Victrex Europa GmbH, Hofheim, Germany) and 60 µm-thick PEKK (OXPEKK Permetta™, Oxford Performance Materials, South Windsor, USA) were flattened by hot embossing with HEX3 (JENOPTIK AG, Jena, Germany) slightly above their glass transition temperatures. Subsequently, the flattened and virgin films were activated using oxygen plasma treatment (RIE System Plasmalab 80 Plus, Oxford Instruments, Wiesbaden, Germany) with powers from 25 to 100 W for PEEK and from 25 to 150 W for PEKK. Contact angles were measured in triplicate 5 s after adding a 4 µL water droplet to the film at room temperature. Surface roughness and island densities of the surfaces were measured using electron microscopy and in-depth using atomic force microscopy (Dimension 3100 instrument, Veeco, Mannheim, Germany) in tapping mode.

RESULTS: The water contact angle for PEEK decreases from 75 to 37 degrees, while for PEKK from 84 to 7 degrees with the increasing oxygen plasma power. Nanostructures tunable with the plasma intensity are seen for both PEEK and PEKK (cp. Fig. 1). The effect of the nanostructures is more pronounced for flattened films. The induced nanostructures give rise to an increased roughness and decreased island density.

DISCUSSION & CONCLUSIONS: Oxygen plasma treatment is a promising method to build nanostructures and simultaneously activates PEEK/PEKK surfaces for cell seeding. Roughness increased, while island density and contact angle decreased with increasing oxygen plasma power.

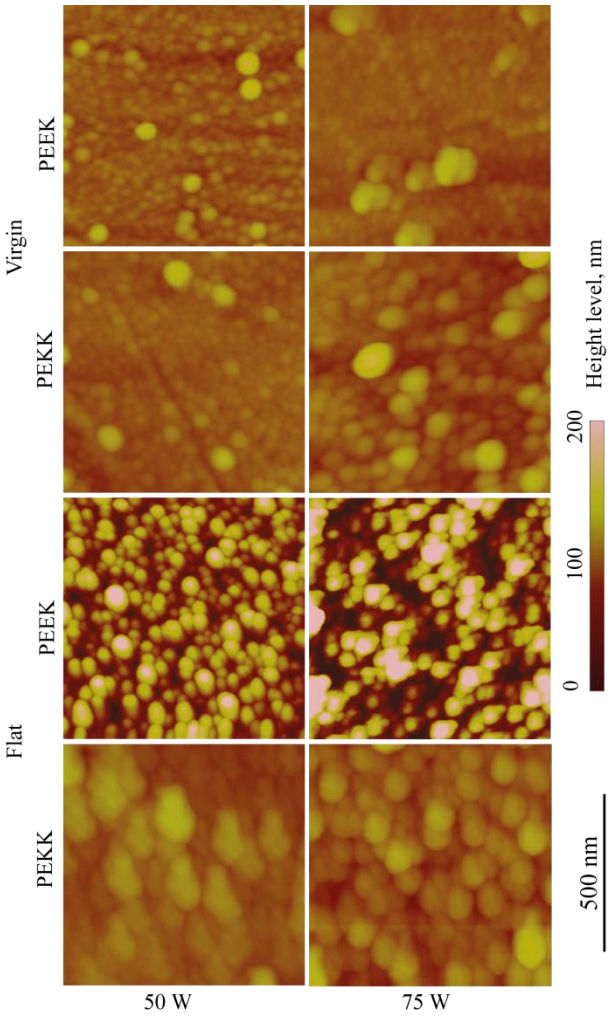

Fig. 1: AFM images of plasma-treated films.

REFERENCE: [1] J. Althaus, C. Padeste, J. Köser, U. Pieles, K. Peters, B. Müller, (2012) *Eur. J. Nanomed.* **4**(1):7-15.

ACKNOWLEDGEMENTS: The authors thank the Swiss Nanoscience Institute and the Swiss Academy of Engineering Sciences for providing financial support. Technical assistance from C. Spreu, S. Stutz, R. Schelldorfer and K. Vogelsang is greatfully acknowledged.

X-ray microtomography of bone and other mineralized tissues

Michel Dalstra[1]

[1] *Section of Orthodontics, Department of Dentistry, Aarhus University, Denmark*

INTRODUCTION: ”Seeing is believing” and “A picture is worth a 1000 words”. These adages show that most people’s mind set is largely pictorial-based. During the last twenty years or so new methods have become available for the three-dimensional (3D) visualization of biological tissues. One of these methods is X-ray micro-computer tomography (microCT), which - being a radiographic technique - is quite well suited for bone and other mineralized tissues. The term *micro* is used to indicate that the method’s resolution is in the micrometer range, although the last few years also *nano*CT has been moving fast forward. The advantage over classical histology and histo-morphometry is that a 3D data-set is produced, which can be used for the quantification of geometrical, anatomical and architectural features, which might be biased when using 2D or semi-3D measurements. In this presentation different aspects of microCT of various mineralized tissues will be reviewed and illustrated with examples.

METHODS: MicroCT can be divided into the table-top variety and synchrotron-based, depending on the X-ray source. A table-top system has its own (conventional) X-ray tube, whereas a synchrotron-based machine is the end station at a beamline of a synchrotron ring. Due to the high brilliance of a synchrotron beam, its mono-chromatic character and the “infinitely” long distance between source and sample (parallel beam), synchrotron-based microCT has less reconstruction artefacts and is considerably less plagued by beam hardening. So, even though resolution for both table-top and synchrotron-based systems lies in the same range (700 nanometer to 40 micrometer, depending on the sample size), synchrotron-based microCT generally produces better quality images. However, limited access to beam time at synchrotron facilities and the availability of tomographic equipment at these locations is a disadvantage.

As a typical scanning session usually takes several hours with the sample inside a warm machine, biological degradation will be an issue. Therefore, biological samples are typically embedded in methylmetacrylate or resin prior to scanning.

Once the samples are scanned, the stack of single-slice reconstructed images makes up the 3D data-set, which can then be read into dedicated image analysis software for visualization and quantification purposes.

RESULTS: MicroCT scans of biological tissues do not only provide a geometrical form of the sample, but also information about the degree of mineralization (Fig. 1). It can therefore also be used to study remodelling processes in bone.

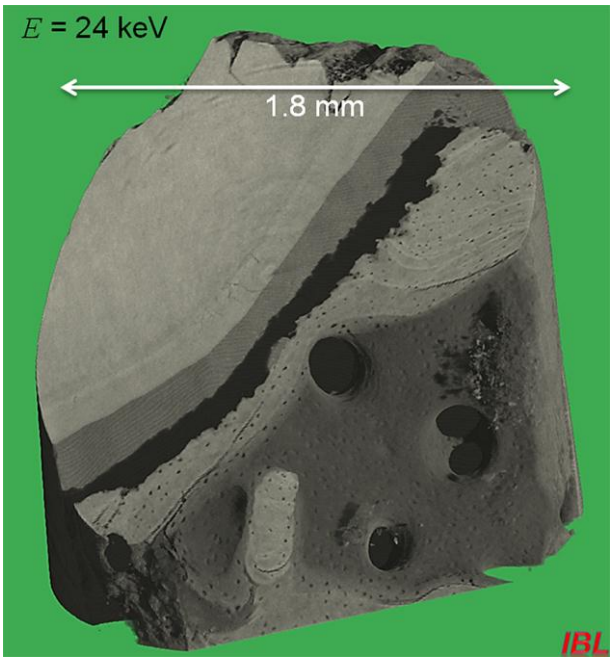

Fig. 1: A 3D-reconstruction of a cylindrical core drill sample from a human molar. Note the seemingly solid and less mineralized root at the back, the gap of the periodontal ligament and the alveolar bone at the front with its lamellar bone organisation and myriad of osteocyte lacunae (scanned at P05 (IBL), PETRA III, DESY).

DISCUSSION & CONCLUSIONS: Coming back to the opening adages from the introduction, microCT has provided new ways to look at and quantify biological tissues and it has become an important tool in bone research.

ACKNOWLEDGEMENTS: Dr.Felix Beckmann and his colleagues from the Helmholtz-Zentrum Geesthacht are kindly thanked for their support using the synchrotron microCT at HasyLab/DESY, Hamburg, Germany.

Porous titanium by powder injection moulding of titanium hydride and PMMA space holders

E. Carreño-Morelli[1], A. Amherd[1,2], M. Rodriguez-Arbaizar[1], D. Zufferey[1], A. Várez[2], J-E. Bidaux[1]

[1] *University of Applied Sciences Western Switzerland, 1950 Sion, Switzerland.*
[2] *University Carlos III of Madrid, 28911 Leganés, Spain*

INTRODUCTION: Porous titanium is used as implant material because of its high specific strength, bone-like stiffness, biocompatibility and good bone cell ingrowth provided that the open pores have sizes between 100 µm and 500µm. Powder metallurgy has been successfully used to produce titanium foams by using the space holder method [1-3]. Recently, Ti grade 4 has been obtained by powder injection moulding (PIM) of titanium hydride, which is cheaper and less reactive than pure titanium [4]. The feasibility of a novel route combining TiH_2 and space holders to produce porous titanium is explored in this work.

METHODS: The starting powder (Fig. 1) was angular TiH_2 (AG Materials Inc., Taiwan, median particle size Dv50 = 20.26 µm). PMMA particles (polymethylmethacrylate) were used as space holders (Goodfellow, UK, Dv50 ~ 600 µm).

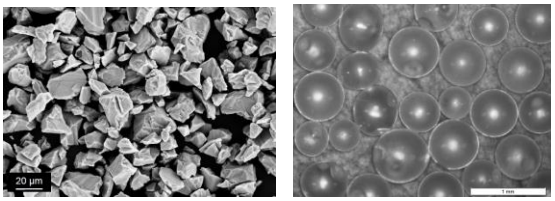

Fig. 1: TiH_2 powder and PMMA space holders.

Feedstocks for PIM were prepared with a binder composed of low density polyethylene, paraffin wax and stearic acid. The solids loading was 60 vol.%, which includes equal parts of TiH_2 (30 vol.%) and PMMA (30 vol.%). Compression test specimens (9 mm diameter × 9 mm height) were injection moulded in an Arburg 221K 350-100 machine. Green parts were solvent debinded in acetone at 35°C for 40h, then thermal debinded and dehydrided at 450°C for 2h under argon, and finally sintered at 1000°C for 4h under argon in a Nabertherm VHT08-16MO MIM furnace (Fig. 2). The density was measured by the Archimedes method and gas pycnometry. Compression tests were performed using a Zwick 1475 machine.

RESULTS: Fig. 3 shows the cross section and the interconnected porosity of a sintered part. The porosity is 50 vol.% (27 vol.% open and 23 vol.% closed). The pore size is between 100 and 500 µm. Compressive strength values determined at 0.2% and 50% strain are 146 MPa and 610 MPa respectively. The Young' modulus is about 12 GPa (Fig. 4).

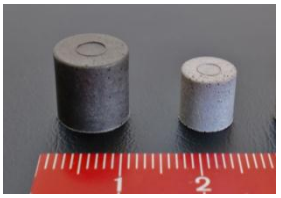

Fig. 2: Green and sintered porous titanium parts.

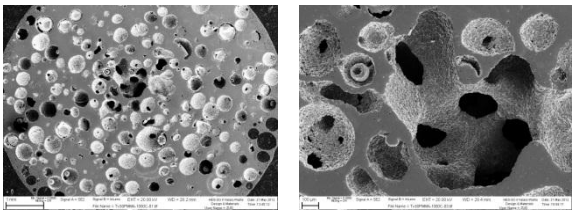

Fig. 3: Microstructure of sintered PIM titanium. Scale bars are 1mm (left) and 100 µm (right).

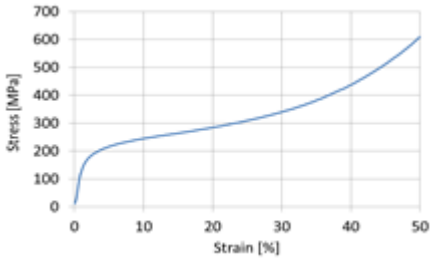

Fig. 4: Compression behaviour.

DISCUSSION & CONCLUSIONS: Open porosity and interconnection diameters could be optimized by varying the space holder volume fraction and sintering conditions. Porous titanium parts have been processed by a novel route from low cost TiH_2 base powder.

REFERENCES: [1] T. Imwinkelried (2007), *J. Biomed. Mater. Res. A*, **81** (4): 964-970. [2] A. Bansiddhi, D. C. Dunand (2008), *Acta Biomater.*, **4**:1996-2007. [3] M. Köhl, T. Habijan, M. Bram, H.-P. Buchkremer, D. Stöver and M. Köller (2009), *Adv. Eng. Mater.*, **11** (12): 959-968. [4] E. Carreño-Morelli, J.-E. Bidaux, M. Rodriguez-Arbaizar, H. Girard and H. Hamdan, Proc. of EuroPM2011, Barcelona, Spain, October 9-12, 2011, **2**:105-110.

ACKNOWLEDGEMENTS: This project was funded by HES-SO under a MaCHoP 06-11 grant and the Erasmus Programme. The technical support of H. Girard is gratefully acknowledged.

Chemical functionalization of bioceramics for the development of bone implants

F. Borcard[1], F. Krauss-Juillerat[2], UT. Gonzenbach[2], L. Juillerat-Jeanneret[3] and S. Gerber-Lemaire[1]

[1]*ISIC, BCH, EPFL, CH-1015 Lausanne, Switzerland,* [2]*Department of Materials, ETHZ, Zürich, Switzerland,* [3]*University Institute of Pathology, CHUV, Lausanne, Switzerland*

INTRODUCTION: Nowadays large bone defects are staggering due to the ageing of the population and the democratization of high-risk sports. [1] Furthermore the present treatments, mainly bone grafts, show several limitations that require the development of new treatments. Tissue engineering is an emerging technique, which represents a promising approach for the treatment of large bone defects. We propose the development of new bone implants based on the chemical functionalization of biomaterials. The functionalized biomaterials are seeded before implantation with histocompatible human bone-derived cells and vascular cell precursors, which together are expected to promote bone reconstruction.

METHODS: Alumina, hydroxyapatite and ß-tricalcium phosphate ceramic foams were prepared according to a new foaming method based on the hydrophobization of the particles allowing the stabilization of the water-air interface and the formation of stable pores. The porous ceramics were then functionalized with a specific chemical ligand designed and synthesized to covalently bind human fetal osteoblasts (FsOs) and promote adhesion of endothelial cells (HUVEC) on the biomaterials leading to a complete colonization of the implant especially in the inner area. Here, the chemical ligand containing the active functionalities and preliminary results of the cell adhesion on the three different porous biomaterials previously functionalized are presented.

RESULTS: The development of the chemical ligand was based on the insertion of specific binding moieties increasing cell interactions with the biomaterials. Pyrrogallol was identified as a highly efficient unit for the functionalization of the materials. [2] The binding occurs by ligand exchange reaction of the hydroxyl or phosphate groups of the materials. For the FsOs binding, a cyclic cyclooctyne was inserted allowing a covalent attachment by click reaction after modification of the cell surface with a non-natural azido amino acid. The azide moiety inserted on the cell surface during the protein synthesis can react selectively with the activated cyclooctyne by a [3+2] cycloaddition without any cytotoxicity. [3-4] Finally, a cyclic peptide containing the Arg-Gly-Asp (RGD) sequence was incorporated in the ligand resulting in a peptide-protein (integrin) interaction of the endothelial cells. [5]

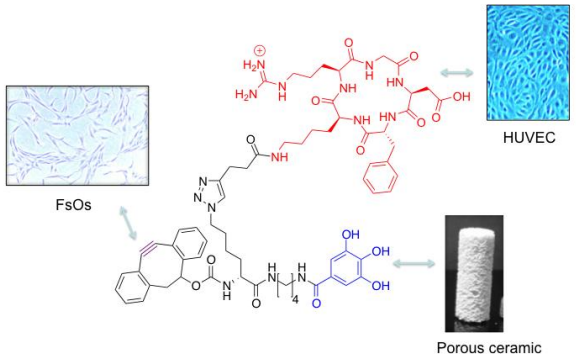

Fig. 1: Chemical ligand designed and synthesized for the enhancement of human fetal osteoblasts endothelial cells adhesion on the biomaterials.

DISCUSSION & CONCLUSIONS: In this approach a chemical ligand containing three defined chemical moieties was synthesized and conjugated to porous ceramics allowing a better colonization of the implant. We showed that after functionalization of the materials the number of both FsOs and HUVEC bound to the materials was increased compared to the non-functionalized materials suggesting potential in the development of bone implants.

REFERENCES: [1] Bohner, M. (2010) *Mater Today* **13**, 24-30. [2] Comas, H. et al. (2012) *Appl. Mater. Interface* **4**, 573-576. [3] Borcard, F. et al. (2011) *Bioconjugate Chem.* **22**, 1422-1432. [4] Krauss Juillerat, F.; Borcard, F. et al. (2012) *Bioconjugate Chem.* **23**, 2278-2290, [5] Borcard, F. et al. (2012) *J. Med. Chem.* **55** (18), 7988–7997.

ACKNOWLEDGEMENTS: We thank the Swiss National Science Foundation (Grant Nos. CR23I3-124753 and CR22I2-140866) for financial support, Dr. L. Menin, J. Artacho, M. Rey, Dr. P. Mievílle, F. Sepulveda and C. Chapuis Bernasconi for excellent technical support.

From implantation to degradation – Are PLLA/MWCNT composite materials really cytocompatible?

M. Obarzanek-Fojt[1], Y. Elbs-Glatz[1], E. Lizundia[2], JR. Sarasua[2], A. Bruinink[1]

[1] Materials-Biology Interactions, Empa, St. Gallen, CH [2] Department of Mining-Metallurgy and Materials Science, University of the Basque Country (EHU-UPV), 48013 Bilbao, E

INTRODUCTION: Biodegradable materials are of interest in orthopaedic application especially in order to avoid a risk of a second surgery. Some of biodegradable materials, like poly-(L-lactic acid, PLLA) show poor mechanical properties. In order to improve mechanical properties [1], the composite of PLLA and multiwall carbon nanotubes at different concentrations (0.1, 0.5 or 1% w/w) was prepared. Although PLLA is a biodegradable material [2] with its turnover of about two to three years in the human body, the MWCNT are yet considered as non-biodegradable molecules. To assure its bioacceptance we evaluated in deep the cell-material interactions, with a special interest in bone tissue regeneration. The effect of MWCNT representing the remnant of the degraded composite inside the body functionalized or not with LA was further used to evaluate the possible cell response when complete degradation of PLLA will take place.

METHODS: The MWCNT were synthesized by Arkema in Catalytic Chemical Vapor Deposition (CCVD) process. PLLA from Purac Biochem (NL) was used as matrix to prepare nanocomposites. The human bone marrow stromal cells (HBMC) cultured in monolayer or three dimensional HBMC cell spheroids were cultured on the composites. Cells potential to differentiate towards osteogenesis was evaluated by qRT-PCR and FACS analysis. MWCNT were suspended either in Pluronic-F127 or functionalized by LA via incubation under the conditions for accelerated *in vitro* degradation (80°C, for 28 days). Effect on cell activity and toxicity was evaluated by microscopic analysis and MTS assay.

RESULTS: The composites were found to be non-toxic as assessed by the ISO10993-5 tests. We observed that HBMC are able to attach and spread on the composite surface and keep their capacity to differentiate toward osteogenesis. HBMC ability to colonize the surface was further verified by use of 3D cell spheroids. We observed significant cell outgrowth and migration on the composite surface. Next, we treated HBMC with MWCNT solution to simulate situation occurring after complete degradation of PLLA. Even though, MWCNT were found in cell cytoplasm after five days treatment, no evidence for the induction of adverse effects on cell proliferation or activity could be detected. In the further approach we investigated effect of MWCNT on HBMC when cultured in the presence of lactic acid. Surprisingly, cultures treated with MWCNT-LA under physiological pH (pre-incubated for 28 days) exhibited significantly lower cell number and total culture MTS conversion activity compared to MWCNT suspension in Pluronic F-127.

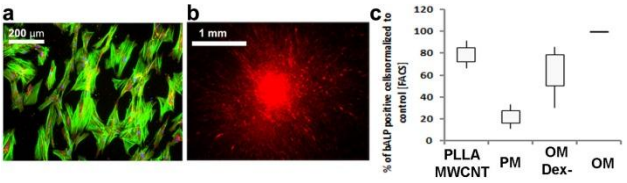

Fig. 1: HBMC culture on PLLA/MWCNT composites. (a) cell attachment, (b) 3D spheroids outgrowth and (c) % of bALP positive cells.

DISCUSSION & CONCLUSIONS: Altogether, this comprehensive study was focused on the evaluation of human bone cell reaction to new implant material and to its degradation products. Our data show lack of toxicity, good bio-compatibility and bioactivity of the PLLA/ MWCNT composite. MWCNTs suspension in Pluronic solution did not affect cell functionality even though detected in cell cytoplasm. However, when evaluated in LA solution we observed change in the suspension quality of MWCNT and significant reduction in cell number relative to controls after 5 days of treatment. This indicates that extensive *in vitro* evaluation including final degradation products may be needed to enable prediction of the overall success or failure of the newly developed composite.

REFERENCES: [1] HH. Lee et al (2011) J Biomed Mater Res B Appl Biomater. Aug;98B(2):246-54. [2] S. Gogolewski et al (1993) J Biomed Mater Res. Sep;27(9):1135-48

ACKNOWLEDGEMENTS: This work has been supported by EC FP7 POCO, Grant agreement number: CP-IP 213939-1.

19th Swiss Conference on Biomaterials

Overview Poster Presentations

SSB Swiss Society for Biomaterials
Société Suisse des Biomatériaux
Schweizerische Gesellschaft für Biomaterialien
Società Svizzera Biomateriali

AO Foundation

Poster Presentations

Poster number	Authors	Title	Page
18	S. Lischer, U. Tobler, Ph. Gruner, K. Maniura-Weber	«Choice of cell type and test method defines the results of a cytotoxicity study of HA coatings according to ISO-norm 10993-	56
19	M. Taherimehr, R. Bagheri, H. Maddah Hoseini, M. Baghaban Eslaminejad	«Evaluation of thermoplastic starch and nano-biocomposite of thermoplastic starch/beta tricalcium phosphate for bone tissue engineering applications»	57
20	G. Mattei, A. Tirella, A. Ahluwalia, N. Tirelli	«Smart, enzymatically cross-linkable hydrogels as three-dimensional models of tissue ageing and fibrosis»	58
21	H. Mirzadeh, A. Mirzaei, Y. Ghazizadeh, M. Daliri	«Nano-fibrous polyurethane/chitosan multi-layers as a novel wound dressing»	59
22	M. Müller J.Becher, M.Schnabelrauch, M. Zenobi-Wong	«Thermoresponsive-biopolymer blends as bio-inks for cartilage engineering»	60
23	E. Öztürk, J. Becher, M. Schnabelrauch, M. Zenobi-Wong	«Sulfated, acrylated hyaluronan hydrogels for chondrogenesis of mesenchymal stem cells»	61
24	G. Palazzolo, N. Broguiere, J. Becher, M. Schnabelrauch, M. Zenobi-Wong	«Sulfation of alginate promotes 3D neuronal growth»	62
25	I. Potapova, D. Eglin, MW. Laschke, M. Bischoff, RG. Richards, TF. Moriarty	«Bioorthogonal reaction for two-step labeling of Staphylococcus aureus with Lysostaphin»	63
26	M. Pusnik, A. Bruinink, M. Rodriguez-Arbaizar, E. Carreño-Morelli	«Opportunities and limits of in vitro cytotoxicity test methods exemplified by powder metallurgy titanium alloys»	64

19th Swiss Conference on Biomaterials

Abstracts Poster Presentations

SSB Swiss Society for Biomaterials
Société Suisse des Biomatériaux
Schweizerische Gesellschaft für Biomaterialien
Società Svizzera Biomateriali

AO Foundation

P1 – A novel self assembled injectable system based on Avidin – Biotinylated nanocomposite microspheres for bone tissue engineering applications

S. Bagheri-Khoulenjan[1], H. Mirzadeh[1], M. Etrati-Khosroshahi[2]

[1] Polymer Engineering Department, Amirkabir University of Technology, Iran. [2] Biomedical Engineering Department, Amirkabir University of Technology, Iran.

INTRODUCTION: Providing a porous and biocompatible injectable system is one of the challenges in non-invasive tissue engineering approaches [1]. Using microsphere based injectable systems can provide an interconnected porous network [2]. In this study, avidin-biotinylated nanocomposite microspheres (based on nanohydroxyapatite/gelatin/chitosan (nHA-i-GC)) which self-assembles via avidin-biotin conjunction is investigated as an injectable system for bone tissue engineering applications.

METHODS: first, the nHA-i-GC nanocomposite microspheres were fabricated using water in oil emulsion [3] and followed by EDC cross-linking. The microspheres were characterized by optical microscope, SEM, TEM, XRD and FT-IR analysis. The cross-linking density and NH_2 content of the microspheres were obtained using TNBS assay. After analyzing the data, the optimized formulations were selected to fabricate the nanocomposite microspheres to be biotinylated. Biotinylation of microspheres was performed using NHS-PEG-Biotin spacer with molecular weight of 3500 D. The biotinylation density of the microspheres was studied by HABA assay.

Effect of particle size, dispersion volume fraction and spacer concentration on rheological properties, porosity, pore size and injectability were investigated after addition of avidin. Design of experiments has been performed using tagoucci model (samples are presented in Table 1). In vitro studies were performed using normal human osteoblast cell culture and MTT assay.

RESULTS: Rheological studies showed that gel strength of this system (storage modulus) varied in the range of 3.2 -38 KPa (Table 1). Porosity of the formed scaffolds was between 50 to 60 %(Table 1). Optical images of formed scaffolds showed the integrity of formed scaffolds (Fig. 1) and pore revealed that size of scaffolds increased by particle size of microspheres. SEM images of cultured cells within the scaffolds showed that human osteoblast could spread within the scaffolds. MTT assays revealed that after one week almost 90% of cells cultured within the scaffolds were alive.

DISCUSSION & CONCLUSIONS: Statistic analysis of Rheology data revealed that dispersion volume fraction has a great impact on gel strength and pore size, respectively. Based on these results, optimum formulation defined as the sample with particle size of 80 µm, dispersion volume fraction of 50% and spacer concentration of 5mg/ml.

Table 1- samples characteristics designed by Taguchi approach.

Run	particle size (µm)	dispersion volume fraction (%)	Spacer concentration (mg/ml)	Biotinylation density(µm/ml)	Porosity	Storage modulus (&Pa)
1	10	50	5	56.2±1.1	54	38
2	10	30	15	70.6±1.9	61	6.78
3	80	50	15	4.5±0.4	51	14.6
4	80	30	5	15.9±0.7	57	3.28
O1	80	50	5	4.5±0.4	54	14.96

As the microspheres could provide a porous structure exactly after formation of scaffolds, osteoblast cells had enough space to attach and spread within the scaffolds. In addition, Avidin-Biotin conjugates (as a setting agent) are more biocompatible than conventional chemical cross linking agents.

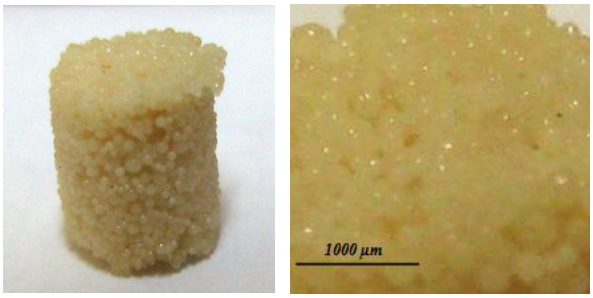

Fig. 1- Images of formed injectable nano-composite (sample O1) after addition of avidin.

REFERENCES:[1]Y. Krishnamachari, M.E. Pearce and A.K. Salem, (2008) Adv Mater, **20**(5):989-994. [2] S.R Van Tomme., C.F. van Nostrum, M. Dijkstra, et al., (2008) *Eur J Pharm Biopharm*, **70**(2): 522-30. [3] S. Bagheri-Khoulenjani, H. Mirzadeh, M. Etrati-Khosroshahi, M.A. shokrgozar, (2013) *J Biomed Mater Res* A

P2 – Production of novel polyhydroxyalkanoate-terpolymers using *Pseudomonas putida* KT40N22

M. Bassas-Galia[1,2], G. Molinari[1]

[1] Helmholtz Zentrum für Infektionforschung, Braunschweig, DE, [2]HESO-SO Valais Wallis, Sion-CH.

INTRODUCTION: Polyhydroxyalkanoates (PHAs) are biodegradable and biocompatible biopolyesters that offer the potential as promising alternative to the traditional plastics since they have shown good properties for industrial and biomedical applications. Mcl-PHAs are amorphous or semi-crystalline elastomers with low T_m (<50°C) and weak tensile strength. On the contrary, scl-PHAs (e.g PHB) are crystalline and have a tensile strength similar to polypropylene (40 MPa) although being more brittle. Combination of scl- and mcl-monomers in the same polymer resulted in a terpolymer of high interest since it combines the strength of PHB and the flexibility of mcl-PHA [1]. In this study it is shown that *P. putida* KT40N22, a recombinant strain expressing a *pha*C gene obtained from a metagenomic library, is able to produce different types of terpolymers, mainly PHB based copolymers containing up to 21 mol% of the mcl-PHA fraction [2].

METHODS: *P. putida* KT40N22 was cultivated in Erlenmeyer flasks (2L) containing 400 mL of LB medium using antibiotics (Gm, Km) [2]. Different substrates were tested: hexanoate, heptanoate, octanoate and decanoate (4 g/L), glucose (3.6 g/L) and oleic acid (10 g/L). After 48-72h of cultivation at 30°C and 180 rpm, cells were harvested and freeze-dried. The lyophilized biomass was extracted and purified as previously described [2]. Polymer formation was monitored along the cultivation time by fluorescence microscopy of the nile red stained cells (Fig.1a). After purification, monomer composition was determined by NMR, thermal properties and molecular weight by DSC and GPC, respectively.

RESULTS: *P. putida* KT40N22 produced P[3HB (94 mol%)-co-3HV (6 mol%)] and P[3HB (7.1 mol%)-co-3HV (92.9 mol%)] when glucose and heptanoate were used as substrate, respectively. A similar polymer to Nodax® was obtained when the strain was grown on hexanoic acid, P[3HB (79 mol%)-co-HHx (21 mol%)], while a terpolymer of P[3HB-co-3HHx-co-3HO] was produced when octanoic, decanoic or oleic acid were used as substrates. NMR spectra indicated that the terpolymer contained 3HB (88-90 mol%), 3HHX (5-10 mol%) and 3HO (2-5 mol%) depending on the substrate.

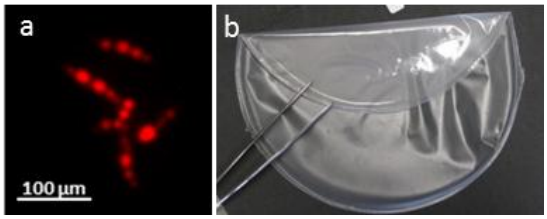

Fig. 1: (a) Fluorescence micrograph of nile red stained cells and (b) P[3HB-co-3HHx-co-3HO] film obtained using sodium octanoate as substrate.

According to the DSC analysis, all the polymers showed a unique glass transition temperature (T_g) although the melting temperature (T_m) could not be detected in all of them (Table 1). Remarkably, the terpolymer obtained using oleic acid as substrate showed a higher melting temperature and higher T_g as obtained for all polymers.

Table 1. Physical characterization of PHA-polymers produced by P. putida KT40N22 grown on different substrates

substrate	T_g (°C)	T_m (°C)	Tc (°C)	M_w (kDa)	PI
hexanoate	-2.2	-	-	236	1.91
heptanoate	-16	100	63	445	1.90
octanoate	-2.4	-	-	259	2.25
oleic acid	-1.0	125/145	69	168	1.96
glucose	0.4	150	51	nd	nd

nd: not determined; Tc: crystallization temperature

DISCUSSION & CONCLUSIONS: Several copolymers were produced and the films cast (Fig. 1b) showed improved material properties. From the results, it appears that the introduction of the 3HO monomer units affect the mechanical properties of the 3HB-based copolymer. Mechanical properties are on track.

REFERENCES: [1] I. Noda, P. R. Green, M.M. Satkowski et al (2005) *Biomacromo1ecules* **6**:580-586. [2] S. Cheema. M. Bassas-Galia, P. S. Sarma et al (2012*) Bioresource Technol* **103**:322-328.

P3 – Effects of TNF-α inhibition on muscle regeneration following muscle trauma

I. Stratos[1,2], AK. Behrendt[1,2], C. Anselm[1], A. Gonzalez[1], T. Mittlmeier[1], B. Vollmar[2]

[1]*Dept. of Trauma & Reconstructive Surgery, Rostock University Medical Center, Rostock, Germany*
[2]*Institute for Experimental Surgery, Rostock University Medical Center, Rostock, Germany*

INTRODUCTION: The regeneration of injured muscle tissue is a complex phenomenon that involves a variety of signaling molecules. It is known that TNF-α has degenerative actions on various tissues and that an up-regulation of TNF-α occurs immediately after muscle injury during the acute post-traumatic inflammatory phase[1]. The aim of our study was to investigate whether blockade of TNF-α using the TNF-α inhibitor "Infliximab" could improve and accelerate muscle regeneration after injury.

METHODS: We anesthetized 42 male Wistar rats (320-390 g bw) with pentobarbital sodium (60 mg/kg bw i.p.) and induced a blunt injury of the left soleus muscle by using an instrumented clamp as previously described[2]. After trauma, animals received a single dose of either 10 mg/kg bw Infliximab i.p. (infliximab, IFX) or equivalent volumes of saline as vehicle solution i.p. (control, CTRL). Subsequent observations were performed at day 1, 4 and 14 after injury (n=7 per time point and group). After stimulation of the sciatic nerve fast twitch (9 mA/75 Hz, 5 times for 0.1 s in 5 s intervals) and tetanic force (9 mA/75 Hz, 5 times for 3 s in 5 s intervals) of the soleus muscle were analyzed. Furthermore, the wet muscle weight was quantified. Moreover, we analyzed the muscle cell proliferation (BrdU IHC) and the coverage of muscle cells as well as the myofiber diameter (HE histology). Data are given as mean ± SEM. Group differences were assessed using Students t-test, a p-value of < 0.05 was considered significant.

RESULTS: Muscle force analysis showed a significant increase of twitch muscle force (Fig.1a, CTRL: 0.30±0.03 N vs. IFX: 0.39±0.04 N; $p<0.05$) and tetanic muscle force (Fig.1b, CTRL: 0.67±0.09 N vs. IFX: 0.80±0.08 N; $p>0.05$) 14 days after injury by TNF-α inhibition. The wet muscle weight was significantly enhanced at day 14 (Fig.1c, CTRL: 310±1 mg vs. IFX: 317±1 mg; $p<0.001$). Quantification of myofiber diameter did not show any significant difference between both groups 14 days after injury (CTRL: 42±1 µm vs. IFX: 43±1 µm) indicating that the observed functional musle restoration in IFX group was not a result of muscle cell hypertrophy.

On the contrary, planimetric analysis of muscle tissue showed at day 14 a significant increase of visible muscle cells in the IFX group compared to the control (CTRL: 59±3% vs. IFX: 71±3% muscle cell coverage to the entire visible muscle tissue; $p<0.05$). BrdU staining showed a maximal proliferative activity at day 4 after injury. Quantitative analysis revealed higher mean values of BrdU positive cells after infliximab treatment (CTRL: 56±7 vs. IFX: 61±6 cells/field; $p>0.05$). At other time points no difference between groups could be observed for the mentioned parameters.

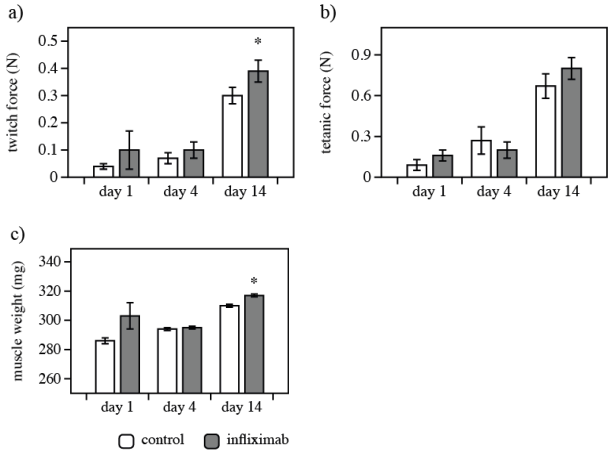

Fig.1: Analysis of muscle twitch (a) and tetanic (b) force and muscle wet weight (c) in infliximab (grey bars) and control (white bars) groups post injury.

DISCUSSION & CONCLUSIONS: The present study demonstrates that infliximab enhances the biomechanical characteristics of the injured muscle by significantly improving the muscle force and the wet muscle weight 14 days after injury. Furthermore, we could show that the functional restoration of the muscle is associated with an increase of visible muscle tissue at day 14 and a slight increase of cell proliferation at day 4. Overall this data support our primary hypothesis that inhibition of TNF-α induces regenerative processes in injured muscle.

REFERENCES: [1] GL. Warren, T. Hulderman, N. Jensen et al (2002) *FASEB* **16**:1630-32. [2] I. Stratos, Z. Li, P. Herlyn et al (2012) *Am J Pathol* **182**:895-904.

P4 – Selenium doped hydroxyapatite coating by biomimetic method on titanium alloy

B. Yilmaz[1], Z. Evis[1,2]

[1] Biomedical Engineering, Middle East Technical University, Ankara, Turkey [2] Engineering Sciences, Middle East Technical University, Ankara, Turkey

INTRODUCTION: Coating of the metallic orthopedic or dental implants with hydroxyapatite (HA) is a commonly used technique to increase the bioactivity and corrosion resistance on the surface. The most recent studies on this topic focus on ion doping into the structure of HA in order to bring functionality to the coating. Ions, such as Zn^{2+}, Fe^{2+}, Cu^{2+}, Mg^{2+}, Mn^{2+}, Sr^{2+}, F^{-}, Cl^{-} and CO_3^{2-} may substitute for Ca^{2+}, OH^{-} and $(PO_4)^{3-}$ in the HA structure[1]. Likewise, selenate ion (SeO_4^{2-}) can be doped to HA and it is a strong candidate for refunctioning the HA coatings with anti-cancer and anti-bacterial properties.

METHODS: Ti6Al4V plates ($20\times20\times2mm^3$) were abraded with #400 SiC paper and ultrasonically cleaned with acetone, ethanol (70%) and distilled water. The plates were immersed in 5M sodium hydroxide (NaOH) at 80°C for 3 days and subjected to a temperature of 600°C for 1 hour. The alkali and heat treated plates were coated in conventional 1.5 times more **concentrated** simulated body fluid $(1.5\times SBF)^2$ and in 1.5×SBF, which was modified to include 0.15 mM SeO_4^{2-}, at 37°C for 7 and 14 days. The surface morphology of the coated plates was observed by a field emission scanning electron microscope (FE-SEM Quanta 400F). The plates were also characterized by Fourier-transform infrared spectroscopy (FTIR, Bruker IFS 66/S) in the range of 4000–400 cm^{-1} and X-ray diffraction (XRD, Rigaku Ultima-IV) operating with Cu-Kα radiation at 40 kV and 30 mA. In addition, inductively coupled plasma-mass spectrophotometry (ICP-MS) analysis was performed by using Thermo Electron X7. For ICP-MS analysis, the coatings on the Ti6Al4V plates were scraped by a spatula and the powders were dissolved in 2% nitric acid (HNO_3) solution.

RESULTS: Fig.1 shows the SEM images of pure and selenium doped HA coatings after immersion for 7 days. The entire surface was successfully coated with a thicker HA layer after 14 days in solution. The selenium doped and pure HA coatings showed the typical FTIR spectrum of carbonated HA regardless of the soaking time. The XRD studies also revealed that both type of the biomimetic CaP coatings gave the standard HA (ICDD card No. 1-1008) XRD peaks.

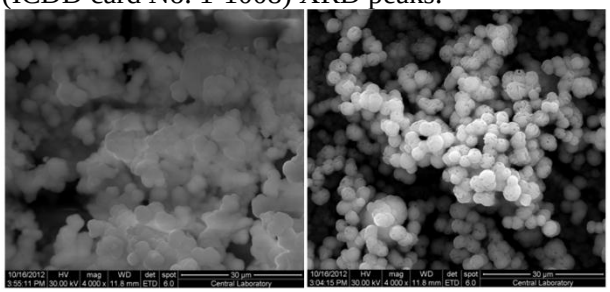

Fig. 1: SEM images of pure (left) and selenium doped (right) HA coatings after immersion of 7 days (4000×)

The calculated Ca/Se atomic ratios of the coatings after soaking in selenate added 1.5×SBF for a period of 7 and 14 days were 3509 and 4851, respectively.

DISCUSSION & CONCLUSIONS: The alkali and heat treatment provided a porous network layer of sodium titanate, on which apatite formation can be induced. The calcium phosphate (CaP) was first nucleated and then grew continuously in the form of half spheres on the titanate layer of the plates. The selenium doped HA coating was shown to have a more uniform morphology when compared to pure HA coating. The XRD patterns showed that both of the coatings were phase pure. Although the FTIR spectra of selenium doped coatings were found to exhibit no significant difference than pure hydroxyapatite, from ICP analysis selenium was shown to incorporate into the structure. In conclusion, selenium doped HA coatings on Ti6Al4V plates were successfully obtained by modification of the composition of conventional 1.5×SBF in 2 weeks. Further studies can be done for evaluating the in-vitro anticancer and antibacterial activities of the selenium doped HA coatings.

REFERENCES: 1 J. Terra, E.R. Dourado, J.G. Eon, et al (2009) Phys Chem Chem Phys 11:568-77. 2 A. Bigi, E. Boanini, S. Panzavolta, et al (2000) Biomacromolecules 1: 752-56.

ACKNOWLEDGEMENTS: This study was supported by the research grant of the Scientific and Technological Research Council of Turkey under the project number TUBITAK-111M262.

P5 – Fast gelling, neurite-outgrowth promoting hydrogels using the Michael addition of thiols on maleimides

N. Broguiere[1], G. Palazzolo[1], M. Zenobi-Wong[1]

[1] *Cartilage Engineering and Regeneration Laboratory,*

Department of Health Sciences and Technology, ETH Zurich, Switzerland.

INTRODUCTION: Poly[ethylene glycol] (PEG) occupies a central role in biomaterials because of the very weak interactivity of PEG with biological systems. In particular, PEG hydrogels provide a blank, hydrated matrix in which bioactive cues such as adhesion peptides or proteins, enzymatically cleavable cross-linkers and releasable factors can be added on demand to control the behavior of cells in vitro and in vivo [1]. PEG gels covalently cross-linked without a source of UV-light usually rely on the Michael addition of thiols on vinyl sulfones. This cross-linking reaction has the disadvantage of becoming very slow (at pH7.4) for the low macromer content (less than 1.5%w/v) that is necessary to support the 3D growth of neural extensions. Here, we use the much more reactive Michael acceptor maleimide to encapsulate primary hippocampal neurons in neurite outgrowth promoting hydrogels.

METHODS: 10%w/v stock solutions of 20kDa 4arm-PEG-maleimide and 3.7kDa PEG-dithiol (Laysan Bio) were prepared in 0.9%w/v NaCl (pH5.0). Dissociated hippocampal neurons were suspended at 5e7 cells/ml in PBS pH7.4 (Gibco). The peptide CSRARKQAAS**IKVAV**SADR-NH2 (Anaspec), used for adhesion, was dissolved in mQ water at 2mg/ml. The stock solutions were then combined to form gels of 30 to 150 l with a 4arm-PEG-maleimide content of 1.2% to 2%w/v, stoichiometric amount of PEG-dithiol, 100 m of adhesion peptide, 5e6 cells/ml, and the leftover volume filled with the saline solution. The dithiol cross-linker was added last and mixed quickly by vortexing. The precursor solution was then swiftly transferred in a custom chamber and left to gel for 3min. Gels were kept in DMEM (Gibco, 61965-026) with 10% FBS (Gibco, 10270-106) overnight, and then transferred to neurobasal medium (Gibco, 21103-049) supplemented with 1x B27 (Gibco, 17504-044) and 1x L-glutamine (Gibco, 25030-024).

RESULTS: Gelling occurred in less than a minute after transferring the precursor solution into the caster. Extensive neurite outgrowth could be observed from the first day after encapsulation, at rates reaching several hundred microns per day.

The gels were very soft (Compressive modulus of 400 to 1500 Pa) and degraded over the course of one to a few weeks.

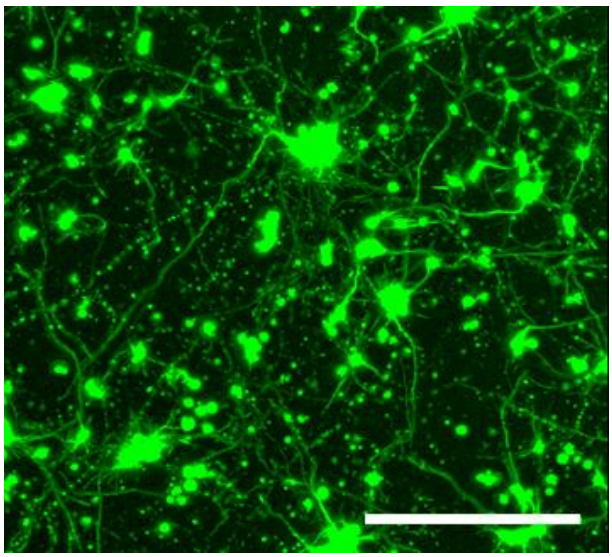

Fig. 1: Encapsulated embryonic E18 rat hippocampal neurons at 3 DIV in 1.2% 4arm-PEG-maleimide gel. Stained for β3 tubulin. Maximum intensity projection of a Confocal Z-stack. Scale bar:100μm.

DISCUSSION & CONCLUSIONS: The cross-linking of PEG with the addition of thiols on maleimides, in contrast with the classical addition on vinyl sulfones, confers fast (at pH6) to extremely fast (at pH7.4) gelation, and degradability over the course of a few weeks. These novel features enable the encapsulation and growth of hippocampal neurons in vitro, and they could be of interest as well for a variety of other tissue engineering applications.

REFERENCES: [1] G.P. Raeber, M.P. Lutolf, J.A. Hubbell (2005) *Biophysical Journal* **89**:1374-1388.

ACKNOWLEDGEMENTS: Hippocampal neurons used in this work were a kind gift from prof. Frischty. We also thank prof. Vörös for useful inputs.

P6 – Tissue Engineered Bone Grafts Based on Biomimetic Nanocomposite PLGA/Amorphous Calcium Phosphate Scaffold and Human Adipose-Derived Stem Cells

J. Buschmann[1], L. Härter[2], S. Gao[2], S. Hemmi[2], M. Welti[1], N. Hild[3], OD. Schneider, [3], WJ. Stark[3], N. Lindenblatt[1], CML. Werner[2], GA. Wanner[2], M. Calcagni[1]

[1]Division of Plastic and Hand Surgery, University Hospital Zurich, Zurich, [2]Division of Trauma Surgery, University Hospital Zurich, Zurich [3]Institute for Chemical and Bioengineering, Department of Chemistry and Applied Biosciences, ETH Zurich, Zurich

INTRODUCTION: For tissue engineering of critical size bone grafts, nanocomposites are getting more and more attractive due to their controllable physical and biological properties. We report *in vitro* and *in vivo* behaviour of an electrospun nanocomposite based on poly-lactic-co-glycolic acid and amorphous calcium phosphate nanoparticles (PLGA/a-CaP) seeded with human Adipose-Derived Stem Cells (ASC) compared to PLGA.

METHODS: We seeded human Adipose-Derived Stem Cells (ASC) onto PLGA and PLGA/aCaP scaffolds and compared their proliferative behaviour. The function of aCaP nanoparticles was tested for triggering osteogenesis of ASC in a suspension. Vascularization capacity into the nanocomposite scaffold was checked by an *in vivo* assay on the chorioallantoic membrane (CAM)[1].

RESULTS: Major findings were that cell attachment, three-dimensional ingrowth and proliferation were very good on both materials. Cell morphology changed from a spindle-shaped fibroblast-like form to a more roundish type when ASC were seeded on PLGA, while they retained their morphology on PLGA/a-CaP. Moreover, we found ASC differentiation to a phenotype commited towards osteogenesis when a-CaP nanoparticles were suspended in normal culture medium without any osteogenic supplements, which renders a-CaP nanoparticles an interesting osteoinductive component for the synthesis of other nanocomposites than PLGA/a-CaP. Finally, electrospun PLGA/a-CaP scaffold architecture is suitable for a rapid and homogenous vascularisation confirmed by a complete penetration by avian vessels from the chick chorioallantoic membrane (CAM) within one week.

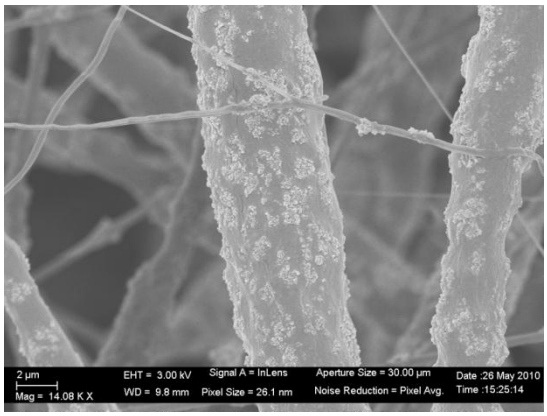

Fig. 1: SEM image of an electrospun PLGA/aCaP nanocomposite.

DISCUSSION & CONCLUSIONS: The combination of an electrospun PLGA/a-CaP nanocomposite with human ASC was suitable for tissue engineering of bone constructs because cells attached and proliferated very well on this scaffold material. Moreover, a-CaP nanoparticles applied in low concentrations triggered osteocalcin expression in human ASC, which makes them *per se* an interesting and potential partner for synthesizing nanocomposites with any other polymer instead of PLGA. Finally, the electrospun PLGA/a-CaP nanocomposite has an excellent architecture with respect to vessel ingrowth as shown by a full and homogenous vascularisation of a ~ 800 µm thick layer within 1 week.

REFERENCES: [1] Buschmann J, Härter L, Gao S, Hemmi S, Welti M, Hild N, Schneider OD, Stark WJ, Lindenblatt N, Werner CML, Wanner GA and Calcagni M. Tissue engineered bone grafts based on biomimetic nanocomposite PLGA/amorphous calcium phosphate scaffold and human adipose derived stem cells, Injury 2012;43(10):1689-1697.

ACKNOWLEDGEMENTS: We thank Miss Gabriella Meier-Bürgisser for measuring the widths of the ASC in the histological cross-sections. Miss Pia Fuchs is acknowledged for help with histological staining.

P7 – Covalent immobilisation of VEGF on electrospun fibres

A. G. Guex[1], D. Hegemann[1], MN. Giraud[2], G. Fortunato[1]

[1] *Empa, Swiss Federal Laboratories for Materials Science and Technology, St.Gallen, CH.*
[2] *Cardiology, Department of Medicine, University of Fribourg, CH.*

INTRODUCTION: Functionalised biomaterials, namely the covalent immobilisation of proteins or growth factors on synthetic scaffolds, are increasingly considered for tissue engineering applications. Cell response is governed by material properties and at the site of interest. Furthermore, implantation of substrate immobilised growth factors represents a safe delivery method, bypassing the problem of rapid diffusion and short blood plasma half-life as encountered for soluble factors [1]. In the current study, we developed a scaffold with covalently bound vascular endothelial growth factor (VEGF) and evaluated its effect on endothelial cell viability and proliferation.

METHODS: Microfibrous poly(ε-caprolactone) (PCL) non-wovens were produced by electrospinning and surface-coated in an RF plasma process (CO_2/C_2H_4 gas). Carboxyl groups were activated by EDC/NHS chemistry, followed by introduction of a linker molecule (HMD). Substrates were then incubated in an EDC-activated VEGF solution of 0.5 μgmL^{-1}, 1μgmL^{-1} or 3 μgmL^{-1}. Scaffolds were characterised by SEM and XPS, VEGF concentration was indirectly quantified by ELISA. Human umbilical vein endothelial cells (HUVEC) were seeded on VEGF functionalised scaffolds and on pure scaffolds in media supplemented with soluble VEGF (50 $ngmL^{-1}$). Cell viability, proliferation and morphology was assessed by MTT, CyQuant and SEM, respectively.

RESULTS: Substrates of homogeneous fibres (3± 0.6 µm) were successfully produced by e-spinning (*Fig 1a*). XPS measurements confirmed the deposition of an oxygen functional hydrocarbon coating [2]. By increasing the CO_2 to C_2H_4 gas ratio from 2:1 to 6:1, the concentration of functional COOH groups at the surface was found to be noticeable higher (0.7 at% vs. 0.2 at%, [3]). Thereby, and by changing the initial VEGF concentration in the reactive solution, distinct scaffolds, providing low (83 ± 37 ng per patch) or high (212 ± 123 ng per patch) VEGF concentrations could be generated (*Fig 1b*). Immobilisation yields were 30% on 2:1 substrates and 50% on 6:1 substrates. VEGF release over time is relatively constant, indicated by a release of 6 $ng{\cdot}mL^{-1}$ during the first two days and 3 $ng{\cdot}mL^{-1}$ on day 4 and 5.

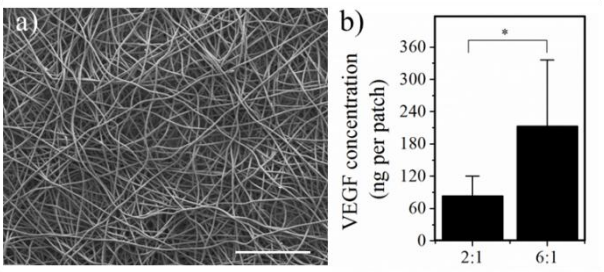

Fig. 1: a) SEM image of electrospun fibres. Scale bar: 250 µm. b) VEGF concentrations, assessed with ELISA.

MTT test revealed viable cells on all substrates. Five days post seeding, HUVEC formed homogeneous cell layers on the substrates, assembling into tightly packed tubes within two weeks. Interestingly, cell proliferation on VEGF functionalised scaffolds was not enhanced, compared to pure substrates.

DISCUSSION & CONCLUSIONS: We present a rapid and safe functionalisation route to successfully couple VEGF to electrospun fibres. Functionalised scaffolds were shown to be suitable for HUVEC culture. Further studies will address the direct quantification of VEGF on the fibres by surface analytical approaches (Tof SIMS, Raman spectroscopy, immunofluorescence) and its stability over time and bench life.

REFERENCES: [1] K.S Masters (2011) *Macromol Biosci*, **11**(9):1149–63 [2]A.G. Guex (2012) *Acta Biomater* **8**:1481-91 [3] E. Körner et al (2011), *Surf Coat Technol* **205**:2978-84.

ACKNOWLEDGEMENTS: This study was financially supported by SNF grant No. 122334.

P8 – Structural investigations of lanthanum and fluoride doped nano hydroxyapatites

S. Gungor Geridonmez[1], MB. Turkoz[2], Z. Evis[3]

[1] Department of Mechanical Engineering, Yuzuncu Yil University, Van, Turkey. [2] Department of Physics, Kirikkale University, Kirikkale, Turkey.[3] Department of Engineering Sciences, Middle East Technical University, Ankara, Turkey. [1]sgungorgerid@gmail.com

INTRODUCTION: Hydroxyapatite (HA) is frequently used in medical applications due to their high biocompatibility in the human body. Compared with pure HA, substitution of La^{3+} in HA structures revealed higher flexural strength, lower dissolution rate and superior biocompatibility [1]. The incorporation of lanthanum increased the surface area of the samples and hardness [2]. Thermal stability and biological properties of HA were enhanced with addition of fluoride ions (F^-) which impose the physical and biological characteristics of HA [3]. However, there are few studies on the influences of a series of rare earth ions on the formation of HA particles. The purpose of this study is to synthesize HA doped with La^{3+} and F^- ions to investigate their microstructures properties and develop new nano-bioceramics for biomedical applications.

METHODS: All pure and doped HA were synthesized by a precipitation method. Calcium nitrate tetra hydrate and di-ammonium hydrogen phosphate were used as main precursors. These precursors were added into distilled water in order to prepare ($Ca(NO_3)_2{\cdot}4H_2O$) and ($(NH_4)_2HPO_4$ solutions with a certain molar ratio. The Ca/P ratio was kept at 1.67. Ammonia was added into the Ca-P mixture solution to adjust the pH of the final mixture to 11-12. After mixing the solution overnight, the mixture was filtered to obtain a wet cake. The wet cake was dried in the furnace at 200°C, calcined at 800°C for 30 min and sintered at 1100°C for 1h. In addition to the main precursors used in the synthesis of pure HA, lanthanum nitrate and ammonium fluoride were used.

RESULTS: The XRD patterns of pure and lanthanum doped samples coincide with the JCPDS data (09-0432) for the pure phase of HA with small amount of $LaPO_4$. According to Table 1, smaller densities were obtained for most of the compositions after sintering at 1100°C except HA10.0La1F. Increasing the amount of La^{3+} ions led to decrease in the density of samples doped with La^{3+} ions after the sintering at 1100°C. The microhardness values of the samples were increased in the samples HA2.5La1F and HA2.5La5.0F.

Table 1. Sintered densities of pure and doped HA after the sintering at 1100°C for 1h .

Material	Sintered Densities
HAP	3.1151
HA1La1F	3.0949
HA2.5La1F	3.0831
HA5.0La1F	3.0855
HA10.0La1F	3.1196
HA2.5La2.5F	3.1029
HA2.5La5.0F	3.0956
HA2.5La10.0F	3.0933

DISCUSSION & CONCLUSIONS: In this study, HA doped with La^{3+} and F^- ions were synthesized by a precipitation method. Doping amount of F^- ions was kept at 1.0, 2.5, 5 and 10 mol.% whereas doping amount of La^{3+} ions was 1.0, 2.5, 5 and 10 mol.%. There was substitution of La^{3+} into HA and decrease in crystallinity and crystallite size on doping was confirmed by XRD. The incorporation of La^{3+} ions decreased the hardness of the samples except HA2.5La1F and HA2.5La5.0F.

REFERENCES: [1] D.G. Guo, A.H. Wang, Y. Han, et al (2009) *Acta Biomater* **5**: 3512-3523. [2] M.I. Ahymah Joshy, K. Elayaraja, R.V. Suganthi, et al (2011) *Current Applied Physics* **11**:1100-1106 [3] A. Machoy-Mokrzynska (1995) *J Inter. Soc. for Fluoride Res.* **28**: 175-177.

P9 – Quantitative characterization of biomaterials and their interaction with living cells by AFM

E. Hartmann[1], T. Müller[1], C. Pettersson[1], T. Neumann[1]

[1] *JPK Instruments AG, Applications department, Berlin, Germany*

INTRODUCTION: Topography, roughness and mechanical properties of biomaterials are crucial parameters influencing cell adhesion/motility, morphology and mechanics as well as the development of stem/progenitor cells [1,2,3,4]. Atomic force microscopy (AFM) is a powerful tool not only to study the morphology in terms of high resolution imaging and roughness measurements, but also to map mechanical and adhesive properties. Combining these remarkable abilities with advanced optical microscopy allows for extensive characterization of biomaterials.

METHODS: AFM is based on a flexible cantilever stylus that is scanned over the sample. The probe-sample interaction induced deflection of the cantilever is finally converted into sample topography and interaction force. The sensitivity of the detection system and the accuracy of piezo actuators with capacitive sensors allow for resolving structures of less than 1 nm and forces on the pN scale. Different imaging modes can resolve structures of biomaterials in physiological conditions without the Abbe diffraction limit. In force spectroscopy mode, interaction forces between the (modified) cantilever and any substrate can be investigated. Using Single Cell Force Spectroscopy (SCFS), cell-substrate or cell-cell interactions can be measured down to single protein unbinding (fig. 1). The cantilever can also serve as nano-indentation tool to analyse mechanical properties like the Young's modulus of biomaterials or cells.

RESULTS: Using AFM imaging, the nanostructure of biomaterials like aligned collagen matrices have been resolved as well as cell alignment on such structures [4,5]. SCFS quantified the adhesion force and the contribution of different components, e.g. from the extra cellular matrix of living cells to implant materials as from cochlear implants [6]. Force-indentation measurements on cells using colloidal probes showed a significant effect of micro-patterned substrates on cellular elasticity [2].

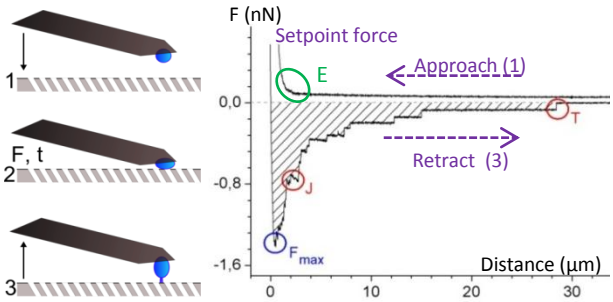

Fig. 1: Sketch of a SCFS experiment. The probe cell is approached to (1) and pressed against the substrate (2) with a defined Setpoint force (F) for a defined time (t). When the cell is separated from the sample (3) interactions like maximum adhesion force (F_{max}) and single unbinding events (force jumps (J) and those that are preceded by membrane tethers (T)) are visible in the force distance curve. The contact part of the Approach curve allows for applying elasticity models (E).

DISCUSSION & CONCLUSIONS:
AFM is a multipurpose technology which is much more than simple imaging. Interaction forces from single molecule unbinding to cell adhesion and analysis of surface and mechanical properties of biomaterials and cells make AFM to a key technology in biomaterial research. Nano-mechanical analysis of cells increasingly gains in importance in different fields in cell biology like cancer research [7] and developmental biology [8]. We present a strategy to comprehensively characterize biomaterials as well as their interaction with cells and influence on cell behavior.

REFERENCES: [1]Elter et al., Eur Biophys J 2011:40(3): 317-327. [2]McPhee et al., Med Biol Comput 2010:48(10):1043-53. [3]Engler et al., Cell 2006:126(4):677-689. [4]Kirmse et al., J Cell Sci 2010:124(11):1857-66. [5]Cisneros et al., Small 2007:3(6):956-63. [6]Aliuos et al., Biomed Tech 2010:55:66-68. [7]Cross et al., Nat Nanotech 2007:2(12):780-783. [8]Krieg et al. Nat Cell Biol 2008:10(4):429-36.

P10 – FEM analysis of porous titanium bone scaffolds

W. Hoffmann[1,2], S. Fabbri[2], R. Schumacher[2], S. Zimmermann[2], M. de Wild[2]

[1] Institute for Surgical Research and Hospital Management, University Hospital Basel, Basel, Switzerland [2] University of Applied Sciences Northwestern Switzerland, School of Life Sciences, Institute for Medical and Analytical Technologies, Gruendenstrasse 40, CH-4132 Muttenz Switzerland, Waldemar.Hoffmann@fhnw.ch

INTRODUCTION: Porous implants are effective clinical choices for the surgical reconstruction of large bone defects [1]. The porosity has two advantages: Firstly, the stiffness can be adapted to the biomechanical loading situation and secondly, the interconnected pores allow vascularisation and therefore support osseointegration. The additive manufacturing method selective laser melting (SLM) allows the physical realization of complex open-porous titanium structures designed in a three-dimensional CAD file [2]. When constructing such a synthetic scaffold, its reaction upon external load has to be considered as a function of the macroscopic lattice geometry in order to optimize fatigue resistance, osseointegration and reduce stress shielding. The resulting structural and mechanical responses like deformation, stiffness and stress distribution are simulated with the numerical technique of finite element method (FEM) [3].

METHODS: The designed three-dimensional lattice consists of translational multiplications of rhombi-dodecahedral (*rdh*) unit cells filling out the entire implant volume, see fig. 1. In order to simulate the mechanical properties as a function of various lattice parameters (strut thickness, cell height, porosity), the scaffold geometry is based on a completely parameterized SOLIDWORKS™ CAD model. Using COMSOL™ Multiphysics 4.3, the CAD geometry and the FEM model is linked associatively. The elasto-plastic material properties of SLM processed titanium are derived from unidirectional static compression tests (Zwick/Roell Allround Line 100 kN, LaserXtens, testXpert II V3.4) [4]. In accordance to typical clinical situations, the applied load is defined as a compressive load. In the FEM simulation, a prescribed displacement is applied. The geometry is discretized by meshing with tetrahedral volume elements, see fig. 1. The elements are refined in the proximity of the geometrical nodes and are adapted to the minimal strut size by the mesh generator. The deformation and von Mises stress distribution of the biomaterial is calculated using the COMSOL™ solver.

RESULTS: As expected, the induced stress is maximised in the nodes, see fig. 2. From the arising reaction forces, the stiffness of the entire scaffolds can be derived in dependence of the parameterized dimensions.

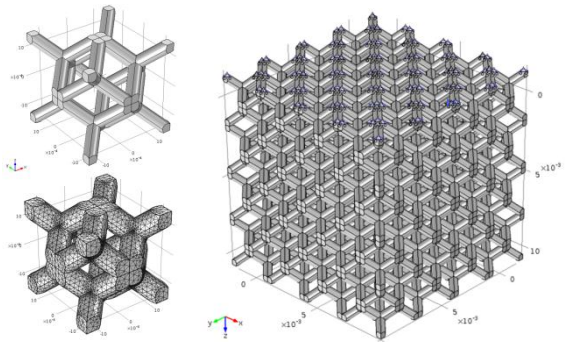

Fig. 1: Rhombi-dodecahedral unit cell, and cubic scaffold consisting of 4^3 rdh unit cells.

DISCUSSION & CONCLUSIONS: A numerical FEM simulation using the COMSOL™ software enables the characterization of the elasto-plastic behaviour of artificial porous structures under unidirectional compressive loadbearing. The stiffness as well as von Mises stress distribution can be evaluated in respect of unit-cell design.

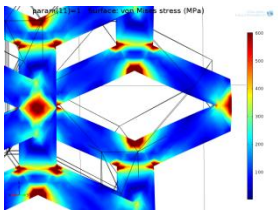

Fig. 2: Details of the deformation and the von Mises stress distribution in the nodes.

REFERENCES: [1] O. Hasart et al. (2010), *Oper Orthop Traumatol.* **22**(3):268-77. [2] T. Bormann et al. (2012), *Journal of Materials Engineering and Performance*, **21**(12), 2519-2524. [3] R. Singh et al. (2010), *Acta Biomaterialia* **6**;2342–2351. [4] P. Lamprecht (2012), bachelor thesis.

ACKNOWLEDGEMENTS: This project was supported by the HLS research fund.

P11 – In-vivo biosensors for biomedical implants based on tribocorrosion concepts and models

A. Igual Muñoz[1], B. Jolles-Haeberli[2], E. Meurville[3], S. Mischler[1]

[1]*Tribology and Interface Chemistry Group, École Polytechnique Fédérale de Lausanne Station 12, CH-1015 Lausanne, Switzerland*

[2]*Center of Translational Biomechanics, École Polytechnique Fédérale de Lausanne and University Hospital in Lausanne, Switzerland*

[3]*Product Design Group, École Polytechnique Fédérale de Lausanne, Switzerland*

INTRODUCTION: Out of the million hip and knee replacement prostheses that are implanted each year in the EU and US, none contain a way to monitor their condition during use, which can allow an early detection of failure or insufficient functionality. This stimulated the development by an EPFL team (InProVE project: Intelligent Prostheses Via Electrochemistry) of a system consisting of implanted sensors and electronics and a remote device, to measure the implant's function and degradation during its life span. While the overall objective is to propose systems that can be used with any metallic implant (including cardiovascular ones), the initial focus is on hip joint replacement prostheses.

METHODS: The basic principle consists in detecting in-vivo changes in electrochemical behavior of the implant through the simple measurement of the current and/or voltage difference between implant and a micro electrode. This signal is monitored by a miniaturized battery less electronic device able to transmit the information outside of the body by wireless telemetry. Due to the high sensitivity of electrochemical properties to the state of the body/metal interface, this method could allow an early detection of problems such as cellular toxicity, metal hypersensitivity, wear and/or corrosion of the implant.

RESULTS: SEM images, Fig. 1a, of the cone-ball taper junction of retrieved MoM hip joints show similar damage than those observed after in-vitro fretting-corrosion tests in which motion caused a measurable electrochemical response, Fig 1b. At the initiation of fretting, current increases abruptly. The enhancement of anodic current by rubbing is commonly observed in tribocorrosion of passive metals, where abrasion of the passive film covering the alloy leads to the exposure to the solution of metal that undergoes anodic oxidation until the passive film forms again. Therefore, electrochemical conditions can give an indication of the degradation state of the implant[1].

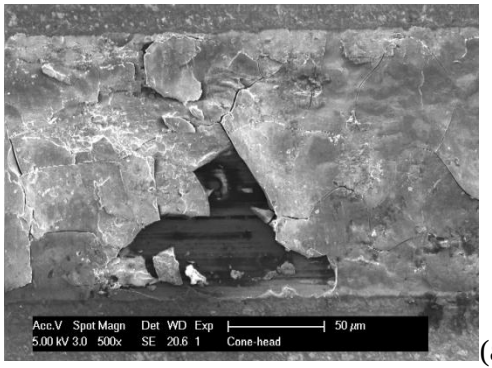

(a)

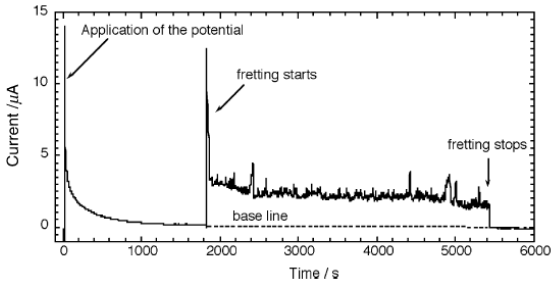

(b)

Fig. 1: (a) Fretting damage on the titanium cone-ball taper junction of a retrieved MoM hip joint. (b) Electrochemical response to fretting under similar conditions[2].

DISCUSSION & CONCLUSIONS: Implantable measuring devices which are powerful enough for electrochemical testing and passive wireless interface antennas for the communication with the external reader already exist. The electrochemical techniques to be used are well understood *in vitro*. The challenge of this project is to combine the two. Another challenge is to properly calibrate the electrochemical sensors (electrodes) and to optimize their use in the living tissue.

REFERENCES: [1] S. Mischler, A. Igual (2013) *Wear* 54:26-35. [2] S. Barril, S. Mischler, D. Landolt (2004) *Wear* 256:963-972

ACKNOWLEDGEMENTS: SEM images were kindly performed by Pierre Mettraux.

P12 – PLGA in situ forming implants for sustained release of BMP-2 and its enhancer

LS. Karfeld-Sulzer[1], JC. Leroux[2], FE. Weber[1]

[1] Oral Biotechnology and Bioengineering Lab, Dept. of Cranio-Maxillofacial and Oral Sugery, University Hospital Zurich, Zurich, CH. [2] Drug Formulation and Delivery Lab, Institute of Pharmaceutical Sciences, ETH Zurich, Zurich, CH

INTRODUCTION: Many large bone defects that are due to trauma, tumor resection, or disease are not able to heal themselves without intervention. Bone morphogenetic proteins (BMPs) are critical in bone formation and their importance has been affirmed with in vivo bone regeneration studies [1]. However, effective applied concentrations are very high, which constitutes an expensive treatment with potential negative side effects. Previously, we have demonstrated that N-methyl pyrrolidone (NMP) is a potent enhancer of BMP activity that can increase bone regeneration markers with lower BMP concentrations [2]. For this therapy to be clinically effective, we aim to deliver NMP along with BMP-2 in a sustained manner. Since NMP is a small, water- and organo-miscible molecule, many traditional drug delivery strategies are not adapted to its sustained release. In the present work, we have employed poly(lactide-co-glycolide) copolymers as injectable in situ forming implants (ISFI) for prolonged NMP and BMP-2 delivery.

METHODS: All polylactide and poly(lactide-co-glycolide) polymers were obtained from Boehringer Ingelheim. Polymers were dissolved overnight at 40 wt% in NMP at 37°C, with or without BMP-2. Release studies were performed by injecting the dissolved polymer into a metal mesh basket and immediately immersing it into phosphate buffered saline (PBS) or PBS-Urea (for BMP-2 release). Samples were maintained at 37°C on a shaker at 100 rpm. NMP concentration was quantified using liquid chromatography-mass spectrometry by quantifying the area under the curve of the UV signal at 210 nm. Initial polymer molecular weights and polymer degradation were analyzed with gel permeation chromatography by refractive index detection and polyethylene glycol standards for molecular weight calibration. BMP-2 concentrations were determined by using a Bio-Dot SF Microfiltration Apparatus (Biorad) to apply samples to a nitrocellulose membrane in a 48-slot format and then proceeding with normal blot procedures with a primary anti-BMP-2/4 antibody. Samples were quantified by comparing the intensity to that of standards.

RESULTS: The release profiles of NMP from polymer implants with different molecular weights (MW) and lactide to glycolide ratios (L:G) were studied. All of the formulations had some amount of initial burst release, but it was limited to less than 30% after 24 h for the lower MW polymers that contained a mixture of lactide and glycolide. A comparison of different MW polymers with L:G = 50:50, shows that the release rate of the lowest MW polymer (inherent viscosity (i.v.) = 0.16-0.24 g/L) was initially lower than that of the i.v. 0.32-0.44 g/L polymer. However, after 10 days, the release from the 0.16-0.24 g/L polymer surpassed the 0.32-0.44 g/L polymer, which may be attributed to polymer degradation. L:G ratio also impacted release characteristics. Release experiments demonstrated that the L:G = 100:0 polymer had a higher burst release, but a longer release period. The L:G = 50:50 polymer showed the least burst, but the fastest overall release. BMP-2 release from low MW polymers with L:G = 50:50 and L:G = 75:25 showed similar release profiles as these polymers' NMP release. The L:G = 75:25 polymer demonstrated a steadier release rate, whereas the L:G = 50:50 delivered most of the BMP-2 between 14 and 21 days.

DISCUSSION & CONCLUSIONS: When the water-insoluble polymers of the ISFI are exposed to water, they undergo a phase transition, forming a membrane on the implant [3]. The rate of transition, which is dependent on polymer properties, impacts the NMP and BMP-2 release rates. NMP and BMP-2 can be retained for at least three weeks, demonstrating that this injectable polymer system is potentially viable for sustained NMP and BMP-2 delivery for increased bone regeneration.

REFERENCES: [1] U.M. Wikesjo, M. Qahash, Y.H. Huang, et al (2009) *Orthod Craniofac Res* **12**:263-70. [2] B.S. Miguel, C. Ghayor, M. Ehrbar, et al (2009) *Tissue Eng Part A* **15**:2955-63. [3] A.J. McHugh (2005) *J Control Release* **109**:211-21.

ACKNOWLEDGEMENTS: We acknowledge the Swiss National Science Foundation for funding.

P13 – HA-PNIPAM biopolymer blends as bio-inks for cartilage engineering

M. Kesti[1,2], M. Müller[1], D. Eglin[3], J. Becher[4], M.0 Schnabelrauch[4], M. Zenobi-Wong[1]

[1] Cartilage Engineering + Regeneration, ETH Zürich, Zürich, Switzerland. [2] Tampere University of Technology, Tampere, Finland. [3] AO Research Institute Davos, Davos, Switzerland. [4] Biomaterials Department, Innovent e.V., Jena, Germany.

INTRODUCTION: Bioprinting is an emerging technology for tissue engineering replacement grafts. Bioprinters are already highly developed for rapid prototyping purposes; however, there is still a lack of suitable biologically relevant printing materials, so called bio-inks. The ideal bio-ink for extrusion printing should be liquid at the beginning to mix it freely with other polymers, peptides or cells and show a flow behavior suitable for the extrusion process (shear thinning). The final construct should be a stable, irreversible crosslinked hydrogel with similar mechanical properties as the surrounding tissue. This study investigates the properties of polymer blends suitable for bio-inks in extrusion bioprinting. Material blends of thermoresponsive and photopolymerizing polymers were used. In fact, these blends are capable of tandem gelation.

METHODS: Hyaluronan grafted Poly(*N*-isopropylacrylamide) (HA-PNIPAM) (Mw 1.6 MDa) was used as the thermoresponsive element of the bio-ink. HA-PNIPAM was blended with hyaluronan (Mw 280kDa), dextran (Mw 15-25 kDa) and chondroitin sulfate (Mw 20kDa) (all methacrylated) to improve mechanical properties of the final gel and to include biological cues. These bio-inks were analyzed with an Anton Paar MCR301 rheometer utilizing cone-plate geometry. Flow curves were recorded to test the printability of the gels while temperature ramps and UV crosslinking under oscillation were performed to investigate the gelling kinetics. Chondrocyte viability was assessed with a live/dead assay at 1 and 7 days after encapsulation.

RESULTS: Rheology measurements of tandem crosslinked biopolymer hydrogels (Fig. 1) illustrate temperature gelling to be independent from the photopolymerizing polymers. UV-crosslinking of the methacrylated biopolymers occurs in the presence of HA-PNIPAM hydrogel as shown by the second increase in the storage and loss moduli. HA-PNIPAM gels instantly after printing which enables accurate printing structures, before chemical irreversible crosslink.

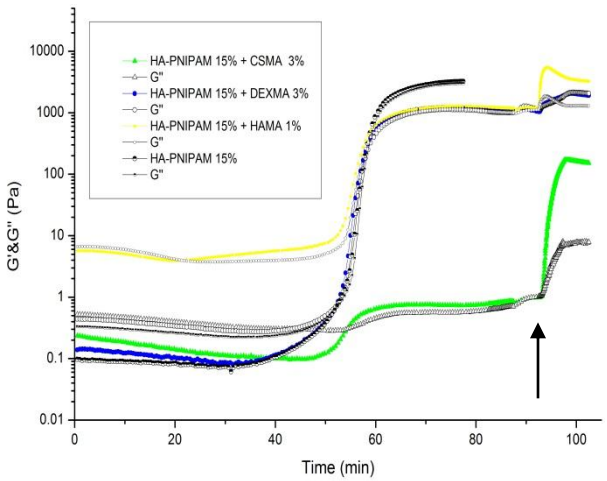

Fig. 1: *Tandem gelation of HA-PNIPAM biopolymer blends with temperature increase of 0.5C°/min between 4-45C°. HA-PNIPAM has lower critical solution temperature of 32 C°. Arrow points the UV- treatment start.*

The cell viability assays have shown over 90% viability after one day culture (Table 1).

Table 1: *Cell viability assay of biopolymers.*

Biopolymer	HAMA 1%	CSMA 3%	CSMA 5%	DEXMA 3%	DEXMA 5%
1 Day viab.	N/A	91%	94%	93%	N/A
7 Day viab.	98%	N/A	97%	58%	85%

DISCUSSION & CONCLUSIONS: The addition of methacrylated biopolymer decreases the initial gel stiffness after temperature gelling but allows instant gelling of the blend. Furthermore, the UV gelation is inversely proportional to the temperature gelation. Cell viabilities remained high except dextran methacrylated 3% and all gels maintained their original shape after 7 days from cell encapsulation. According to these preliminary results we can predict similar cell viabilities for the 3D hydrogel structures.

ACKNOWLEDGEMENTS: The work was funded European Union Seventh Framework Programme (FP7/2007-2013) under grant agreement n^{0}NMP4-SL-2009-229292.

P14 – Establishment of a novel organic/inorganic matrix system — a possible stepping stone to controllable vasculo–/angiogenesis

H. Kirch[1], J. Nickel[1], J. Probst[2], H. Walles[1]

[1] Department for Tissue Engineering and Regenerative Medicine, University Hospital Würzburg, Röntgenring 11, 97070 Würzburg, Germany; [2] Fraunhofer Institute for Silicate Research ISC, Neunerplatz 2, 97082 Würzburg, Germany

Introduction: The induction and control of vasculo- and/or angiogenesis is one of the more persistent problems in tissue engineering. Despite vigorous research efforts incorporating numerous different approaches, we are still far from controlling these processes. Based on prior data from our lab, a new silica gel based fibre material is combined with a proprietary collagen matrix "SISmuc" (acellularized porcine jejunum without serosa) and both human mesenchymal stem cells (hMSCs) and human microvascular endothelial cells (hmvEC) to achieve vasculo- and later angiogenesis in the scaffold. Due to the fibrous structure of the scaffold, guidance for the newly formed blood vessels may be achieved.

Materials & Methods: In this study, the material to be tested is a silica gel based fibre shaped as non-woven mat. Blanked disks (see Fig. 1) with diameter of 20 mm and approx. 1 mm thickness are seeded with $2x10^6$ hMSCs and cultured until the 3D-structure is saturated with cells and ECM after around 2-3 weeks (see Fig. 2). Concurrently, the SISmuc is seeded with hmvECs and cultured accordingly. The saturated scaffolds are then wrapped in the SISmuc, loosely stitched together and cultured for 2 weeks. As control, unmodified blanked disks and ones impregnated with collagen gel are used.

Outlook: In the future, we plan to upscale the system beyond the diffusion limit of ~200 µm. Additionally, our upscaling technique will allow the generation of an additive gradient to create a variety of effects, e.g. geometrically defined co-differentiation into chondrogenic and osteogenic lineage to create a bone-cartilage-interface.

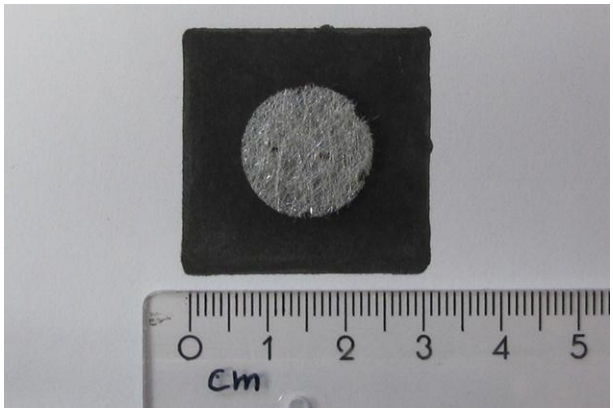

Figure 1: Scaffold disk blanked from the fibre mat. Note: Disk is slightly shrunken due to extended storage in an incubator (approx. 3 months).

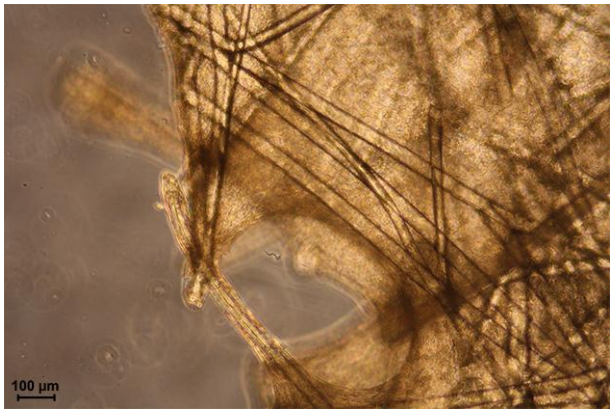

Figure 2: hMSCs on the edge of the scaffold. Note the saturation with ECM between the fibres.

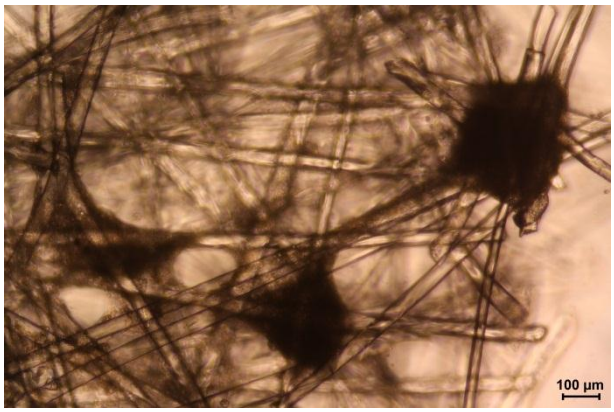

Figure 3: Adipogenically differentiated preadipocytes on the scaffold. Note the higher concentration of cells on intersections of fibres.

P15 – Interaction of blood components with titanium implant surfaces affects the osseointegration of bone implants

BS. Kopf[1], S. Lischer[1], S. Berner[2], K. Maniura-Weber[1]

[1] *Laboratory for Materials Biology Interactions, Empa, Lerchenfeldstr.5, 9014 St.Gallen, CH*

[2] *Institute Straumann AG, Peter Merian-Weg 12, 4002 Basel, CH*

INTRODUCTION:
Upon implantation the initial interaction of blood components and proteins with titanium (Ti) implant surfaces may affect the eventual adhesion, migration and differentiation of primary human osteogenic cells since blood protein adsorption and blood coagulation are greatly influenced by the topography and chemistry of Ti surfaces [1,2]. Thus, it may be of major importance to understand the early interaction between blood and the implant and how this steers osseointegration. In this study we investigated the blood coagulation on hydrophobic and hydrophilic micro-roughened Ti-surfaces. Additionally, we assessed the adsorption of blood proteins (fibrinogen, albumin and fibronectin) and found that the amount of protein layer formed from blood *in vitro* incubation of implant materials is decisive for later cell response. Further, bone cells/implant interactions and the differentiation potential of the osteogenic cells in such pre-formed microenvironment was evaluated.

METHODS: Material: Hydrophobic (SLA®) Ti and hydrophilic (SLActive®) sand-blasted and acid-etched Ti surfaces, which are commercially available implant surfaces from Institute Straumann AG.
Methods: The proliferation and differentiation potential of primary human bone cells (HBCs) were investigated. HBCs were cultivated on SLActive® and SLA® Ti surfaces, which had previously been incubated for 10 min with partially heparinized (0.5 IU/ml) human whole blood from healthy volunteers (with ethical approval). Blood coagulation was investigated by microscopy. Mineralization of cells was confirmed after 21 to 28 days using Xylenol Orange staining. Protein adsorption on the surfaces was investigated by application of fluorescently labeled proteins and intensity measurements using a microarray scanner (GenePix 2000A).

RESULTS: Enhanced blood coagulation was observed on SLActive® vs. SLA® Ti surface 10 min post incubation (Fig.1). Additionally, increased amounts of the proteins fibrinogen, albumin, and fibronectin over time had adsorbed on SLActive® vs. SLA® surfaces.
HBCs cultivated on SLActive® surfaces, previously incubated with blood, mineralized faster and to a higher extend compared to cells on pre-treated SLA® surfaces.

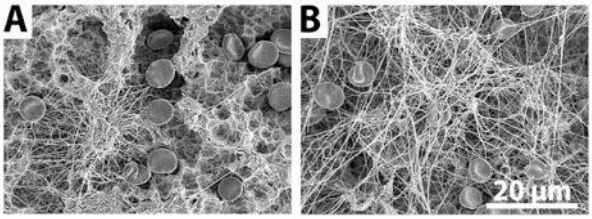

Fig.1: Fibrin fiber deposition on (A) SLA® and (B) SLActive® Ti-surface after incubation with partially heparinized blood for 10 min.

DISCUSSION & CONCLUSIONS:
The surface hydrophilicity of SLActive® Ti implant enhances blood coagulation, protein adsorption and promotes subsequent differentiation of HBCs in *in vitro* studies. Our results correlate with the reported enhanced osseointegration of SLActive® Ti implant as demonstrated in preclinical and clinical investigations [3-7]. In summary studying the interaction of blood components with implant surfaces might represent a predictive screening tool for novel implant surfaces.

REFERENCE:
[1] Hong *et al*., Biomaterials (1999), 20(7):603-11
[2] Milleret *et al*., Eur Cell Mater (2011), 21:430-44
[3] Buser *et al*., J Dent Res (2004), 83:529-533
[4] Ferguson *et al*., J Biomed Mater Res A (2006), 78: 291-297
[5] Schwarz *et al*., J Periodontol (2007), 78:2171-2184
[6] Schwarz *et al*., J Clin Periodontol (2008), 35:64-75
[7] Lang *et al*., Clin Oral Implants Res (2011), 22:349-356

ACKNOWLEDGEMENTS:
We thank the Swiss Commission for Technology and Innovation CTI (Grant no: 13747.1) for financial support.

P16 – Novel Hyaluronan scaffolds via diglycidyl ether crosslinking

A. La Gatta, A. Papa, A. D'Agostino, M. Cammarota, M. Frezza, M. De Rosa, C. Schiraldi

Department of Experimental Medicine, Faculty of Medicine, Second University of Naples, Naples, Italy

INTRODUCTION: Hyaluronic acid (HA) is recognized as a performing biopolymer for tissue engineering purposes due to a unique combination of properties among which magnificent biocompatibility, non immunogenicity, capacity to degrade in safe products, high hygroscopicity [1]. Actually HA has been widely used in the development of matrices conceived as scaffolds. When used for this purpose, HA has to be stabilized (mainly through crosslinking) to achieve the proper stability (resistance to chemical and enzymatic degradation) and mechanical performance in the biological environment. Many crosslinking strategies have been employed among which crosslinking processes involving the hydroxyl groups of the biopolymer. The latter are mainly achieved using a diglycidyl ether as the crosslinker [1]. This report presents an approach for the fabrication of HA based scaffolds using 1,4-butandiol diglycidyl ether as the crosslinker and their characterization.

METHODS: A 12,5%w/w aqueous solution of a low molecular weight HA (M_w = 220kDa) was lyophilized in order to obtain a microporous substrate, which was crosslinked in a non solvent for the biopolymer with increasing 1,4-butandiol diglycidy ether (BDDE) amounts (22-112% equivalents with respect to the hydroxyl groups on HA). Swelling properties of the resulting hydrogels, that proved not soluble in water, were investigated in water and phosphate buffer saline (PBS, pH 7.4, 0.165M ionic strength) by means of gravimetric measurements. Additionally, the swelling degree was evaluated as a function of ionic strength (0-0.165M) and pH (3-9) of the swelling medium. *In vitro* enzymatic degradation studies were performed by incubating materials with BTH at 100 and 1000U/mL at 37°C; degradation was monitored by measuring the amount of solubilized HA during incubation by the carbazole assay[2]. The stability of the hydrogels in cell culture medium (DMEM added with Calf Bovine Serum 10%v/v) at 37°C was evaluating likewise. A biological evaluation of the materials including cytotoxicity and cytocompatibility tests was performed using NIH 3T3 fibroblasts and performing the MTT test for the quantitative analyses [3].

RESULTS: The crosslinking process performed led to products insoluble in aqueous environment presenting an interconnected porous 3D architecture as confirmed by SEM observation. Swelling studies revealed that materials were able to absorb large amounts of water increasing their dry weight up to one hundred folds. Swelling capability was found coherently dependent on the ionic strength and pH of the swelling medium and on the BDDGE amount used. Hydrogels, when equilibrated in physiological solution, showed pores ranging from 70 to130µm and G' values were in the range 2-10kPa. The matrices exhibited high stability in cell culture conditions and to enzymatic degradation. Materials proved, beside the absence of cytotoxicity, appropriateness to promote cell adhesion and proliferation.

DISCUSSION & CONCLUSIONS:
Novel heterogeneous conditions were exploited for HA crosslinking aiming at producing scaffolds for tissue engineering purposes. The main achievement consists in that the novel conditions (BDDGE and heterogeneous reaction) permitted to obtain insoluble, directly structured and potentially applicable scaffolds with the lower content of crosslinker reported to date. The in vitro physico-chemical and biological characterization outcomes propose the hydrogels as promising substrates for soft tissues regeneration [4,5].

REFERENCES: [1] Schiraldi, C.et al., In *Biopolymers*; Elnashar, M., Ed.; published by Sciyo, Rijeka, Croatia 2010; pp. 387–412. [2] La Gatta A. et al., *Anal Biochem.* **2010**, 404, 21-29. [3] La Gatta A. et al., *J Biomed Mater Res.* **2009**, 90A, 292-302. [4] Hwang, H.D et al. *Colloids Surf B Biointer.*, 91, 106-113 (2012). [5] Yoon, I.S. et al. *J Biosci Bioeng,. 112*(4), 402-408 *(2011).*

P17 – Hip simulator study imitating edge loading

R. Lerf[1], J. Señaris[2], D. Delfosse[1]

[1] Innovation & Technology, Mathys Ltd Bettlach, Bettlach; [2] Complexo Hospitalario Universitario de Santiago de Compostela, Santiago de Compostela

INTRODUCTION: Edge loading in acetabular hip implants is generally due to mal-orientation or low tissue tension. It is known that edge loading of metal-on-metal THA may lead to higher metal wear and ion release with corresponding adverse body reactions. The inclination angle of the acetabular cup has been positively correlated with the wear rate of explanted components [1]. However, only limited data is known about wear rates of edge loaded hard – soft hip bearings.

METHODS: For the hip simulator study, seleXys cup inlays, size 28/EE, (Mathys Ltd Bettlach, Switzerland) were used. Standard PE parts and vitamys® inlays (highly cross-linked, vitamin E stabilised UHMWPE) were tested in the same run. PE inlays were machined out of sintered GUR 1020 slabs, packaged and gamma-sterilised in inert atmosphere at 30 kGy. The vitamys® material was made in-house by adding 0.1 wt.-% of vitamin E to GUR 1020 powder from Ticona GmbH, Kelsterbach/Germany. Cross-linking used 100 kGy gamma-irradiation and the final sterilisation was gas plasma. Cup inclination was varied: besides the protocol of ISO 14242 with an inclination angle corresponding to 45 ° in the medial-lateral plane, a steep cup position corresponding to 80 ° was tested, too. To our knowledge, this is the highest inclination angle ever tested in a hip simulator. The testing was conducted in a servo-hydraulic six-station hip simulator (Endolab, Thansau/Rosenheim, Germany) at a temperature of 37±1°C. Tests were run at the RMS Foundation (Bettlach, Switzerland) for five million cycles. The test fluid was diluted bovine serum stabilised with sodium azide and EDTA. At lubricant change interval of 500'000 cycles, the inlays were measured gravimetrically with an accuracy of 0.01 mg.

RESULTS: The wear rate of the standard UHMWPE inlays tested with an inclination of 80° was 16% lower than those of the inlays with 45 ° inclination. For the vitamys® inlays, wear rates were about the same for both inclination angles (cf. Figure 1). After the test, the 45 ° inlays were polished tribologically on about 2/3 of the articulation surface (vitamys®, Figure 2a) or almost the whole articulation (standard PE). The polished surface of the 80 ° inclination samples was on the caudal wall of the inlays while on the pole the tool-marks were still present (Figure 2b, vitamys®). Hence, the hard – soft bearings tested showed no significant effect due to inclination angle on the wear rate. This is true for a position as steep as 80 °, just before subluxation would occur.

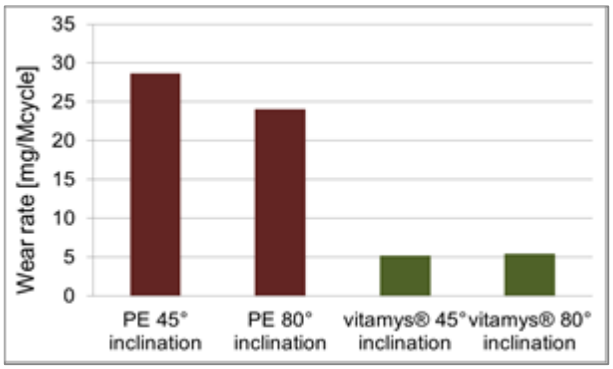

Fig. 1: Wear rates of conventional UHMWPE and vitamys® under standard hip simulator settings (45° inclination) and mimicking edge loading (80° inclination).

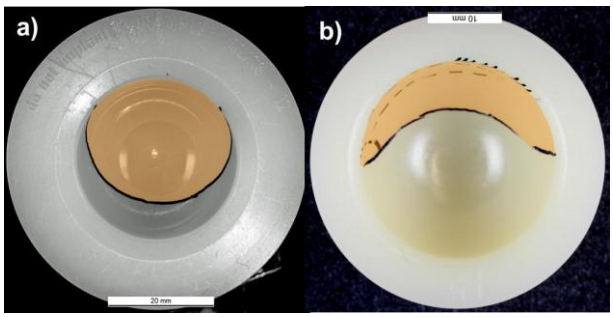

Fig. 2: Articulation surface of a vitamys® inlay after 5 million cycles (worn area in amber):
a) Inclination 45°
b) Inclination 80°.

DISCUSSION & CONCLUSIONS: Based on the present hip simulator study, it seems that metal-on-polyethylene bearings are exempt from accelerated wear rate when subjected to edge loading conditions. Using the newest generation of HXLPE, stabilised with vitamin E, combines superior oxidation resistance [2], low wear and highest forgiveness for component mal-orientation.

REFERENCES: [1] Morlock MM et al., JBJS Am 2008;90 (Suppl 3), 89-95 [2] Lerf R et al., Biomaterials 2010;31: 3643–3648.

P18 – Choice of cell type and test method defines the results of a cytotoxicity study of HA coatings according to ISO-norm 10993-5

S. Lischer[1], U. Tobler[1], Ph. Gruner[2] K. Maniura-Weber[1]

[1] *Empa, Swiss Federal Laboratories for Materials Science & Technology, Laboratory for Materials-Biology Interactions, Lerchenfeldstr. 5, CH-9014 St. Gallen*

[2]*Medicoat AG, Gewerbe Nord, CH-5506 Mägenwil*

INTRODUCTION: Total hip arthroplasties have become a standard surgical procedure with a high success rate[1]. Orthopedic joint prostheses that mostly consist of titanium are often coated with bioactive ceramics like hydroxyapatite (HA) to improve their bioactivity and with this their osseointegration. Although HA coated hip endoprosthetic devices have been used for more than 20 years in orthopaedic surgery[2] regular cytotoxicity tests are required to prove that the material batches are safe. The standardised biological evaluation of medical devices is based on the ISO-norm 10993-5 that proposes three tests for cytotoxicity assessment: extract test, direct and indirect contact test[3]. The ISO-norm recommends the use of cell lines like 3T3 or L929 mouse fibroblasts due to their reproducible growth rate and homogenous cell population but these cells are not relevant for the intended application of the biomaterial[3]. The use of primary human cells mimics more closely the *in vivo* situation and allows the study of specific cell type reaction. The aim of our study was to compare the cell behaviour of cell lines and primary cells by testing the cytotoxicity of HA coatings.

METHODS: HA coatings were incubated in extract media at 3 cm^2/ml at 37 °C for 72 h, thereafter the extract was added to a 24 h pre-seeded cell culture of human primary bone cells (HBC) or 3T3 mouse fibroblasts for 5 days. The cytotoxic effect on cellular activity and proliferation was quantified by MTT and DNA assay. The growth rate of 3T3 cells and HBCs was determined by DNA quantification.

RESULTS: The cytotoxic potential of HA coatings was analysed with primary human bone cells and 3T3 mouse fibroblasts using the extract test. The quantitative analysis of the cytotoxicity assay showed that the tested HA coatings are cytocompatible to both cell types. However, the sensitivity of the primary human bone cells and the mouse fibroblast cell line 3T3 to HA was different. The cell activity of 3T3 cells decreased to lower levels with the extract but was still around 70 %, which defines the threshold for an extract to be toxic. In contrast human bone cells showed a slight increased cell activity with increasing concentration of the extract.

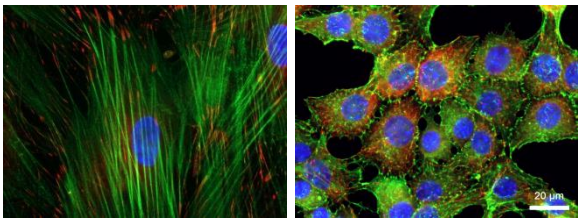

Fig 1: HBCs and 3T3 cells on TCPS control.

The origin and cell behaviour of cell lines and primary cells is very different. 3T3 cells showed a faster cell proliferation, HBCs have larger cell morphology and exhibited a more pronounced actin cytoskeleton.

DISCUSSION & CONCLUSIONS: This work demonstrates that cell lines and primary cells show different cell behaviour and sensitivity in testing the cytotoxicity of HA coatings. By using primary human cells which will actually be in contact with the biomaterial *in vivo*, a more suitable model for the *in vivo* situation of HA coatings is provided.

REFERENCES:

[1]Layrolle et al., (2011), 1.112 - Calcium Phosphate Coatings. In: Editor-in-chief: Ducheyne, P. (ed.) Comprehensive Biomaterials. Oxford: Elsevier., [2]Shepperd et al., (2005) A contemporary snapshot of the use of hydroxyapatite coating in orthopaedic surgery. J Bone Joint Surg Br, 87-B, 1046-1049. [3]Bruinink et al., (2012) Evaluation of Biocompatibility using in vitro methods: Interpretation and Limitations. Adv Biochem Engin/Biotechnolog 126:117-152

P19 – Evaluation of thermoplastic starch and nano-biocomposite of thermoplastic starch/beta tricalcium phosphate for bone tissue engineering applications

M. Taherimehr[1], R. Bagheri[1], H. Maddah Hoseini[1], M. Baghaban Eslaminejad[2]

[1] *Polymeric material research group, Department of Material Science and Engineering, Sharif University of Technology, Tehran, Iran*

[2] *Department of Stem Cells and Developmental Biology at Cell Sciences Research Center, Royan Institute for Stem Cell Biology and Technology, ACECR, Tehran, Iran*

INTRODUCTION: Biodegradable polymers and their composites that are used as implant materials need to be biocompatible and their degradation products should not be cytotoxic [1-2]. In this work, Thermoplastic starch (TPS) as a biodegradable and non-toxic polymer and its composites with beta tricalcium phosphate (β-TCP) were analysed in terms of degradation, and biomineralization, when they were immersed in simulated body fluid (SBF). Ceramic- matrix dispersion was evaluated by using scanning electron microscopy (SEM); β-TCP powder was characterized using dynamic light scattering (DLS) and X-ray diffraction (XRD) as well. Mechanical properties and in-vitro biocompatibility of the TPS and nanocomposites were also investigated.

METHODS: Cornstarch, glycerol, $CaCO_3$, and $CaHPO_4$ were used in this research. β -TCP nano powder was prepared by using mixture of $CaHPO_4$ and $CaCO_3$ with a molar ratio of 1:2. The phase compositions and sizes of the β -TCP nanoparticles were analysed by XRD and DLS, respectively. For producing TPS and nanocomposites, starch (70 wt %) and glycerol (30 wt %) and β-TCP (0, 3, 5, and 10 wt. %) were mixed using ultra-sonication and fed into a twin screw extruder. Standard tensile and impact test specimens were made via injection molding technique. These tests were undertaken as outlined in ASTM D638 and ASTM D256. Moreover, Weight loss, swelling degree in simulated body fluid (SBF) [2] and MTT assay were investigated. SEM was incorporated to evaluate dispersion of β-TCP nanopowder in the matrix as well as biomineralization of the nanocomposites after incubation in 5-SBF [3].

RESULTS: XRD and DLS results show that β-TCP is the major phase in synthesised powders and the mean particle size of β-TCP nanopowders were 61.1nm. Table 1 shows results of tensile and impact tests of the samples. Figure 1 shows SEM micrograph of the TT10 before and after treatment in 5-SBF (EDAX result, Ca/P: 1.67). The effect of extracts of TPS and TT10 on MSCs viability was evaluated: TPS: 99.1%, TT10: 97.2%. The percentages of degradation and water absorption in SBF after 28 days were 47% & 460% for TPS and 51% & 492% for TT10, respectively.

Table 1. Mechanical properties.

Samples	Tensile Modulus (MPa)	Ultimate Tensile Strength (MPa)	Impact Energy (kJ/m^2)
TPS	66.54	1.67	4.18
TT3	96.72	2.27	2.32
TT5	160.34	2.62	1.91
TT10	390.5	4.68	0.94

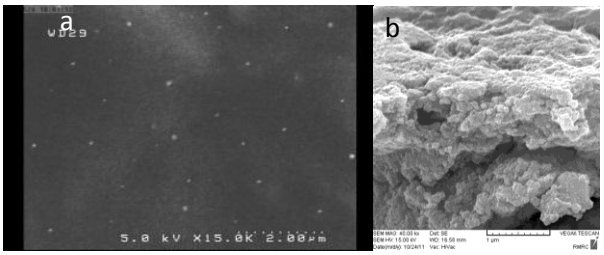

Fig. 1: (a) SEM micrograph of TT10 (15kx), (b) SEM micrograph of biomineralized TT10 (40.0kx)

DISCUSSION & CONCLUSIONS: SEM micrograph of TT10 demonstrates that β -TCP particles homogenously dispersed in the polymeric matrix. The composite exhibited improved tensile modulus and ultimate tensile strength though its deformation and toughness have declined significantly. Because of high hydrophilicity, TPS and TT10 presented high water absorption ability and degradation rate. TT10 had no negative impact in cytotoxicity assay and showed excellent compatibility.

REFERENCES: [1] DA Wahl and JT Czernuszka (2006) *J European Cells and Materials* **11**:43-56. [2] Q. Cai, Q. Feng, H. Liu, et al (2013) *J Materials Letters* **91**: 275-278. [3] R. Shi, A Zhu, D. Chen, et al (2010) *J Applied Polymer Science* **115**: 346-357. [4] M.G Raucci, V Guarino and L Ambrosio (2010) *J Composites Science and Technology* **70***:* 1861-1868

P20 – Smart, enzymatically cross-linkable hydrogels as three-dimensional models of tissue ageing and fibrosis

G. Mattei[1,2,4], A. Tirella[2,3], A. Ahluwalia[2], N. Tirelli[4]

[1] Department of Civil and Industrial Engineering, University of Pisa, IT. [2] Research Centre "E. Piaggio, University of Pisa, IT. [3] Institute of Clinical Physiology, CNR, Pisa, IT. [4] School of Materials, University of Manchester, UK

INTRODUCTION: Nowadays, scientists are shifting their focus from 2D cell monolayers grown on plastic to 3D cell cultures, implementing more relevant in-vitro models to predict the complex behaviour of biological systems [1]. Our study is focused on the development of 3D pathophysiological models of soft organs, presenting the use of synthetic hydrogels as 3D models of biological hardening (contraction, ageing and fibrosis) phenomena. In fact, tissue ageing and fibrotic pathologies are generally associated with an enzyme-mediated stiffening of extracellular matrices (ECMs) and/or production of reactive oxygen species (ROS) [2]. Therefore we developed materials that can produce both effects, either in isolation or in combination to study cell response to this cues.

METHODS: Hydrogels with tunable elastic moduli were obtained following a two-step crosslinking procedure: first, a healthy hydrogel is obtained via photo-polymerisation of appropriate mixtures of mono- and di-acrylate poly(ethylene glycol) derivatives containing different amounts of primary amines. Afterwards, the healthy hydrogel is modified to a pathological/aged one, by adding an amine cross-linker which causes hydrogel stiffening with or without ROS release. Hydrogel design was based on two major hypotheses: i) healthy hydrogel mechano-structural properties are mainly dictated by the acrylate/diacrylate molar ratio (A/DA), and ii) hydrogel stiffening towards pathological/aged models is a function of the amino content, expressed here as amine/acrylate molar ratio (NH_2/A). Three different hydrogel families in terms of A/DA were investigated keeping a constant total PEG content of 5% w/v. Each A/DA family was functionalised with three different amine contents (NH_2/A=0.00, 0.05, 0.10). NH_2/A was considered and compensated for while preparing hydrogel precursor solutions to obtain the desired A/DA, generating a library of hydrogels were the densities of cross-links (hence the resulting healthy stiffness) could be varied independently on the amine content. Healthy hydrogels were then exposed to either lysyl oxidase (LOx, an enzyme typically involved in ECM cross-linking) or to glyoxal (GO, a low molecular weight amine cross-linker, used as a positive control for LOx cross-linking). The reactions were optimised on soluble model systems prior to their application in hydrogels.

RESULTS: Rheological (G'), compressive (E) and swelling (Q) properties of healthy hydrogels were found to be decoupled from their amino content and dictated only by different A/DA, confirming the experimental hypotheses for hydrogel design (Table 1).

Table 1. Healthy gel properties (mean ± std. dev.)

A/DA	G' (kPa)	E (kPa)	Q
0.25	1.22 ± 0.04	3.81 ± 0.12	20.0 ± 0.3
0.50	0.59 ± 0.06	1.81 ± 0.08	24.4 ± 1.1
0.75	0.28 ± 0.03	0.81 ± 0.05	31.0 ± 1.0

GO and LOx amino cross-linking reactions exhibited similar kinetic and conversion: about 40% of initial free -NH2 in the gel reacted, resulting in a compressive averaged hydrogel stiffening of 126 ± 13 Pa per mmol of reacted amine. These values match those of healthy and fibrotic liver [3].

DISCUSSION & CONCLUSIONS: A library of hydrogels with tunable mechanical properties (function of A/DA ratio and total PEG content) was developed. Hydrogels reproducing the healthy modulus of specific tissue/organ of interest can be easily obtained, while different stages of organ disease/ageing can be obtained via a subsequent LOx crosslinking reaction.

REFERENCES: [1] H. Geckil, F. Xu, X. Zhang, et al (2010) *Nanomedicine* **5(3)**:469-84. [2] C. Frantz, K. Stewart, and V. Weaver (2010) *Journal of cell science* **123**:4195-200. [3] W. Yeh, P. Li, Y. Jeng, et al. (2002) *Ultrasound in Medicine and Biology* **28(4)**:467-74.

P21 – Nano-fibrous polyurethane/chitosan multi-layers as a novel wound dressing

H. Mirzadeh[1], A. Mirzaei[1], Y. Ghazizadeh[1], M. Daliri[2]
[1] *Amirkabir University of Technology (Tehran Polytechnic,) Tehran, Iran*

[2]*National Institute of Genetic Engineering and Biotechnology, Tehran, Iran*

INTRODUCTION: Chitosan is a non-toxic, antibacterial, biodegradable and biocompatible biopolymer. Based on these properties, chitosan is widely used for biomedical applications such as tissue engineering. However, chitosan has poor mechanical properties. In contrary, polyurethane has good biocompability, flexibility and mechanical properties. Therefore, polyurethane and chitosan as a composite possesses good advantages for wound dressing applications. Recently, electrospining process has been widely used to produce nanofibrous mats that can mimic extracellular matrix (ECM) [l].

In this study, for the first time, nanofibrous polyurethane/chitosan multi-layers mats were prepared by electrospinning of chitosan and polyurethane solutions on a same collector.

METHODS: Various grades of chitosan (Sigma–Aldrich) with different degree of deacetylation (DD) and molecular weights by dissolving 2- 3 wt% in Trifluoroacetic acid/dicholoromethane 70/30(v/v) solvent systems and were electrospun with applied voltage 15- 20 kV. Caprolactone based polyurethane (Sigma–Aldrich) was dissolved in two different solvent systems including tetrahydrofuran/dimethyl formamide and tetrahydrofuran/dimethylacetamide (all Merck) 60/40(v/v) and electrospun by applied voltage 7-12 kV. The efficacy and potential of the electrospun polyurethane/chitosan nanofibrous mats as wound dressing were evaluated by both in *vitro* and *in vivo* assays. The morphology of electrospun mats and cells were examined by scanning electron microscopy.

RESULTS: Electrospinnability of both chitosan and polyurethane solutions were found by changing solvents, concentrations of the solution and applied voltages as key parameters to achieve nano-fibrous mats. The obtained nano-fibers were smooth and beads free. Fourier transform infrared microscopy (FTIR) results showed no significant structural difference between chitosan powder and salt treated electrspun nanofibers. For cell culture assays on multi-layers mats, all results were compared with the corresponding chitosan and polyurethane one layer mats, separately. The multi-layers mats showed an excellent fibroblast cell attachment and proliferation and after 48 h cell culture, a confluent monolayer of cells was formed on them (Fig. 1). *In vivo* study on rats using multi-layers mats as wound dressing showed improvement of wound healing significantly, in comparison with those wounds which were left without multi-layers electrospun mats.

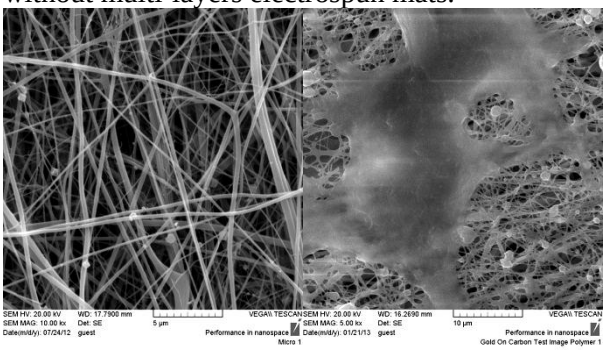

Fig. 1: SEM Images of electrospun nanofiber PU/CS mat (left) and fibroblast cell on mat (right)

DISCUSSION & CONCLUSIONS: It was found that DD of chitosan has more pronounced effect on the polymer concentration window of electrospinnability rather than molecular weight. Higher dielectric constant of the polyurethane solvent system led to eliminate the beads on fiber and reducing the average fiber diameter and consequently cause more cell stimulation and proliferation due to more contacts with cell membrane. Based on *in vitro* and *in vivo* results we conclude that a PU/CS mat has an excellent potential for wound healing [2].

REFERENCES: [1] J.A. Matthews, G.E. Wnek, D.G. Simpson, and G.L. Bowlin (2002) *Biomacromolecules, 3 (2) pp 232-238.* [2] A. Mirzaei, H. Mirzadeh, Y. Ghazizadeh (2012) Preparation of Chitosan Electrospun Nanofibers as Wound Dressing, *ISPST2012, Amirkabir University of Technology, Tehran, Iran, 21-25 October 2012.*

ACKNOWLEDGMENTS*:* The authors appreciate Iran National Science Foundation (INSF) for financial supporting of this research work.

P22 – Thermoresponsive-biopolymer blends as bio-inks for cartilage engineering

M. Müller[1], Jana Becher[2], Matthias Schnabelrauch[2], M. Zenobi-Wong[1]

[1]*Cartilage Engineering + Regeneration, ETH Zürich, Zürich, Switzerland. 2Biomaterials Department, Innovent e.V., Jena, Germany*

INTRODUCTION: An ideal bio-ink for extrusion printing should be liquid at the beginning to mix it freely with other polymers, peptides or cells. After mixing, the flow behavior must be compatible with the extrusion printing process. For printing fidelity, cessation of flow upon deposition is also necessary. We investigated the properties of blends of themoresponsive and photopolymerizable polymers for their suitability as bio-inks in extrusion bioprinting.

METHODS: Methacrylated Pluronic F127 (PF127-DMA) was used as the thermoresponsive element of the bio-ink. PF127-DMA was blended with hyaluronic acid, dextran and chondroitin sulfate (all methacrylated). The blends were analyzed with an Anton Paar MCR301 rheometer utilizing a cone-plate geometry. Flow curves were recorded to test the printability of the blends. Temperature ramps and UV crosslinking under oscillation were performed to investigate the gelling kinetics of the two gelation steps. Chondrocyte viability was assessed with a live/dead assay at 1 and 7 days after the encapsulation with UV-crosslinking in the PF127-biopolymer hydrogel blends.

RESULTS:

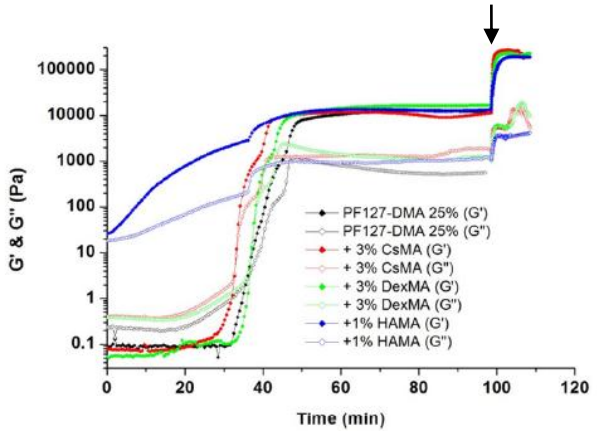

Fig. 1: Tandem gelation curves for PF127-DMA mixed with 1% hyaluronic acid methacrylate (blue curve) and 3% methacrylated chondroitin sulphate (red curve) or dextran (green curve) respectively. Full symbols represent the G' values, empty symbols the G'' values. The arrow indicates the onset of UV exposure.

The rheological measurements of PF127-DMA blended with the biopolymers reveal that the gelation temperature is slightly decreased upon the addition of 3% chondroitin sulfate methacrylate and 1% hyaluronic acid methacrylate (see Fig. 1). This effect was less pronounced in the blend with dextran methacrylate. After UV-crosslinking, the final mechanical properties are similar for all the conditions (Fig. 1).

Preliminary results with PF127-DMA-biopolymer blends show that chondrocytes have improved viability after one day of culture within the hydrogel compared to pure PF127-DMA hydrogels, however cell viability dropped by day 7 for all conditions. Due to the good 3D printing properties of the PF127 (see Figure 2) it is desirable to improve the long term viability and use PF127 based inks for bioprinting.

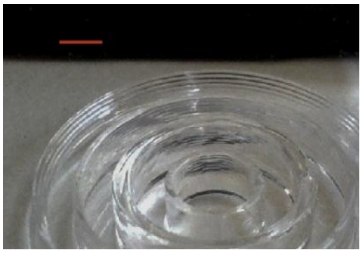

Figure 2: 3D printed construct with PF127. The red bar indicates2 mm

DISCUSSION & CONCLUSIONS: Rheological measurements indicate that the addition of biopolymers can influence the gelation temperature of PF127-DMA without influencing final storage moduli. Therefore the good printability of Pluronic is conserved in the blends. In case of negatively charged biopolymers the gelation temperature seems to decrease whereas for neutral biopolymers such as dextran methacrylate there is hardly any change. The mechanical properties are similar between the pure and blended PF127-DMA which indicates that the PF127-DMA network is responsible for the mechanical strength. Methods to improve cell viability by encapsulating the cells are being investigated.

ACKNOWLEDGEMENTS: The work was funded European Union Seventh Framework Programme (FP7/2007-2013) under grant agreement n^{0}NMP4-SL-2009-229292.

P23 – Sulfated, acrylated hyaluronan hydrogels for chondrogenesis of mesenchymal stem cells

E. Öztürk[1], Jana Becher[2], Matthias Schnabelrauch[2], M. Zenobi-Wong[1]

[1]Cartilage Engineering+ Regeneration Laboratory, ETH Zürich, Switzerland [2]Biomaterials Department, Innovent e.V., Jena, Germany

INTRODUCTION: Hydrogel-based scaffolds inspired from extracellular matrix(ECM) components have been a popular approach for cartilage tissue engineering. Hyaluronan (HA) is an anionic, non-sulfated biopolymer abundant in cartilage with high water retention properties. Although HA is attractive for its biocompatibility and degradability, its non-adhesiveness prevents cell spreading. We investigated the effect of sulfate groups on acrylated HA (HA-A) for promoting spreading of re-differentiating chondrocytes and the potential of sulfated, acrylated HA (HA-AS) for chondrogenesis of mesenchymal stem cells (MSC).

METHODS: HA-A and HA-AS hydrogels were formed with UV photocrosslinking via LAP. Hydrogels of different polymer concentrations were mechanically tested for elastic moduli with a texture analyzer (Stable Microsystems). Bovine chondrocytes (bCh) were isolated from six month-old calf knees and cultured until passage 3. De-differentiated bChs were encapsulated in HA-A and HA-AS hydrogels and cultured up to four weeks while cell morphology was monitored. Human bone marrow- derived MSCs were also encapsulated in HA-A and HA-AS hydrogels and cultured in chondrogenic media for 7 days. MSCs were cultured in pellets as control. Expression of chondrogenic markers were assayed with qRT-PCR.

RESULTS: The concentration of HA-AS for stable hydrogels that could be cultured up to 4 weeks was found to be 5% (w/v). The elastic modulus of 5% HA-AS gels was measured as 0.96 kPa (Fig. 1). HA-A hydrogels were much stiffer than HA-AS gels at comparable concentrations. A range of concentrations of HA-A hydrogels were tested to have a similar stiffness to that of 5% HA-AS and 0.4% HA-A with a modulus of 1.07 kPa was chosen for comparison in further experiments. Sulfated HA hydrogels induced spreading of bChs starting from the second week of culturing (Fig. 2) whereas the cells encapsulated in non-sulfated hydrogels kept a round morphology for 4 weeks. MSCs encapsulated in HA hydrogels were superior to pellets regarding the expression of collagen2 and Sox9 genes. Furthermore, the sulfated hydrogels resulted in decreased expression of hypertrophic markers such as collagen 10 and MMP-13 compared to non-sulfated hydrogels.

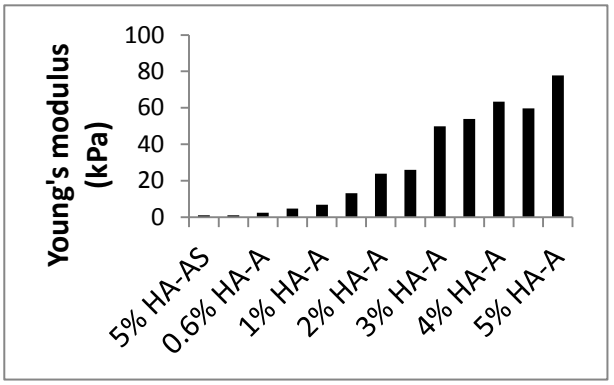

Fig. 1: Elastic moduli of 5% (w/v) HA-AS and 5%-0.4% HA-A hydrogels.

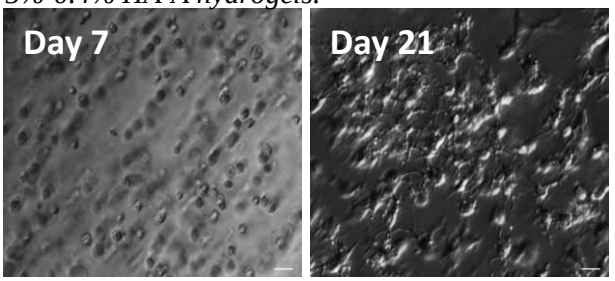

Fig. 2: Morphology of passage 3 bChs in 5% (w/v) HA-AS hydrogels. (Scale: 20 µm).

DISCUSSION & CONCLUSIONS: Sulfated and acrylated HA overcomes the non-adhesive properties of native HA hydrogels. It presents a useful tool for applications where spread cell morphology could be desired and beneficial for functional tissue formation or regeneration. Hence, it is shown to be a promising approach for chondrogenesis of bone marrow- derived MSCs which show increased expression of chondrogenic markers and prevention of hypertrophic markers compared to non-sulfated hydrogels and pellet culturing.

ACKNOWLEDGEMENTS: The work was funded by the European Union Seventh Framework Programme (FP7/2007-2013) under grant agreement n^{0}NMP4-SL-2009-229292.

P24 – Sulfation of alginate promotes 3D neuronal growth

G. Palazzolo[1], N. Broguiere[1], J. Becher[2], M. Schnabelrauch[2], M. Zenobi-Wong[1]

[1] *Cartilage Engineering + Regeneration Laboratory, ETH Zurich, Zurich, CH*

[2] *Innovent Technologieentwicklung, Jena, Germany*

INTRODUCTION: Heparan sulfate proteoglycans are key regulators in brain delevopment[1]. In particular, sulfation revealed to be essential for neural differentiation[2]. Here we show that sulfation of a natural polysaccharide, alginate, generates a scaffold ideal for promoting neuronal growth.

METHODS: Cortical neurons were obtained by dissociation of the E17 rat embryo cortex with 0.05% papain for 15 min. Dissociated neurons were encapsulated at the density of 10 million cells/ml in 2% (w/v) sulfated alginate dissolved in 150mM NaCl. Hydrogel disks (30 µL) were polymerized into casters (Qgel, AG) soaked in 102 mM $CaCl_2$ for 8min. Disks were then transferred in 51 mM $CaCl_2$ for 8 min, washed 3 times x 2 min in 3 mM $CaCl_2$. Eventually the gels were cultured for 1 day in DMEM + 10% FCS + 1.75mM $CaCl_2$, after which they were maintained in Neurobasal medium + B27 +1.75 mM $CaCl_2$ up to 20 days. As control, cells were either cultured in 0.4% and 2% pure alginate or in 2D culture plastics coated with poly-L-Lysine and laminin. A viability assay (LIVE/DEAD® kit, Invitrogen) was carried out after 7, 14 and 21 days in culture, according to the manufacturer's instructions. Hydrogel disks (150 µL) were prepared as described above for the rheology experiments which were conducted on an Anton Paar MCR301 rheometer using a 10mm-diameter parallel plate geometry.

RESULTS: We found that primary neurons maintain 70% viability over 21 day culture in 3D sulfated alginate, which is comparable to 2D cultures, and undergo extensive neurite formation (Fig. 1), while poor cell viability and no neurite formation is observed in pure alginate. Shear stress experiments showed that at low frequency sulfated alginate has a storage modulus of 50 Pascal (Fig. 2) while for pure alginates the storage moduli are usually in the range of thousands Pascal[3].

DISCUSSION & CONCLUSIONS: Sulfated alginate promotes extensive neuronal growth, possibly related to both softness and biological cues, due to the sulfate groups. Therefore it represents a promising biomaterial for neural tissue engineering applications.

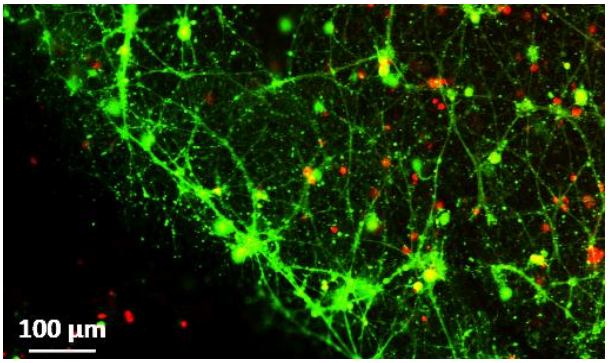

Fig. 1: Viability of primary rat cortical neurons after 21 days in 2% sulfated alginate. Green: live cells; red: dead cells.

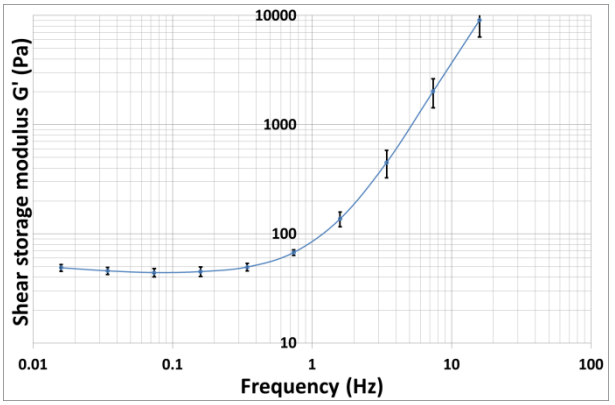

Fig. 2: Shear storage modulus of cell-encapsulated 2% sulfated alginate. Data from three separate measurements are shown as means + s.e.m.

REFERENCES: [1]D. Stickens, B.M. Zak, N. Rougier et al (2005) *Development* **132**:5055-5068. [2]M. Forsberg, K. Holmborn, S. Kundu et al (2012) *J Biol Chem* **287**:10853-62. [3]M. Davidovich-Pinhas, H. Bianco-Peled (2010) *Carbohyd Pol* **79**:1020–1027

ACKNOWLEDGEMENTS: This research has been supported by the 3D NeuroN project (http://www.3dneuron.eu) in the European Union's Seventh Framework Programme, Future and Emerging Technologies (grant agreement n° 296590) and by the European Union Seventh Framework Programme (FP7/2007-2013) under grant agreement n° NMP4-SL-2009-229292 (Find&Bind). Authors thank Prof. Jean-Marc Fritschy (University of Zurich) for providing the rat embryo cortex.

P25 – Bioorthogonal reaction for two-step labeling of Staphylococcus aureus with Lysostaphin.

I. Potapova [1], D. Eglin [1], MW. Laschke [2], M. Bischoff [3], RG. Richards [1], TF. Moriarty [1]

[1] AO Foundation, Davos, CH. [2] Institute for Clinical and Experimental Surgery and [3] Medical Microbiology and Hygiene, University of Saarland, D

INTRODUCTION: Current clinical infection diagnostics is time consuming and invasive and relays on microbiological cultures. Meanwhile probes enabling rapid and specific detection of infection *in vivo* shall improve the situation. We investigated the potential of Lysostaphin as a specific probe to detect staphylococci in a new labeling protocol. Azido (N_3) - modified Lysostaphin and DIBO-dye were used in a two-step bacteria-labeling protocol. N_3 and DIBO (di-benzocyclooctyne) are the counterparts of a bioorthogonal "click" reaction. In the first step, Lysostaphin-N_3 bound specifically to *Staphylococcus aureus*. In the second step, bound N_3 clicked to DIBO thus achieving *S. aureus* selective labeling (Figure 1). This two-step approach effectively distinguished *S. aureus* from *Escherichia coli*; was non-toxic and proved to work *in vivo*. The two-step labeling protocol is a promising approach for diagnostic imaging of staphylococci in clinical settings.

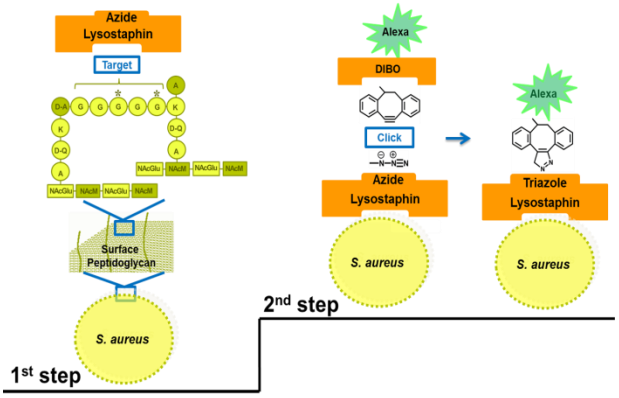

Fig 1: Two step labeling of S. aureus: 1st Step Lysostaphin-Azide targets surface peptidoglycan of S. aureus; 2nd Step DIBO-Alexa reacts with Lysostaphin-Azide.

METHODS: *S. aureus* NCTC 10788 and *E. coli* NCTC 12241 (from National Collection of Type Cultures), primary sheep osteoblasts and C57BL/6 mice were used for this study. DIBO-Alexa488 (Invitrogen ®), DyeLight488 (Thermofisher ®), NHS-N_3 (Lumiprobe ®), Lysostaphin (Sigma-Aldrich ®) were purchased. *In vitro* we used standard microbiological protocols to assess antimicrobial and labeling activity of Lysostaphin-N_3 and DIBO-dye "click" probes, and pre-labeled Lysostaphin-Dye and non-labeled Lysostaphin controls. Flow cytometry, Fluorescence microscopy, and Spectrophotometry were employed. The cytotoxicity of the probes on osteoblasts was performed using Presto Blue Cell Viability test (Invitrogen ®). *In vivo* we used Fluorescence Intravital Microscopy and mice blood infection model (approved by the local governmental animal care committee).

RESULTS & DISCUSSION: The modified Lysostaphin-N_3 partially lost its antimicrobial property, but still bound *S. aureus* efficiently and clicked DIBO-dye afterwards. There was no significant cytotoxicity of "click" reagents on sheep osteoblasts. *In vitro* the two-step labeling with Lysostaphin-Click was more efficient than the one-step with Lysostaphin-Dye. *In vivo* the one-step and two-step labeling were qualitatively different. In the two-step protocol the "click" probe labeled adherent to blood vessels and extravasated into the soft tissue bacteria (Figure 2) better.

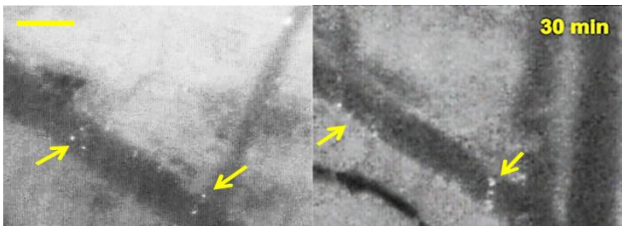

Fig 2: In vivo labeling of intravenous S. aureus in mice 30 minutes after the injections. Left: One-step; Right: Two-step protocol. Arrows point labeled bacteria. Scale bar 100 µm.

OUTLOOK: Currently we extend the study towards labeling *S. epidermidis*, and *S. aureus* intracellular and in biofilms.

ACKNOWLEDGEMENTS: MSc Ewa Czekanska, Sascha Kleer, Prof Dr Michael D. Menger.

P26 – Opportunities and limits of *in vitro* cytotoxicity test methods exemplified by powder metallurgy titanium alloys

M. Pusnik[1], A. Bruinink[2], M. Rodriguez-Arbaizar[3], E. Carreño-Morelli[3] and M. Zinn[1]

[1]Institute of Life Technologies, HES-SO Valais, Sion, CH. [2]Materials-Biology Interactions, EMPA, St. Gallen, CH. [3]Institute of Systems Engineering, HES-SO Valais, Sion, CH.

INTRODUCTION: Testing for *in vitro* cytotoxicity aims at obtaining data for a test material from simplified *in vitro* systems that can be used to make a prognosis for a key step within the processes occurring after implantation in the human body. Depending on the application of the test specimens, one can choose from a number of different assays to assess its bioacceptance in terms of absence of cytotoxicity. While guidelines (e.g. ISO, ASTM) describe a number of mandatory test procedures for official approval, additional tests have to be performed to properly evaluate the *in vitro* effects of test specimen on cells. However, in most cases it is difficult to select the appropriate assay. In addition, the conclusions that can be made out of the results are often limited [1]. They give trends rather than enable clear-cut recommendations. In this work we evaluate for the bioacceptance of different Ti alloys by two different assays; the agar overlay test and the extraction test, both described by the ISO 10993-5 guidelines. Opportunities and limits of cytotoxicity testing based on these and other methods will be discussed.

METHODS: Various Ti alloy samples were prepared by powder injection moulding. Sintered parts were sterilized by autoclaving or hydrogen peroxide gas plasma. The agar overlay test as well as the extraction tests were performed according to the ISO 10993-5 guideline. In case of the agar overlay test cells were vitally labelled using neutral red before use. After 24, 48 and 72 h of treatment toxicity was assessed taking the size of the zone without cells as an index. In case of the extract test cytotoxicity was assessed after 24h of treatment using neutral red and MTT (or WST-8) assays. From the obtained extracts the ions were quantified by ICP-EOS.

RESULTS: Large differences in outcome were obtained by evaluating the titanium alloys using agar overlay and extract tests with the agar overlay test being most sensitive. Only in the case of the agar overlay, the test cells were strongly affected by the samples after 24h. Basically, no such toxic effect could be observed using the extract test after the same treatment period.

DISCUSSION & CONCLUSIONS: Titanium is a widely used FDA approved implant material and passed all officially required *in vitro* as well as *in vivo* tests. Nevertheless, controversial data are reported (and also found in our lab) regarding the cytotoxic effects of Ti (alloy) materials (from no to moderate cytotoxicity). This was seen not only for the different alloys but also for the different cell assays, which most likely resulted from differences in preparation methods of the specimens and cell assay set-ups used.

The ISO 10993-5 extract test norm is rather flexible regarding extract medium, extraction method, treatment period and method to quantify cytotoxicity. As a result the outcome of different labs cannot be compared. The indirect extract test (which the overlay test in principle represents) in contrast is less prone to variations in experimental set-up. Furthermore, it might mimic better the local concentrations of the released constituents occurring *in vivo* in the tissue being in direct contact with the implant. In our hands this test showed to be most sensitive.

Thus while generally *in vitro* cytotoxicity testing represents a great opportunity to pre-evaluate the influence on cells regarding the released constituents of the test material, a careful, well documented and broad evaluation of assays is required in order to get an overall clear-cut impression concerning this key issue of bioacceptance.

REFERENCES: [1] A. Bruinink and R. Luginbuehl (2011) Evaluation of Biocompatibility Using In Vitro Methods: Interpretation and Limitations Adv. Biochem Eng Biotechnol, 117-52.

ACKNOWLEDGEMENTS: Authors would like to thank Umberto Piantini and Fabrice Micaux for their technical support and the HES-SO Valais for the financial support under Socle R&D 2012 Grant.

P27 – Development of a novel cytocompatible and photopolymerizable hydrogel precursor: hyaluronate vinyl ester

X-H. Qin, H. Redl, R. Liska

TU Vienna, Austrian Cluster for Tissue Regeneration, AT

INTRODUCTION: Cytocompatible and photocurable hydrogel precursors are important materials for tissue engineers to repair cartilage defects in a non-invasive manner.[1] Up to date, PEG diacrylates (PEGDA) have been widely used in the biomaterials community due to their high reactivity. However, irritancy and potential cytotoxicity of unreacted acrylate groups might preclude PEGDA from further clinical applications.[2] Our previous work has proved that vinyl esters are much less cytotoxic monomers when compared with acrylates.[3] In this study, we report the design and synthesis of a novel hyaluronan derivative (hyaluronate vinyl esters, HAVE) which is cytocompatible and photocrosslinkable. Importantly, the unique molecular design of HAVE enables that major degradation products out of HAVE hydrogels are PVA and adipic acid (both FDA-approved).

METHODS: HAVE with varying degree of substitution (DS) were prepared by lipase-catalyzed transesterification reaction between hyaluronate (10 K) and divinyl adipate. The products were purified by ion-exchange dialysis and subsequent lyophilization. Chemical structure and DS of HAVE were confirmed via ^{1}H-NMR. The photoreactivity and degradation behaviour of HAVE were evaluated via in-situ photo-rheometry. MTT assay was applied to measure the cytotoxicities of the macromer solutions and extractions of hydrogel pellets against MG63 cells.

RESULTS: ^{1}H-NMR results proved that a wide range of DS (0.05-0.68) was accessible by tuning the reaction time and stoichiometry. Photo-rheometry measurements showed that both the photoreacitivy and crosslinking degree of HAVE depends on the DS degree. Fig. 1 shows that HAVE could be photopolymerized with temporal control. Although photoreactivity of vinyl esters is generally lower than acrylates references, we were able to improve HAVE's reactivity by using the robust thiol-ene chemistry. In addition, biochemical response of HAVE hydrogels to hyaluronidase-induced degradation is shown in Fig. 2. Cleavage of linkages between HA repeating units leads to an enzyme-dose dependent decrease in the elastic modulus (G') over time. MTT assay proved that HAVE macromers and pellets presented negligible cytotoxicities on MG63 cells.

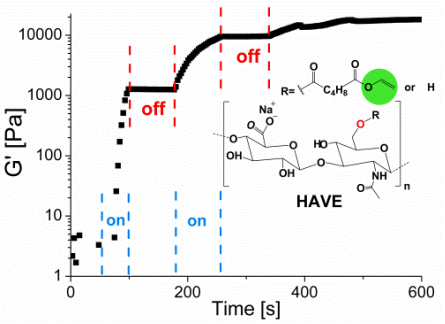

Fig. 1: Chemical structure of HAVE and in situ photo-rheometry measurements for elastic modulus of network formed at 10% HAVE(DS-0.15) solution, 0.5% I2959, 10 mW cm^{-2}, interrupted for 80 s at 100s and again at 260s, 25 °C.

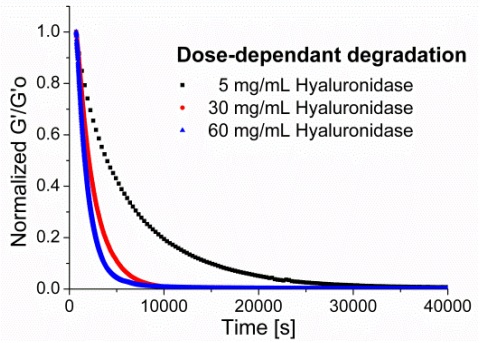

Fig. 2: Elastic modulus evolution due to enzymatic degradation of hydrogel networks at 37°C with 5, 30, or 60 mg/mL hyaluronidase. (G'$_0$: initial elastic modulus of network formed at 4°C)

DISCUSSION & CONCLUSIONS: Molecular design and synthesis of a novel hydrogel precursor is presented. In all, HAVE proves to be a promising material for the creation of cytocompatible hydrogels with user-defined properties. Further exploration of HAVE hydrogels as artificial ECM is under way.

REFERENCES: [1] J. Elisseeff, K. Anseth, et al (1999) *PNAS* **96**: 3104-07. [2] J. Torgersen, X. Qin, et al (2013) *ADV FUNCT MATER*, in press. [3] C. Heller, R. Liska, et al (2009) *J POLYM SCI POL CHEM* **47**: 6941-54.

ACKNOWLEDGEMENTS: XH Qin acknowledges the PhD fellowship sponsored by CSC council and FFG agency.

P28 – A new miniaturized optical device for the clinical assessment of dental erosion-in vitro test with extracted human teeth

E. Rakhmatullina[1], A. Bossen[2], C. Meier[2], A. Lussi[1]

[1]*Department of Preventive, Restorative and Paediatric Dentistry, University of Bern, CH.*
[2]*OptoLab, Bern University of Applied Sciences, CH.*

INTRODUCTION: Enamel is a hardest tissue of our teeth which is mostly (90%) composed of calcium deficient hydroxyapatite (HA) mineral. Regular acidic challenges such as excessive consumption of energy drinks, colas, fruit juices, vinegar, causes demineralization of the HA-based tissue and might result in a complete elimination of the enamel in the most severe cases. The timely clinical diagnostics and prevention of the erosion progression are important for dental health and a life quality of patients. Unfortunately, currently used visual examination allows erosion diagnosis only at late stages, when the extent of tissue loss results in the alteration of tooth shape, appearance or optical properties. Here, we developed a pen-size optical instrument which can be used for the fast quantification and monitoring of dental erosion at early stages.

METHODS: Polished embedded enamel samples were prepared from the buccal sites of the extracted human teeth as described earlier [1]. Different severity of the erosion was modelled by the in vitro etching of the enamel in 1% citric acid (pH=3.6) for 0.5-10 minutes duration.

The miniaturized optical device was supplied by the FDS100 photodiode (1mW, 635nm), a focusing lens providing 23º angles of incidence and reflection and a system of prisms (Fig. 1). The measurement principle is based on the detection of the specular reflection intensity (%) from the enamel surface. The entire device has dimensions of a pen and operates together with the custom-made software.

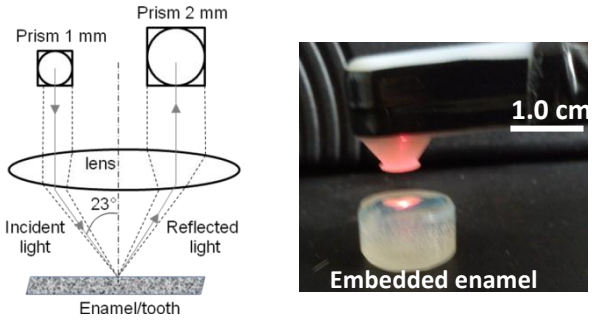

Fig. 1: Scheme of the optical system of the instrument (left) and an image of the measurement head (right).

RESULTS: Figure 2 shows reduction of the reflection intensity with the erosion progression. After 1min of erosion, a 30% reduction of the reflection signal was measured. The early erosion stages (0.5-2 min) were characterized by nearly exponential decay of the reflection signal. A good correlation was found (r^2=0.984) between erosion analyses by the current miniaturized and the prototype [1, 2] devices.

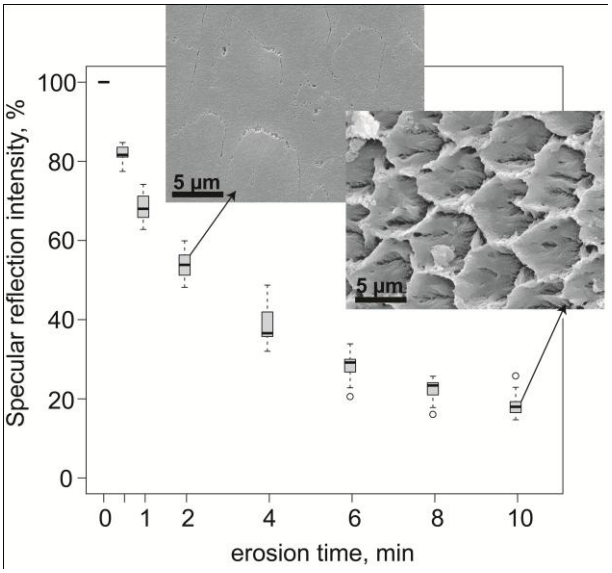

Fig. 2: Decrease of the reflection intensity with erosion progression and examples of SEM images of enamel surfaces (2 and 10 min of erosion).

DISCUSSION & CONCLUSIONS: The assembled optical device could successfully detect various severities of dental erosion. As was shown previously [1, 2], the decay of the reflection intensity was related to the rise of surface roughness and appearance of a typical honeycomb topography during enamel etching (SEM images, Fig. 2). Due to a small size, fast and simple measurements, the proposed instrument will be further tested in clinical erosion diagnosis.

REFERENCES: [1] E. Rakhmatullina, A. Bossen, C. Höschele, et al (2011) *J Biomed Opt* **16**:107002-13. [2] A. Lussi, A. Bossen, C. Höschele, et al (2012) *J Biomed Opt* **17**:097009-21.

ACKNOWLEDGEMENTS: The authors thank the Swiss Dental Association (SSO, project № 253-10) for the financial support.

P29 Remineralisation of carious lesions by self-assembled peptide supramolecular networks

S.Stevanovic[1], L.Kind[1], A.Wüthrich[1], U.Pieles[1], M. Hug[2], D. A. Lysek[2]

[1]FHNW - School of Life Sciences, Muttenz, CH, [2] Credentis, Windisch, CH

INTRODUCTION: The investigation of a non-invasive, regenerative remineralisation method of sub-surface carious lesions/ early caries lesions in tooth enamel is the field of attention in this project. The short peptide P11-4 self-assembles in a supramolecular 3D network after applying in the carious lesion. The hypothesis is, that this self-assembled structure triggers nucleation of de-novo hydroxyapatite (HA) nanocrystals and consequently results in lesion-remineralisation. Studies were performed with human teeth but due to the limited availability and great structural variability of human teeth, a bioceramic tooth model was developed to standardize this test system. Based on this artificial tooth model the study of demineralization and remineralisation of white spot lesions in enamel was simplified.

METHODS: Artificial lesions in human teeth were generated by incubation in acidic demineralisation buffer. P11-4 was directly applied on the lesion and then incubated in remineralisation buffer. The treated lesions were analysed by matrix-assisted desorption/ ionization–time of flight (MALDI-TOF) spectroscopy and μ-computer tomography (μ-CT).

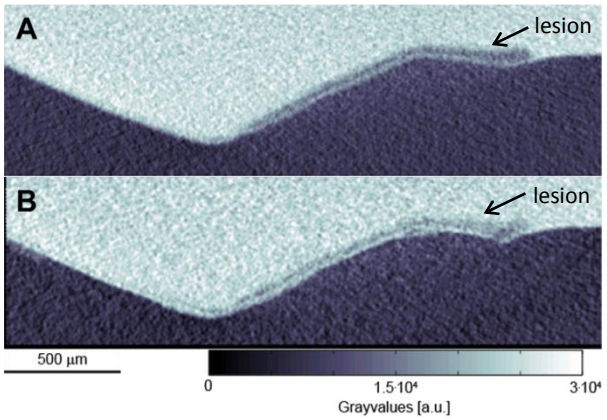

Fig. 1: μ-CT image of an artificial lesion in a human tooth before remineralisation (A) and after two weeks in remineralisation buffer (B)

Tooth models (PB) with characteristics of tooth enamel and dentin were achieved by compression of HA material, followed by thermal treatment. Two types of PB (enamel and dentine-like) were firmly assembled with phosphoric acid. To induce artificial lesions, the enamel-like PB was incubated in acidic solution. Analytic was performed by porosity by mercury intrusion porosity (MIP), Brunauer, Emmett, Teller (BET) gas adsorption, SEM and μ-CT.

RESULTS: Remineralisation of the artificial lesion was observed with μ-CT. Increased density was clearly visible after two weeks (figure 1). Moreover after incubating the tooth in remineralisation buffer for two weeks, P11-4 was still detected in the lesions with by an adapted MALDI-TOF method. The approach of producing and assembling PB (figure 2) as well as introduction of artificial lesions in PB was successful.

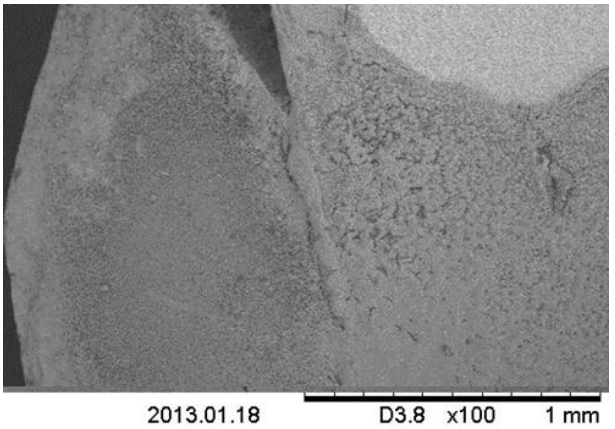

Fig. 2: SEM picture of the with phosphoric acid assembled artificial bodies

DISCUSSION & CONCLUSIONS: The investigations of surface caries lesions after treatment with P11-4 showed an induced remineralisation. At present only a few alternative approaches have been followed in order to regenerate the caries lesions [1]. The developed phantom bodies provide a standardized test system to study new compounds to cure caries. Furthermore studies on restorative remineralisation therapy by 3D-self-assembled peptide either in natural teeth or in phantom bodies are in process.

REFERENCES: [1] L. Rimondini, B. Palazzo, et al (2007) *Material Science Forum* **539-543**:602-605.

ACKNOWLEDGEMENTS: Support by the Swiss-Nanoscience Institute (SNI) and Swiss National Science Foundation (SNSF) is gratefully acknowledged.

P30 – Bioprinted agarose patterns to study cellular interactions

D. Studer [1,2], M. Müller [1], K. Maniura-Weber [2], M. Zenobi-Wong [1]

[1]Cartilage Engineering and Regeneration, ETH Zürich, CH. [2]Materials-Biology Interactions Laboratory, Swiss Federal Laboratories for Materials Science and Technology, St.Gallen, CH.

INTRODUCTION: Many biological processes are governed by the diffusion of soluble factors from cells in 3D. Bioprinting, a novel tool for the deposition of cell-laden hydrogels with micrometre precision [1], allow the study of the spatial-temporal dependence of such processes. The major challenge in the application of bioprinters, is the choice of material used as bioink. In this project, 3% low gelation temperature (LGT) agarose was chosen based on its printability and high cell viability to produce patterns with high precision.

METHODS: 4% LGT agarose (Sigma) was produced in PBS at 50°C. The resulting solution was mixed with a cell suspension at 37°C (10 Mio/ml of bovine chondrocytes) to yield a final concentration of 3%. The cell/hydrogel mixture was extruded through a printhead at 37°C onto a pre-cooled PLL-coated glass slide using the following parameters:

Table 1.: Printing parameters

Needle diameter	150 µm
Pressure	1,5 bar
Feed rate	1000 mm/min
Valve opening time	0.13 ms

After deposition, cold PBS was added on top of the structure, further replaced by cell culture medium and incubated at 37°C and 5% CO_2. For imaging of patterns with ApoTome (Zeiss), cells were pre-labeled with cell tracker red (Invitrogen). Further, the viability was assessed after 24 hours using a live/dead staining kit (Invitrogen).

RESULTS: Different patterns were printed with 3% agarose containing bovine chondrocytes. The resolution of the extruded strands is 300 µm with distance between strands ranging from 10 to 500 µm. The viability 24 hours after bioprinting was determined to be 85%, a value comparable to non-printed agarose hydrogels.

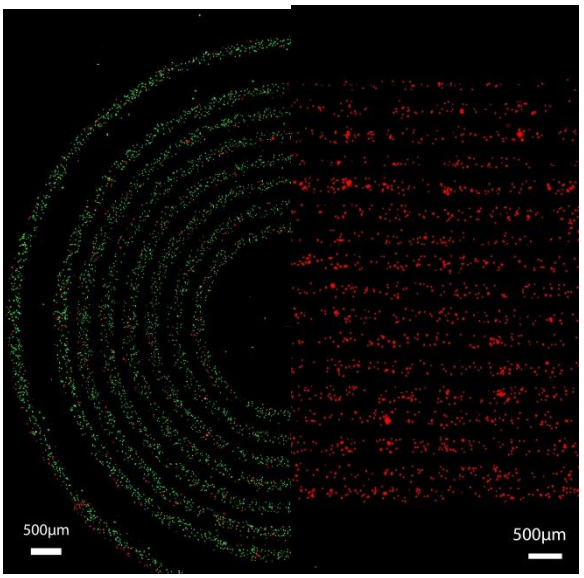

Fig. 1: Bioprinted patterns of live/dead stained (left) and cell tracker red labelled chondrocytes (right)

DISCUSSION & CONCLUSIONS: LGT agarose was successfully established as a bioink for the production of cellular patterns with high cell viability. The resolution in the micrometre range allows the investigation of cell-cell communication through diffusion of soluble cell secreted substances including growth factors. This system will be applied to study the effect of IGF-1 overexpressing cells on neighbouring chondrocytes placed at increasing distances from the source.

REFERENCES: [1] B Derby (2012) Printing and Prototyping of Tissues and Scaffolds, *Science* 338, 921

ACKNOWLEDGEMENTS: This work was supported by the Swiss National Science Foundation (Grant CR23I2_130678).

P31 – Gelatin-Chitosan-Hyaluronan as a new scaffold for liver tissue engineering

A. Tahmasbi Rad[1,2,*], M. Solati-Hashjin[2,3], L. Tayebi[1]

[1]Helmerich Advance Technology Research Center, Oklahoma State University, Tulsa, US; [2] Nanobiomaterials laboratory, Faculty of Biomedical Engineering, Amirkabir University of Technology, Tehran, Iran; [3]Department of Biomedical Engineering, Faculty of Engineering, University of Malaya, Kuala Lumpur, 50603, MALAYSIA; Armin.Tahmasbi@gmail.com*

INTRODUCTION: Liver tissue engineering requires a suitable extracellular matrix for hepatocyte cell culture due to strict requirement of anchorage-dependent growth [1].

Chitosan is highly biocompatible, non-toxic, biodegradable and non-immunoreactive to the human body compared to most synthetic polymers [2-3]. Gelatin is partially hydrolyzed form of Collagen which has great ability to enhance cell attachment [4]. Hyaluronic acid (HA) contains viscoelastic property, has been used in drug delivery systems and TE. HA is the first macromolecule that appears in the ECM during tissue repair and also plays an important role in cell migration and differentiation [5].

In the present study, we use the composite of these materials as a new scaffold for liver tissue engineering.

METHODS: Gelatin at 6.4% (w/v) concentration was poured in a 5% Acetic Acid solution. Then, Chitosan mixed with a 2.1% (w/v) concentration via homogenizer at 29,000 rpm, using a cold water bath (Sample A). Hyaluronic Acid was added with 0.1, 0.2 and 0.3 and 0.4% (w/v) (respectively samples B, C, D and E). Afterward, the solutions were frozen and after been treated by freeze-lyophilization at -53°C and 0.05 milibar for 24 hours, the scaffolds were immersed in 50 mM 1-ethyl-3-(3-dimethylaminopropyl) carbodiimide hydrochloride (EDC)/ 8mM N-hydroxysuccinimide (NHS)/ 95% alcohol crosslinking solution at 4°C twice for 48h. The cross-linked scaffolds were freeze-dried again under the same condition.

Further studies on equilibrium swelling, Porosity measurement, In vitro degradation, FTIR spectra and X-ray diffraction, Thermogravimetric (TG) and Differential Scanning Calorimeter (DSC) analysis and scaffold morphology (SEM) were done. Biocompatibility of the scaffolds was evaluated by Cell attachment and Proliferation (by using GS5 hepatocyte cells), and protein detection (Western blot).

RESULTS: The HA containing freeze-dried samples showed a range of 150-280 micrometers in porosity width and more than 1000% water swellability after six hours. The FTIR spectra illustrate the functional groups of each part with extra bonds between them. Finally the highest amounts of cells in attachment and proliferation tests were observed on the surface of the "B" sample. Also the cells in sample "B" expressed much more Alphafetoprotein and Actin.

DISCUSSION and CONCLUSION: The blend of 6.4% Gelatin, 2.1% chitosan and 0.1% Hyaluronan was selected as the optimum compound for making scaffold for liver tissue engineering.

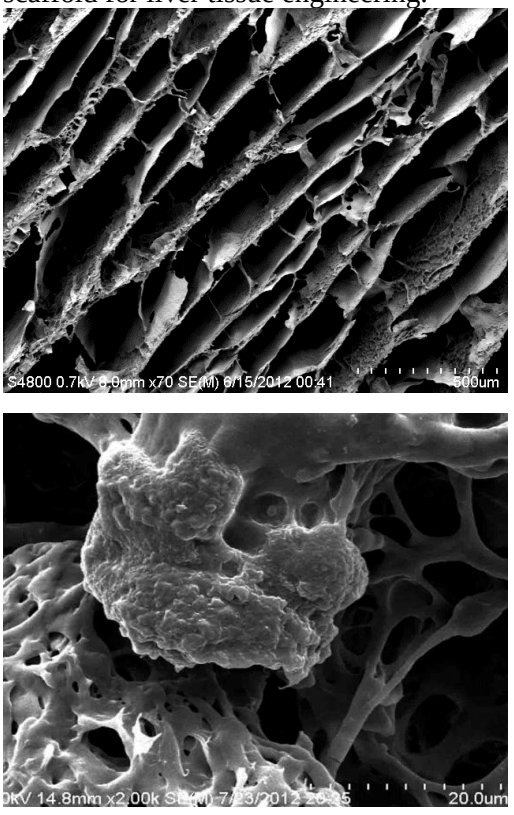

Fig.1. The SEM images of the porous "B" scaffold, the sample which shows the highest amount of the cells in proliferation and attachment tests significantly.

REFERENCES [1]Seog-Jin Seo *et al*., Biomaterials, 2006; 27 1487–1495. [2] Mao JS *et al*., J Biomed Mater Res B 2003; 64A(2):301–8.[3] Li JL *et al*., J Biomed Mater Res A, 2003; 67:938–43. [4] Young BR *et al*., J Colloid Interface Sci, 1988; 124:28–44. [5] Taek Gyoung Kim *et al*., Acta Biomaterialia, 2008; 4, 1611–1619

ACKNOWLEDGMENTS

The authors would like to thank **Marlik institute of innovation and technology** due to their supports.

P32 – Hyaluronic acid conjugates and their complexation with gentamicin for local infection prophylaxis

GA. ter Boo[1,2], DW. Grijpma[2], FT. Moriarty[1], D. Eglin[1]
[1] *AO Research Institute, AO Foundation, Davos, CH.* [2] *Department of Biomaterial Science and Technology,University of Twente, Enschede, NL*

INTRODUCTION: Infection is a common problem upon fracture fixation in trauma patients. For open fractures infection rates might even exceed 30%[1]. Delivery systems that release antibiotics locally can deliver high concentrations at the target site and circumvent systemic toxicity. Hyaluronic acid (HA) conjugates were prepared to complex and deliver antibiotics locally. The properties of the HA conjugates and their complexes with gentamicin (GM) are described here.

METHODS: Materials: The HA used had a Mn of 170.6 kDa. Radical polymerization was used to prepare amine terminated poly(N-isopropylacrylamide) (pNIPAm-NH_2). Jeffamines (JFMs) were a gift of Huntsman GmbH (Germany). Methoxy poly(ethyleneglycol) amine (mPEG-NH_2) was purchased from Jenkem Technology (United States). HA conjugates were synthesized by a direct amidation reaction of HA tetrabutylammonium (TBA) by pNIPAm-NH_2, JFM or mPEG-NH_2 as described elsewhere[2]. ^{1}H NMR was used to determine the degree of substitution (DS) for these compounds. Complexes were prepared by mixing of equal volumes of 5mM HA conjugate and 2mM GM solutions in MQ. Scanning electron microscopy (SEM) was used to observe their morphology.

RESULTS: HA conjugates were successfully synthesized and their DS was calculated by ^{1}H NMR.

Table 1. Mn and DSs of HA conjugates

HA Conjugate	PO/EO ratio (JFM)	Mn (kDa)	DS
pNIPAm	NA	12.0	11.7%
pNIPAm	NA	16.9	8.0%
pNIPAm	NA	41.3	3.6%
JFM M-600	9/1	0.6	29.9%
JFM M-1000	3/19	1.0	14.0%
JFM M-2005	29/6	2.0	42.3%
JFM M-2070	10/31	2.0	30.6%
mPEG	0/1	5.0	29.6%

The DS of pNIPAm for OH (-COOH) decreased with increasing Mn of pNIPAm-NH_2 (Table 1). The JFMs DS values did not show this trend for increasing Mn, possibly because of their low Mns and differences in PO/EO ratio. These HA conjugates were complexed with GM. Unconjugated sodium HA mixed with GM forms insoluble complexes that precipitate from solution. However, HApNIPAm 12 kDa solutions stay clear upon mixing with GM even after 1 week incubation at RT. SEM revealed that the complexes are bead-shaped with diameters in the µm range (Fig 1). HAJFM M-1000 and M-2070 solutions became turbid but no precipitate formed upon mixing, whereas HAJFM M-600 and M-2005 flocculated. HAmPEG solutions stayed clear.

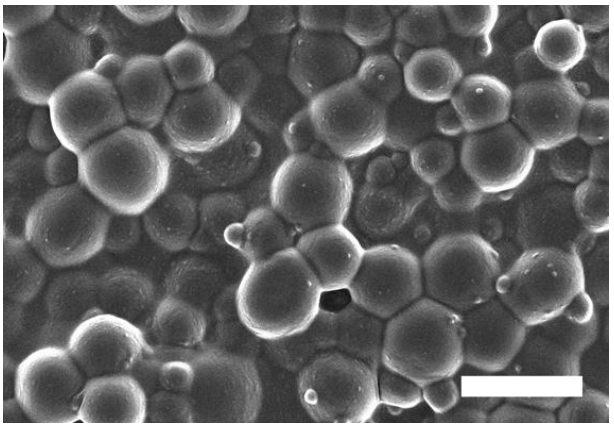

Fig. 1: SEM image of HApNIPAm 12 kDa-GM complexes. The scale bar represents 20 µm

DISCUSSION & CONCLUSIONS: HApNIPAms formed micron sized complexes upon mixing with GM. HAJFM-GM complex stability depends on the hydrophilicity / hydrophobicity ratio of the conjugate, since the more hydrophilic conjugates formed complexes which stayed in solution, whereas the more hydrophobic conjugates came out of solution. Release of GM in time is now investigated by; 1. Incubating samples with S.aureus NCTC 12973 2. *o*-Phthaldialdehyde assay and 3. HPLC analysis.

REFERENCES: [1]A. Trampuz, A.F. Widmer (2006) *Curr Opin Infect Dis* **19**:349-356 [2]M. D'Este, M. Alini, D. Eglin (2012) *Carbohydrate Polymers* **90**:1378-1385

P33 – Calcium phosphate micro-and nanocrystals synthesized in an organic solvent

J. Thüring[1,2], L. Galea[1], M. Bohner[1], M. Niederberger[2]
[1]RMS Foundation, Bettlach, CH. [2]ETH Zürich, Department of Materials, Zürich, CH.

INTRODUCTION: Calcium phosphates (CaPs) belong to the biomaterials which are the most known and applied in terms of bone defect treatment. Several production methods like high temperature processes or precipitation in aqueous solutions result in crystalline products composed for example of β-tricalcium phosphate (β-TCP; β-$Ca_3(PO_4)_2$) or monetite (DCP; $CaHPO_4$). But most of these methods lead to agglomerated and polydispersed particles. Therefore, our aim is to assess a new approach to synthesize non-agglomerated and monodispersed CaP crystalline micro- and nanoparticles based on the precipitation of CaPs crystals in organic solvents.

METHODS: Similar to the work of Tao et al.[1], the CaP particles were produced with a single batch method. For this a calcium salt solution was mixed with a phosphate salt solution. Ethylene glycol was used as solvent. The temperature was typically in the range of 90 to 170°C. After a certain reaction time single crystalline particles precipitated out of this solution. The resulting product was filtered and analyzed by SEM, XRD, and laser diffraction analysis.

RESULTS: By changing parameters like temperature, pH, reaction time and precursor concentration, we were able to synthesize particles varying in size, shape and composition as shown in *Fig. 4*. The size dispersion for batches resulting in β-TCP particles with a phase pure composition was below 10 % and in ideal cases even below 5 %. The size ranged from about 0.1 µm (nanoparticles) to 1.2 µm (hexagonal platelets) or in special cases even up to 8 µm when mixed with DCP (s. huge hexagonal platelet in *Figure 1b*). The parallelepiped-shaped DCP platelets had a length up to several micrometers. Their size dispersion was below 20-30 %, depending on the reaction temperature. The urchin-shaped monetite particles had a diameter of 2.8±0.7 µm; with a size dispersion of 25 %. All particles were non-agglomerated as indicated by the narrow and monomodal particle size distribution curves obtained by laser diffraction.

DISCUSSION & CONCLUSIONS: As our first research efforts show, it is possible to synthesize non-agglomerated and monodispersed calcium phosphate particles. Their size, shape and composition can be influenced by varying the reaction parameters.

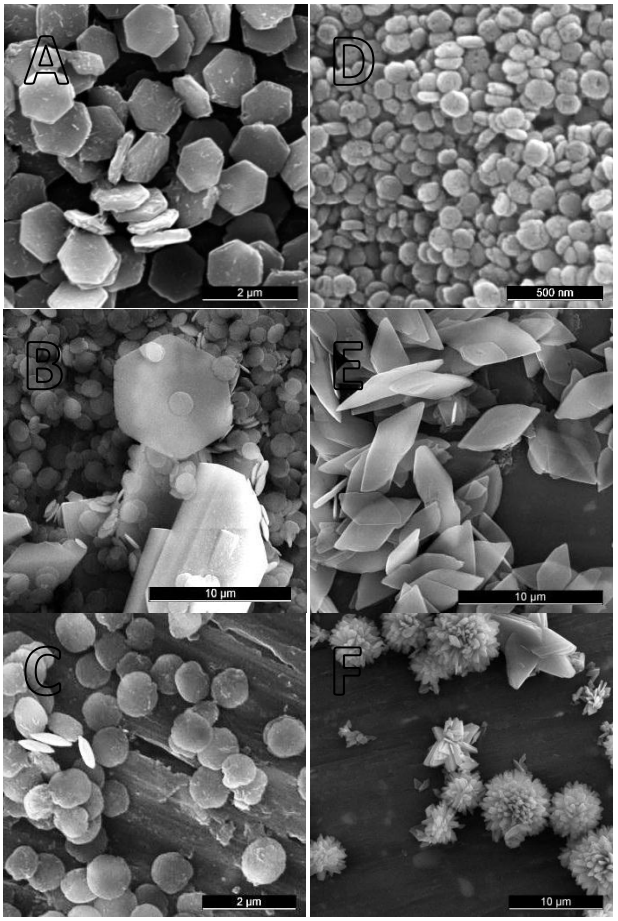

Fig. 4: SEM images: a) β-TCP hexagonal platelets, b) huge β-TCP hexagonal platelet together with monetite particles and other β-TCP hexagonal platelets c) "M&M"-shaped β-TCP particles, d) β-TCP nanoparticles, e) parallelepiped-shaped monetite platelets and f) urchin-shaped monetite balls. The scale bar measures 500 nm for d), 2 µm for a)+c) and 10 µm for b),e),f).

REFERENCES: [1] J. Tao, W. Jiang, H. Zhai, H. Pan, X. Xu, and R. Tang (2008) *Crystal Growth & Design*, **8**(7), 2227.

P34 – Nanostructured nanofibers for drug release and tissue engineering

G. Yazgan[1,2], S. Zuber[1], AM. Bühlmann-Popa[1]

[1] EMPA, Swiss Federal Laboratories for Materials Science and Technology, St. Gallen, CH. [2] Cartilage Engineering and Regeneration Group, ETHZ, Zurich, CH.

INTRODUCTION: Emulsion-electrospinning is a versatile technique for the production of core-sheath fibers and the encapsulation of large quantities of drugs or proteins in the core. In the present study, we aim to synthesize bicomponent nanostructures with a sheath having controlled porosity via mini-emulsion electrospinning. The advantage of the technique is the possibility for scaling up and the transfer to industry. Since it is a relatively new technique, protocols from well-established, conventional solution electrospinning can give a hint how to obtain porous fibers via mini-emulsion technique. In literature, it has been reported that the porous fiber morphology can be achieved by spinning onto a collector which is embedded in a liquid N_2 bath[1], high volatile solvents[2] and ternary system of a non-solvent/solvent with polymers[3].

METHODS: Polymer solutions of poly (L-lactic acid) (PLA) and polystyrene (PS) in $CHCl_3$ were prepared. Additionally, the same polymer solutions containing Span80 as a surfactant were prepared as the continuous phase for the emulsion systems. An aqueous solution of poly(vinyl caprolactam) (PVCL) was added drop wise into the oil phase. Subsequent ultrasonication of the emulsion provided a homogeneous miniemulsion.

Non-solvent/solvent/polymer system After preparation of W/O mini-emulsions, less volatile non-solvents (hexadecane, *o*-xylene or toluene) for the polymer forming the dispersed phase were added and stirred. Afterwards, the emulsions were processed into fibrous nonwovens by electrospinning. *Cryogenic liquid bath* The electrospinning collector was immersed in a liquid N_2 bath. Collected fibers were either dried at room temperature (RT) or in vacuum to be characterized by SEM and TEM later on.

RESULTS: All of the non-solvent containing emulsion systems were successfully processed into fibers; however, interestingly enough, the emulsion spinning did not result in a porous sheath. On the other hand, spinning of PLA solution into liquid N_2 bath resulted in pores both for vacuum dried and RT dried samples. However, PS solution electrospinning resulted in either non-fibrous polymeric structures or low yield of pores depending on the drying condition. Besides, the emulsion system of PVCL and PS yielded with a porous morphology. (Figure1) Parameters need to be optimized to achieve homogeneous structures.

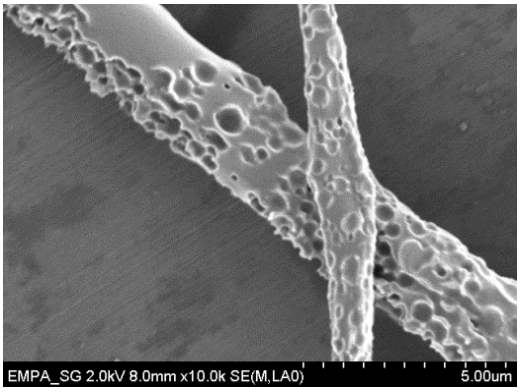

Fig. 1: SEM micrograph of electrospun fibers into liquid nitrogen from 15 %w/v PS in $CHCl_3$ as continuous phase and dried under vacuum

DISCUSSION & CONCLUSIONS: The pores are generally a result of solvent evaporation from the phase separated electrospinning jet. Since both methods yield successful bicomponent fibers, further emphasis must lie on the improvement of a porous sheath.

New approaches for enhanced phase separation, such as addition of non-solvents for the polymer forming the continuous phase or cooling the electrospinning environment will be investigated next.

REFERENCES: [1]McCann, J.T., M. Marquez, and Y. Xia, Journal of the American Chemical Society, 2006. 128(5): p. 1436-1437. [2]Bognitzki, M., et al., Advanced Materials, 2001. 13(1): p. 70-72. [3]Qi, Z., et al., Materials Letters, 2009. 63(3–4): p. 415-418.

ACKNOWLEDGEMENTS: Work was done in the frame of the NFP62 project IRENA kindly financed by the Swiss National Science Foundation.

19th Swiss Conference on Biomaterials

Overview Last Minute Poster Presentations

Last Minute Poster Presentations

19th Swiss Conference on Biomaterials

Abstracts Last Minute Poster Presentations

SSB Swiss Society for Biomaterials
Société Suisse des Biomatériaux
Schweizerische Gesellschaft für Biomaterialien
Società Svizzera Biomateriali

AO Foundation

P35 – The Degradation of PLGA Scaffolds under Dynamic Loading

R. Bohm[1], M. Zaucha[1], S. Biechler[1], S. Williams[1]

[1] *ElectroForce Systems Group, Bose Corporation, Eden Prairie, MN, USA*

INTRODUCTION: Poly(lactic-*co*-glycolic acid), or PLGA, is commonly used in medical applications because it is biocompatible and biodegradable. The degradation rate of PLGA under static loading conditions and/or in the presence of common solvents has been studied extensively. However, the effect of dynamic mechanical loading on scaffold degradation has not been thoroughly investigated. The relationship between dynamic conditioning and degradation of biomedical materials, such as PLGA, needs to be examined because these materials are subjected to dynamic mechanical forces in vivo. In this study, a disk of PLGA was cyclically compressed and degradation was assessed and compared to statically loaded and unloaded controls.

METHODS: A 5110 Test Instrument (Bose Corporation, Eden Prairie, MN) was used to simultaneously perfuse and axially load the sample in a sterile, culture environment. The PLGA sample was mounted between two porous platens. To apply dynamic loading, a PLGA scaffold was compressed (5 to 30 g sine wave) and saline was perfused through the sample at a rate of 5 mL/min for 8 days (Exp Group). During the test period, axial displacement, load, chamber pressure and scaffold diameter were monitored. Three additional groups without axial loading were used for control comparisons: dry scaffolds (Ctrl Group); hydrated scaffolds with perfusion only (+Perf Group); hydrated scaffolds without perfusion or axial loading (-Perf Group).

RESULTS: The height and modulus of the dynamically loaded PLGA sample decreased during the first 2 days of the conditioning period and then stabilized during the last 6 test days. At the end of the conditioning period, a stress-strain analysis was performed to compare the degradation of the experimental group (Exp) to the three control groups (Ctrl, -Perf and +Perf). The four sample groups were mechanically tested to obtain force-displacement relationships. The Green strain and 1st Piola-Kirchhoff stress were calculated to account for alterations in sample geometry between the four groups. As shown in the resulting stress-strain curves (Fig. 1), full dynamic loading with axial compression and liquid perfusion (Exp) resulted in increased sample compliance, as compared to all other groups without axial loading. Samples with liquid perfusion alone, or static loading, (+Perf) also had greater compliance (degradation) after the test period as compared to the hydration group in stagnant saline (-Perf). Dry samples that weren't subjected to any loading or hydration (Ctrl) had the least compliance, indicated by the steep stress-strain curve in Fig. 1.

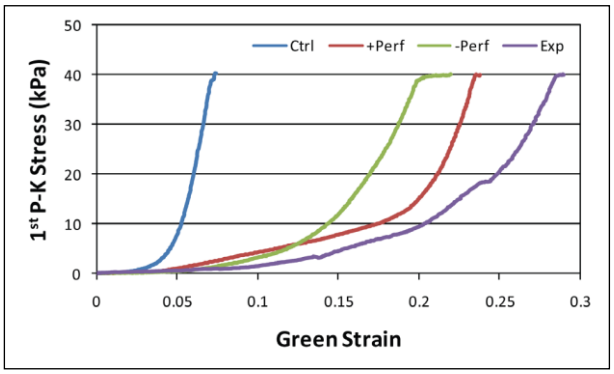

Fig. 1: Stress-strain plots showed that axial compression and liquid perfusion resulted in the most compliant PLGA scaffold group (Exp), and dry scaffolds were stiffer than any hydrated groups (Ctrl). The addition of static perfusion (+Perf) increased the scaffold compliance as compared to stationary fluid (-Perf).

DISCUSSION & CONCLUSIONS: In this study, PLGA samples were investigated under cyclic loading, static loading and unloaded conditions to investigate the importance of dynamic scaffold conditioning on degradation characterization. After an extended conditioning period, mechanical analysis showed that PLGA degradation, as indicated by increased sample compliance, was greater with dynamic compression and liquid perfusion than with static perfusion alone. While static perfusion resulted in greater degradation than unloaded, hydrated samples, the difference between dynamically compressed and statically perfused samples appears to be large. Ultimately, this data validates the importance of considering dynamic conditioning when characterizing scaffold degradation.

ACKNOWLEDGEMENTS: This template was modified with kind permission from eCM Journal.

P36 – Effects of crosslinker type on NVP based hydrogels for nucleus pulposus replacement

A. Khoushabi[1], P-E. Bourban[1], AC. Borges[1], A. Schmocker[2], A. Mermillod-Blardet[1], D. Pioletti[3], C. Schizas[4], C. Moser[2], JA. Månson[1]

[1]Laboratory of composite and polymer technology, [2]Laboratory of applied photonics devices, [3]Laboratory of biomechanical orthopedics, Ecole Polytechnique Fédérale de Lausanne (EPFL), Station 12, CH-1015 Lausanne, [4]Centre Hospitalier Universitaire Vaudois, Switzerland

INTRODUCTION: Low back pain caused by degeneration of intervertebral disc is one of the most common health problems in the adult population. The current available treatments are limited to heavily invasive surgical approaches that do not preserve the disc biochemical and biomechanical functions.

Replacing the gelly core of the intervertebral disc so-called nucleus pulposus (NP) is a minimally invasive approach to back pain treatment. Hydrogels have received a great deal of attention as NP replacement due to their potential in mimicking the NP performance.

A new photo-polymerizable, 1-Vinyl-2-pyrrolidone (NVP) based hydrogel has been recently developed as NP replacement candidate [1]. The present work investigates the influence of two different crosslinkers, trimethacrylated tween 20 (T3) and Triethylene glycol dimethacrylate (TEGDM), on the NVP based hydrogel. The swelling ratio and elastic modulus of the hydrogels with different formulations (i.e. water content and crosslinker concentration) are measured and compared to those of natural human NP reported in the literature [2,3]. The results can be used to select an appropriate hydrogel for NP replacement.

MATERIALS & METHODS: Commercial NVP, 4-(2-hydroxyethoxy) phenyl - (2-hydroxy-2-propyl) ketone and TEGDM are used and T3 is synthesized from tween 20 as described in [4].

Hydrogels candidate precursors are made with different formulations and cured under UV illumination. Synthesized hydrogels are then immersed in phosphate buffer solution for 2 days.

The swelling ratio (SR) is calculated by dividing the hydrogel absorbed water weight to the initial weight. Compression test is performed on swollen hydrogels to obtain the elastic modulus, using the linear part of the stress–strain curve (strain range 20–25%).

RESULTS: Figure 1 illustrates the SR and elastic modulus of the hydrogel with different crosslinkers and those of NP reported in the literature [2,3]. Note that different formulations have been examined for each candidate crosslinker. As expected, increasing the NVP to crosslinker molar ratio increases the SR and decreases the elastic modulus of the hydrogels.

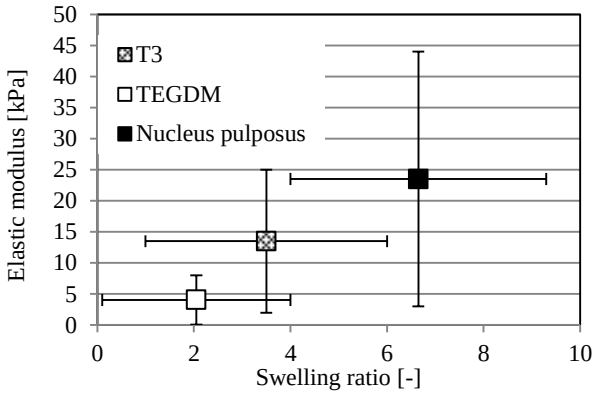

Fig. 1: Elastic modulus and swelling ratio of the NVP/T3, NVP/TEGDM and nucleus pulpous reported in the literature.

DISCUSSION & CONCLUSIONS: Elastic modulus and SR values obtained from the hydrogels synthesized using T3 crosslinker are found in NP-properties range. TEGDM hydrogels have lower SR and elastic modulus, however TEGDM provides a more practical curing process. Reinforcing fibres addition to the hydrogel precursor can be considered to obtain the desired properties in this context. Further investigation should be done to choose the most appropriate hydrogel formulation in presence of reinforcement fibres.

REFERENCES: [1]A.C. Borges, et al (2011) Acta Biomaterialia **7**:3412-21 [2]J.C. Atridis, et al (2005) J Ortopaedic Research **15**(2):318-22 [3]Cloyd, et al (2007) European Spine Journal **16**(11):1892-8 [4]A.C. Borges, et al (2012) J Materials Science And Engineering: C **32**:2235-41

ACKNOWLEDGEMENTS: Financial support from Swiss National Science Foundation under the grant 10024003165465 is acknowledged.

P37 – Polyurethane membrane for annulus fibrosus rupture closure

Z. Li[1], T. Pirvu[1], SBG. Blanquer[2], DW. Grijpma[2], S. Grad[1], M. Alini[1], D. Eglin[1]

[1]AO Research Institute Davos, Davos, CH. [2]Dept. of Biomaterials Science and Technology, University of Twente, Enschede, The Netherlands.

INTRODUCTION: The incidence of reherniation through ruptured annulus fibrosus (AF) ranges from 10% to 15% in patients with herniated discs treated with discectomy. In this study, we produced polyurethane (PU) membranes containing leachable poly(ethylene glycol) (PEG) for the application of AF rupture closure. An initial organ culture study was conducted to investigate the capability of the PU membrane to retain a Tissue Engineering (TE) construct and reduce the reherniation risk.

METHODS: Segmented PU was synthesized as already reported [1]. Preparation of PU membranes with/without PEG (Mn 0.6 kDa) consisted in the solubilisation of PU 10 w:v % with addition of 0 and 1 w:v % of PEG in a mixture of solvents. The solutions were poured into a flat tray and left evaporating for 1 week before drying under vacuum. Half of the samples were washed repeatedly with water for 1 week to remove leachable PEG. Tensile tests were conducted on dry samples using an Instron mechanical testing system model 4302 (High Wycombe, Bucks, UK). A feasibility study was conducted in organ culture of bovine caudal discs under physiological loading conditions. A defect through the AF of the discs was created with a biopsy punch. The AF cavity was refilled with a TE construct. The PU membrane without PEG was sutured (4 point-suture) with the surrounding AF tissue to close the AF defect. After one week of pre-culture, discs were loaded with 4 hours sinusoidal dynamic load per day for 7 continuous days, at 0.06±0.02 MPa, 0.2 Hz. Disc dimensions were measured with a calliper after dynamic loading and after overnight free swelling. Stability of the membrane was macroscopically assessed. Safranin O/Fast Green staining was performed.

RESULTS: PU membranes with PEG showed an increase of elongation at break and a decrease of strength (Fig. 1). The original property of the PU membrane was recovered after leaching of the PEG. The organ culture study showed that after 4 hours of dynamic loading, the disc height decreased by 5-7% compared with the initial height. All the discs recovered their initial height after overnight free swelling. Safranin O/Fast Green staining and macroscopic observation showed that the PU membrane sutured with adjacent AF tissue maintained the TE construct inside the AF cavity under dynamic loading (Fig. 2).

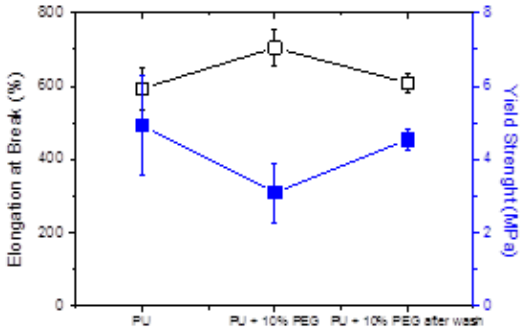

Fig. 1. Elongation at break and Yield strength of PU membrane containing 0 and 10 w:w% PEG and after washing (Mean, ± SD, N = 6).

No protrusion of nucleus pulposus tissue was observed after one week of pre-culture and a second week of dynamic load (Fig. 2).

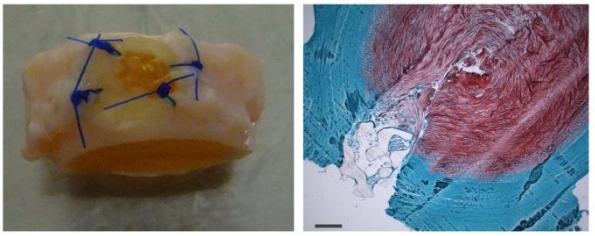

Fig. 2. Discs with AF defect implanted with TE construct and covered with PU membrane after 2 weeks of culture with dynamic load during the second week. Left: macroscopic view. Right: Safranin O/Fast Green stained section, scale bar 1000 µm.

DISCUSSION & CONCLUSIONS: Temporal modulation of PU membrane mechanical properties can be achieved by addition and leaching of PEG. Sutured PU membrane retained an AF TE construct in a disc under mechanical load. PU membranes may be suitable as an AF rupture closure device to reduce disc reherniation risk.

ACKNOWLEDGEMENTS: This study is funded by the AF Rupture Collaborative Research Program from AO Exploratory Research Board.

REFERENCE: 1. Boissard CI, et al. Acta Biomater. 2009;5(9):3316-27.

P38 – Local delivery of D-amino acids reduce bacterial burden in contaminated rat segmental defects

EM. Prieto[1], CJ. Sanchez Jr[2], CA. Kruger[2], KJ. Zienkiewicz[1], KS. Akers[2], SA. Guelcher[1], JC. Wenke[2]

[1] Department of Chemical Engineering, Vanderbilt University, Nashville, TN, USA. [2] US Army Institute of Surgical Research, San Antonio, TX, USA

INTRODUCTION: The healing of open bone fractures is often complicated by infection which causes delayed union or amputation. Even though current treatments include wound debridement and the administration of antibiotics, new methods are required to target bacterial persistence in biofilms. Recently, D-amino acids (D-AAs) have been identified as molecules with minimal toxicity that can inhibit biofilm formation and promote biofilm disassembly [1]. The current study aimed to evaluate whether local delivery of D-AAs from a porous scaffold reduces bacterial burden in a contaminated rat bone defect model.

METHODS: A 1:1:1: mixture of D-Trp:D-Met:D-Pro was incorporated into polyurethane (PUR) scaffolds as a labile powder (PUR-DAA). D-AA release profiles from the foam were measured using HPLC (Fig. 1A). The efficacy of PUR-DAA foams against biofilms was tested *in vitro* and *in vivo*. Cylindrical PUR-DAA foams were implanted in contaminated 6-mm defects in Sprague-Dawley rat femurs [2] and the bacterial counts in the host bone, hardware, and scaffold were quantified after 2 weeks. Two *S. aureus* strains were used to contaminate the defect: Xenogen 36 (weak biofilm former- Caliper Life Science, Hopkinton, MA) and UAMS-1 (strong biofilm former-received from Kai Leung at ISR). Two initial bacterial loads were tested: 10^2 and 10^5 CFUs.

RESULTS: The D-AA concentrations used were not cytotoxic for fibroblasts and osteoblasts as suggested by *in vitro* viabilities higher than 70% after D-AA treatment. Polyurethane scaffolds with 0, 0.1, 1, 5, or 10 wt% D-AA mixture were 88-91% porous with a pore diameter of about 370 μm. The release kinetics of D-Pro, D-Met, and D-Trp was characterized by an initial burst followed by a sustained release for 14 days (Fig. 1A). *In vitro* culture showed that the D-AA mixture reduced the bacterial load on the foam ~5 orders of magnitude compared to the empty scaffold (Fig. 1B). When tested in the contaminated defect *in vivo*, the release of D-AA mixture from the foam had a minimal effect on the defects contaminated with the low biofilm-producing XEN (Fig. 1C). However, the number of contaminated bone samples (Fig. 1D) and the bacterial load on the host bone of defects contaminated with 10^2 CFUs of the heavy biofilm-producing UAMS-1 significantly decreased compared to the empty scaffold.

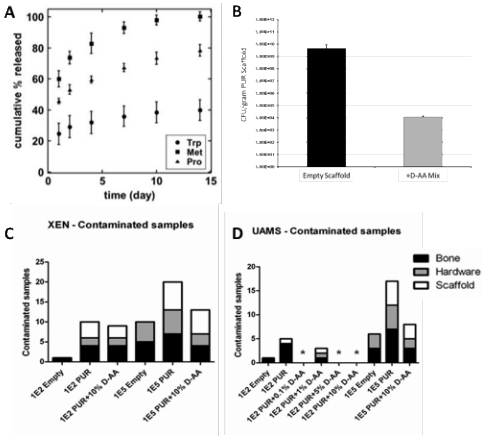

Fig. 1: Characterization of the PUR-DAA scaffold. (A) In vitro release kinetics. (B) Effects of D-AAs on S. aureus UAMS-1 contamination in vitro. Effects of D-AAs on infection for 6-mm femoral defects contaminated with 10^2 or 10^5 CFUs (C) S. aureus Xen 36 or (D) S. aureus UAMS-1.

DISCUSSION & CONCLUSIONS: These results suggest that local delivery of D-AAs from polyurethane scaffolds reduces the probability of infection in a contaminated bone defect. As anticipated, the heavy biofilm-producing UAMS-1 strain is more responsive to D-AAs than the low biofilm-producing Xen-36 strain. While more studies are needed to optimize D-AA dose, the local delivery of a combination of D-AAs is a promising therapeutic strategy to reduce the bacterial burden in contaminated wounds.

REFERENCES: [1] I. Kolodkin-Gal, D. Romero, S. Cao, et. al. (2010) *Science* **328**:627-629. [2] B. Li, K.V. Brown, J.C. Wenke, et al (2010) *J Control Rel* **145**:221-30.

ACKNOWLEDGEMENTS: This work was supported by the Orthopaedic Trauma Extremity Research Program (Department of Defense).

Meeting Location

Room Aspen, Congress Center, Davos

www.davoscongress.ch